Dynamic Analysis of Rotating Structures

Ashok Kaushal

A Thesis

in

The Department

of

Mechanical Engineering

Presented in Partial Fulfillment of the Requirements
for the Degree of Master of Engineering at
Concordia University
Montréal, Québec, Canada

August 1985

ABSTRACT

Dynamic Analysis of Rotating Structures

Ashok Kaushal

The objective of this thesis is to study the dynamic behavior of rotating structures. The structure, depending on the aspect ratio is modelled as either a rotating beam or a rotating plate.

Energy formulation and finite element modelling are carried out for a rotating beam type structure. Natural frequencies and mode shapes for such a structure are determined. The effect of the setting angle, hub radius and rotational speed on these natural frequencies and mode shapes are also presented and discussed.

Beam characteristic orthogonal polynomials are generated for analyzing rotating and non-rotating plates. Experimental results for a plate with all edges free are obtained and compared to validate the computed analytical results.

ACKNOWLEDGEMENT

The author is sincerely grateful to his supervisor Dr. R.B. Bhat for his enthusiastic guidance and continuous encouragement during the course of this work.

The help and assistance provided by friends and colleagues, especially by Mr. K.G. Balasubramaniam and Mr. Anil Dhir is greatly acknowledged. Thanks are also due to Ms. Lilian Jacob for her cooperation and understanding during the course of this work.

Further, the author is grateful to his parents for their abundant moral support and understanding throughout the course of this investigation.

Last but not least, the author is thankful to Mrs. Ilana Crawford for typing the thesis.

TABLE OF CONTENTS

NOMENCLATURE

a,b	plate side dimensions
E	Young's modulus of elasticity
D	flexural rigidity of the plate
h	thickness of the plate
I_x	moment of inertia of the beam cross-section
L	length of the beam
p	natural frequency
R	hub radius
$\tilde{R}_o$	dimensionless parameter
$\tilde{r}$	dimensionless parameter
R_1, R_2 and R_3	radius of curvature
T_f	flexural kinetic energy
T_R	rotational kinetic energy
U	strain energy
W	deflection of the plate
xyz and XYZ	coordinate axes
$\tilde{z}$	dimensionless parameter
ω	rotational speed
θ	setting angle
ν	Poissons ratio
α	dimensionless parameter
α_1	plate side ratio
ρ	density of the material
η	dimensionless parameter
ε, β_1	angles

LIST OF FIGURES

LIST OF TABLES

CHAPTER 1

INTRODUCTION, LITERATURE SURVEY AND OBJECTIVES

CHAPTER 1

INTRODUCTION, LITERATURE SURVEY AND OBJECTIVES

1.1 General

The design of rotating structures such as helicopter rotors, long and flexible rotating space booms and wind turbines requires a good understanding of their vibrational behavior in operation. Centrifugal forces are set up in these structures due to their rotation, which deflect the structure and at the same time cause in-plane strains resulting in the stiffening of the structure.

Due to the change in structural characteristics with the speed of rotation, the natural frequencies and associated modes of free vibration will be much different from those under non-rotating conditions of such structures. The resonant frequencies of these rotating structures can only be established with absolute certainty by means of experiments in a spinning rig, in which the structure is excited by a piezo-electric element cemented to the rotating structure, and a detector crystal is used to measure the response.

1.2 Literature Survey

The determination of natural frequencies and mode shapes of rotating structures, such as turbine blades is highly important in the design of turbomachines, because blade failures are normally attributed to fatigue which occurs when the blade vibrates under resonant conditions. It thus becomes imperative that one should be able to determine the natural frequencies and mode shapes of such rotating structures as accurately as possible.

Since the blades are idealized as beams for high aspect ratios and plates for low aspect ratios, the vibrations of rotating cantilever beams and plates have been studied in several investigations. The methods of solution of such rotating structures can broadly be classified as belonging to either the continuum model approach or the discrete model approach. In the continuum model approach, applications of the potential energy method, the complementary energy principle or the Galerkin process for the solution of such structures have been thoroughly investigated and developed. The resulting differential equations obtained using these methods are solved using a Runge-Kutta procedure. In the discrete model approach, the Holzer-Myklestad, Stodola, polynomial frequency equation transformation, station function, finite difference and finite element methods are well developed. All these discrete model approaches suffer from the drawback of the discretization process of the distributed mass and elasticity, thus yielding lower bound solutions.

Various investigators in this field considered either one or a combination of a few of the blade parameters such as rotational speed, pretwist etc. to determine their effects on the natural frequencies. A general survey of such works is presented by Rao [1].

Energy expressions for a rotating beam undergoing transverse vibrations were derived by Carnegie [2] and he obtained the fundamental frequency of vibration using Rayleigh's method. Schilhansl [3] derived the equation of motion for the bending vibrations of a rotating cantilever beam with uniform cross-section and solved it by successive approximations to determine the effect of rotation on the fundamental frequency. Rubenstein and Stadler [4] and Pnuelli [5] investigated the vibrations of rotating cantilever beams and found that the rotation of the beam tended to increase the natural frequencies of flexural vibration compared to those for the non-rotating beam. Subrahmanyam, Kulkarni and Rao [6] used Reissner method to obtain the natural frequencies of rotating blades of a symmetric aerofoil cross-section with allowance for shear deflection and rotary inertia and showed that the method gives results which are superior to those obtained by using the potential energy expression in the Ritz method. Sutherland [7] has used a Myklestad type method by a suitable modification of the equations, relating the shears and the moments of consecutive stations on the beam, to take into account the effect of the centrifugal forces. Kumar [8] also used Myklestad method to obtain both out of plane and in-plane vibration frequencies of rotating beams with tip mass. Isabson and Eisley [9] used the extended Holzer-Myklestad procedure and Slypex [10] used the Stodala method to determine the natural frequencies of pretwisted cantilever blades. The method of Frobenius was used to solve for the natural frequencies and mode shapes of centrifugally stiffened beams by Wright, Smith, Thresher and Wang [11]. The effects of hub radius and tip mass on the bending natural frequencies of rotating beams were studied by Handléman, Boyce and Cohen [12], Lo, Goldberg and Bogdanoff [13] and Boyce and Handleman [14]. In these studies it was observed that the hub radius influenced the bending natural frequencies significantly in various modes. The effect of the setting angle on the natural frequencies was studied by Wang et al [15]. An improved strain energy formulation in Rayleigh-Ritz method was used by Kaushal and Bhat [16] to obtain the natural frequencies of a rotating cantilever beam. The shear distribution was integrated along the beam subject to appropriate boundary conditions to obtain the moment distribution and using this information the strain energy was obtained. Bhat [17] studied the transverse vibrations of a rotating cantilever beam with tip mass by using beam-characteristic orthogonal polynomials in Rayleigh-Ritz method.

The idealization of rotating structures as rotating cantilever beams is acceptable for high aspect ratios but at low aspect ratios these structures are expected to behave like plates, rather than beams.

In 1909, Ritz postulated his famous variation method [18] and presented as a demonstration a solution for the force vibration of a completely free rectangular plate, the deflection function for which was assumed to be a series of multiplications of free-free beam vibration mode shapes [19]. His example has been followed by numerous investigators who have used series of appropriate beam functions to numerically investigate various types of plate problems.

The flexural vibration of rectangular plates by using beam vibration mode shapes as admissible functions in both the Rayleigh and Rayleigh-Ritz methods of analysis has been treated extensively by Young [20], Leissa [21], and Dickinson [22].

The convergence and accuracy of Ritz's method has been discussed by various authors including Trefftz [23], Courant [24], and Collatz [25].

While Ritz's method is well known, it has not been used as much as might be expected for plate-vibration problems. This is probably due, at least in part, to the great amount of computational labor which is required both to set up and to solve the necessary equations. The amount of computation involved depends to a large extent upon the set of functions that are used to represent the plate deflection. For these functions, some investigators have used combinations of the characteristic functions which define the normal modes of a vibration of a uniform beam. Pickett [26] used polynomial functions as an application to a plate equilibrium problem. Bassily and Dickinson [27] used degenerated beam functions to study flexure problems concerning static deflection or free vibration of plates involving free edges. An alternative set of admissible functions, derived from the mode shapes of vibration of plates having two parallel edges simply supported and boundary conditions on the other two edges appropriate for the plate under consideration, was suggested by Dickinson and Li [28]. Even though these functions, which were called the "simply-supported plate functions", provided superior results for plates supported in some manner along all four edges, they did not yield satisfactory results when some of the plate edges were free. Laura [29] used "polynomial coordinate functions" to approximate the fundamental natural frequencies of systems, however, a basic limitation of this type of approximation is the difficulty in evaluating the higher frequencies. Goldfracht and Rosenhouse [30] used a bipolynomial series to approximate the deflection shapes of plates and obtained the natural frequencies and mode shapes of fixed plates with partial rotational flexibility of the edges employing Galerkin's method. They provided explicit algebraic expressions for the first nine modes. The deflection shapes defined by the bipolynomial series and are not orthogonal to each other and hence the resulting expressions become quite cumbersome. Bhat [31] proposed a set of beam characteristic orthogonal polynomials that can be used as plate deflection functions to obtain the natural frequencies and mode shapes of rectangular plates in Rayleigh-Ritz method. The orthogonal polynomials for the beam were constructed using Gram-Schmidt process [32], the first member of the set satisfying both the geometrical and natural boundary conditions of the beam and all the rest satisfying the geometrical boundary conditions.

Finite element method was used by Putter and Manor [33] to solve for the natural frequencies in flexural vibrations for a rotating beam with tip mass. Hoa [34] also utilized the finite element technique to study the effect of setting angle and hub radii on a rotating beam with tip mass. Dokainish and Ratwani [35] using this technique determined the natural frequencies and the mode shapes of a cantilever plate mounted on the periphery of a rotating disc. From the results of computations carried out for various values of the aspect-ratio, hub radii and setting angles, they derived empirical formulae giving the effect of these parameters on the natural frequencies. Henry and Lalanne [36] derived the total potential energy of a thin rotating plate. They minimized this energy by using the finite element method and obtained the natural frequencies and mode shapes by a simultaneous iterative technique.

In summary, from a review of the existing literature, it is found that although the problem of rotating structures has been investigated, there is still a lot of scope for further research. In this investigation various new techniques are proposed to analyze such structures giving superior results as compared to the above mentioned. The details are discussed in the next section.

1.3 Scope of the Present Investigation

The objective of the present work is to analyze a class of rotating structures by using improved methods in calculating their natural frequencies and mode shapes. These structures depending on their aspect ratios are idealized either as beams or plates.

In the present study, Chapter 2 deals with such a rotating type structure being modelled as a rotating beam. An improved strain-energy formulation in Rayleigh-Ritz method is carried out and the natural frequencies along with the mode shapes are obtained for different rotational speeds and various parametric combinations. The setting angle of the blade with respect to the plane of rotation and radius of the hub on which the structure is mounted are also taken into account in the formulation. The results are compared with the conventional Rayleigh-Ritz method and with those obtained using other methods.

In Chapter 3, a general purpose finite element package 'SPAR' is utilized to model this rotating beam type structure. The natural frequencies are obtained for different parametric combinations and compared.

The fourth Chapter deals with the rotating type structure being modelled as a plate. A class of beam characteristic orthogonal polynomials, constructed using Gram-Schmidt process, are employed as deflection functions for plates. Rayleigh-Ritz method is used to obtain their natural frequencies and mode shapes. Experimental results for a plate with all edges free, verifying the analtyical formulation, are also presented in this Chapter.

Finally, conclusions and recommendations for future work are presented in the fifth Chapter.

CHAPTER 2

DYNAMIC ANALYSIS OF A ROTATING BEAM TYPE STRUCTURE USING IMPROVED STRAIN ENERGY IN RAYLEIGH RITZ METHOD

CHAPTER 2

DYNAMIC ANALYSIS OF A ROTATING BEAM TYPE STRUCTURE USING IMPROVED STRAIN ENERGY IN RAYLEIGH RITZ METHOD

Dynamic behavior of rotating beam is of interest since it is possible to develop such a model for several engineering structures. Some examples are steam and gas turbines. Centrifugal forces are set up in these structures due to their rotation, which cause in-plane strains, resulting in the stiffening of the structure. In addition, Coriolis effects are also present which modify the structural characteristics. Due to the change in structural characteristics with the speed of rotation, the natural frequencies of the structure will change and it is imperative that the speed of operation be away from the natural frequencies for satisfactory operation.

In this chapter, the dynamics of a rotating beam type structure is studied using conventional Rayleigh-Ritz method with an improved strain-energy formulation. The setting angle of the beam with respect to the plane of rotation and radius of the hub on which the structure is mounted are also taken into account in the formulation. The variation of natural frequencies and mode shapes with the speed of rotation are plotted for several parameter combinations such as setting angle, hub radius, etc.

2.1 Rayleigh-Ritz Method

The Rayleigh-Ritz method is widely used to obtain approximate values for the natural frequencies and mode shapes of structures. The method provides upper bound values for the system natural frequencies.

In this method, a deflection shape of the form,

$$y = \sum_{n=1}^{N} C_n \phi_n(x) \tag{2.1}$$

is chosen where $\phi_n(x)$ are any admissible functions satisfying atleast the geometrical boundary conditions and C_1, C_2, ... C_n are constant coefficients. The parameters C_n's and $\phi_n(x)$ form a generating set. In limiting the generating set to a finite number of functions, the analysis can be interpreted as approximating a continuous system as a n-degree of freedom discrete system. The coefficients are adjusted by minimizing the frequency with respect to each of the coefficients, which results in n algebraic equations in the n unknown coefficients, C_n, involving p^2. The ~~solution~~ of these equations then gives the natural frequencies and mode shapes of the system.

For a conservative system, the maximum kinetic energy is equal to the maximum strain energy. By using this property, an expression for the natural frequency is obtained in terms of the undetermined coefficients C_n as,

$$p^2 = U_{max}/T^*_{max} \tag{2.2}$$

where T^*_{max} is the expression for kinetic energy without the term p^2, the square of the frequency of vibration. Minimizing p by differentiating it with respect to each of the coefficients, C_n

$$\frac{dp^2}{dC_n} = 0 \tag{2.3}$$

results in the equation

$$\frac{dU_{max}}{dC_n} - p^2 \frac{dT^*_{max}}{dC_n} = 0 \tag{2.4}$$

This is a standard eigen-value problem and the solution yields the natural frequencies and the corresponding coefficients C_n can be used in equation (2.1) to obtain the approximate mode shapes.

2.2 Analysis

The cantilever beam considered is mounted on the periphery of a rotating disc as shown in Fig. 2.1. The xyz coordinate axis system is chosen such that x and y axes are in the plane of beam cross-section and are the principal centroidal axes of inertia in that plane. The z-axis is along the beam. XYZ is another set of orthogonal axis system where Z axis is along the beam and XZ plane contains the plane of disc rotation. Origin of both xyz and XYZ coordinate systems are at the root of the beam where it is fixed to the disc. The angle θ between the Y and x axes is the setting angle.

Strain Energy

Let M be the bending moment and β be the slope of the elastic curve, the strain energy stored in an infinitesimal beam element is given by [37] as,

$$dU = \frac{1}{2} M \, d\beta \tag{2.5}$$

Assuming small deflections from Fig. 2.2

$$\beta = \frac{dy}{dz} \; ; \; \frac{1}{R_1} = \frac{d\beta}{dz} = \frac{d^2y}{dz^2} \tag{2.6}$$

From the theory of simple bending of beams, the flexure equation

$$\frac{1}{R_1} = \frac{M}{EI_X} \tag{2.7}$$

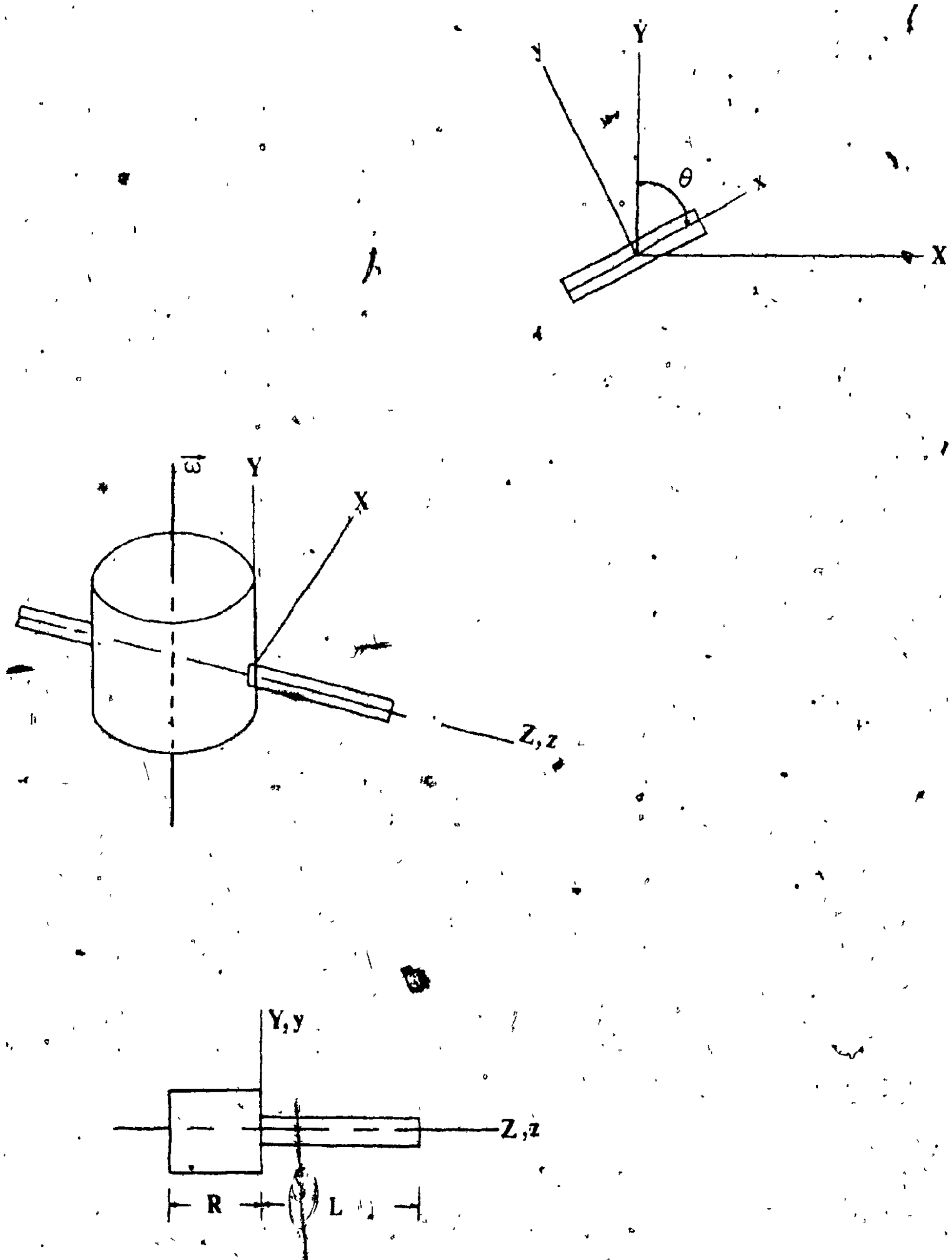

Fig. 2.1: Rotating Cantilever Beam

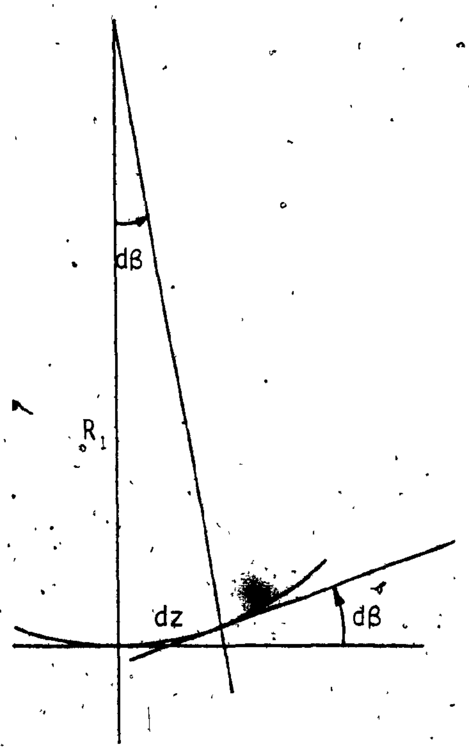

Fig. 2.2: Geometric Parameters Considered for Deflection

is used where R_1 is the radius of curvature.

Substituting for $d\beta$ and $\frac{1}{R_1}$, the strain energy U may be written as,

$$U_{max} = \frac{1}{2}\int \frac{M^2}{EI_x}dz = \frac{1}{2}\int EI_x\left(\frac{d^2y}{dz^2}\right)^2 dz \tag{2.8}$$

where the integration is carried out along the length of the beam.

Let $\tilde{z} = \frac{z}{L}$ be the non-dimensional axial length. Substituting this in (2.8) and integrating along the length of the beam, the expression for strain energy is,

$$U_{max} = \frac{1}{2L^3}\int_0^1 EI_x\left(\frac{d^2y}{d\tilde{z}^2}\right) d\tilde{z} \tag{2.9}$$

Kinetic Energy

The total kinetic energy of the system is the sum of the kinetic energy due to the flexural motion of the beam T_f, and that due to rotation, T_r.

a) Flexural Kinetic Energy

The kinetic energy of the blade in flexural vibration can be considered to be made up of two parts. They are the translational kinetic energy, T_b, and that due to rotating inertia, T_t.

For an element dz, the instantaneous kinetic energy dT_b of the mass concentrated at the centroid is given by

$$dT_b = \frac{1}{2} m \dot{y}^2 dz \tag{2.10}$$

where $m = \rho A$.

Hence, the total instantaneous kinetic energy T_b is,

$$T_b = \frac{1}{2} m \int_0^L \dot{y}^2 \, dz \tag{2.11}$$

The instantaneous kinetic energy dT_t, due to rotation about the centroid is,

$$dT_t = \frac{\rho I_x \, dz (\dot{y}')^2}{2} \tag{2.12}$$

Therefore, the total instantaneous kinetic energy T_t, thus becomes

$$T_t = \frac{1}{2} \int_0^L \rho \, I_x \, (\dot{y}')^2 \, dz \tag{2.13}$$

The combined kinetic energy T_f, is the sum of equations (2.11) and (2.13) and can be written as,

$$T_f = \frac{1}{2} \int_0^L [\rho A \dot{y}^2 + \rho I_x (\dot{y}')^2] \, dz \tag{2.14}$$

b) Kinetic Energy due to Rotation

Figure 2.3 shows the blade mounted on the periphery of the rotating disc. For a short element dz, each view shows both the rest position A and the deflected position B, displacements occuring in both the $\eta_1 z$ plane (Fig. 2.3(a)) and $\xi_1 z$ plane (Fig. 2.3(b)).

When the blade deflects in the $\xi_1 z$ plane, Fig. 2.3(b), the line of action of the centrifugal force, dF, on the element dz remains parallel to the z axes. Hence the force component dF_ξ in the ξ_1 direction is zero and the kinetic energy dT_ξ stored by the element is also zero. Thus,

$$dT_\xi = 0 \tag{2.15}$$

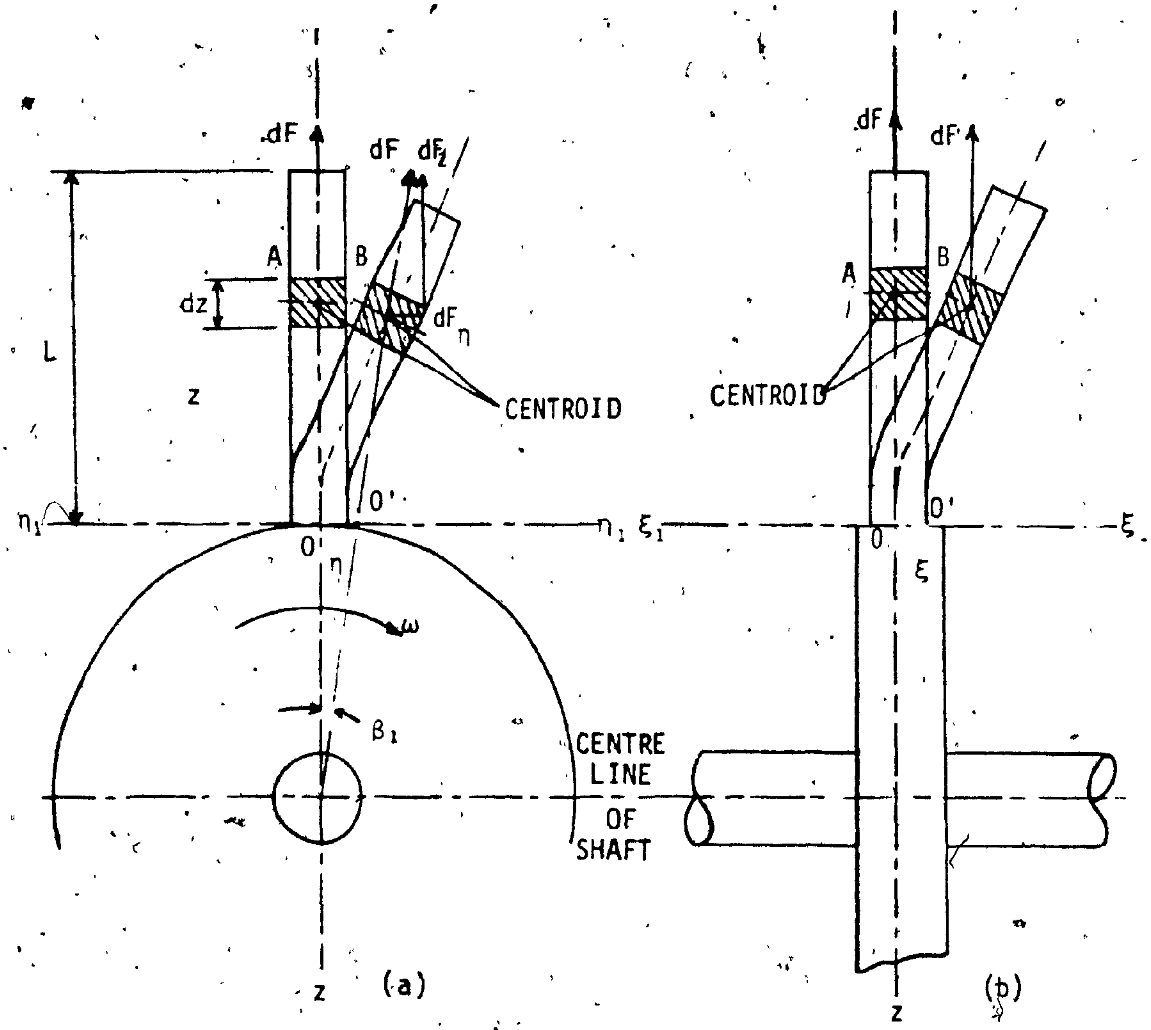

Fig. 2.3: Beam-Hub Radii Assembly

With the element dz in the deflected position B, Fig. 2.3(a), the force dF can be resolved into two components dF_η and dF_z, in the circumferential and radial directions η_1 and z respectively.

The circumferential component dF_η of the centrifugal force dF is given by,

$$dF_\eta = dF \sin \beta_1 \tag{2.16}$$

where $dF = m\omega^2(R+z)\,dz$ (2.17)

and $\sin \beta_1 = \dfrac{\eta_1}{R+z}$ (2.18)

In the above equations, R is the disc radius, ω is the angular velocity of rotation of disc and m is mass of blade per unit length.

Substitution of equations (2.17) and (2.18) into (2.16) gives,

$$dF_\eta = m\omega^2\eta_1\,dz \tag{2.19}$$

Since the η_1 component of the centrifugal force, dF_η, increases linearly from zero at the next position A, regarded as datum, to a value given by equation (2.19) at B, the average force during a displacement η_1 is thus, $dF_\eta/2$. With the force and motion in the same direction, the corresponding gain of the kinetic energy dT is given by,

$$dT_\eta = \frac{dF_\eta\,\eta}{2} = \frac{m\omega^2\eta_1^2 dz}{2} \tag{2.20}$$

and for the entire blade $T_\eta = \displaystyle\int_0^L \frac{\omega^2\eta_1^2 dz}{2}$ (2.21)

The centrifugal force dF acting on the element in the undeflected position A is given by (2.17). In the deflected position B the force component dF_z in the z direction is

$$dF_z = dF \cos\beta_1 \tag{2.22}$$

For small displacements, $\cos\beta_1$ approaches unity; the force component in the z direction can, thus, be regarded as constant and given by equation (2.17).

The z component of kinetic energy dT_z stored by the element can be written as,

$$dT_z = -dF_z\Delta = -dF\Delta \tag{2.23}$$

where Δ is the total displacement of the element dz in moving from rest position A to the deflected position B.

To determine Δ from Fig. 2.4 ,

$$dz^2 = d\delta^2 + (dz - d\Delta)^2 \tag{2.24}$$

where $d\delta = [d\xi_1^2 + d\eta_1^2]^{\frac{1}{2}}$ (2.25)

represents the increase of total transverse displacement δ.

From (2.24), $d\Delta = \frac{1}{2}\left(\frac{d\delta}{\partial z}\right) dz$ (2.26)

Combining (2.25) and (2.26)

$$d\Delta = \frac{1}{2}\left\{\left(\frac{\partial\xi_1}{\partial z}\right)^2 + \left(\frac{\partial\eta_1}{\partial z}\right)\right\} dz \tag{2.27}$$

and the total displacement Δ, of the element at z is, thus, given by

$$\Delta = \frac{1}{2}\int_0^z \left\{\left(\frac{\partial\xi_1}{\partial z}\right)^2 + \left(\frac{\partial\eta_1}{\partial z}\right)^2\right\} dz \tag{2.28}$$

For small displacements, and making use of equations (2.17) and (2.28),

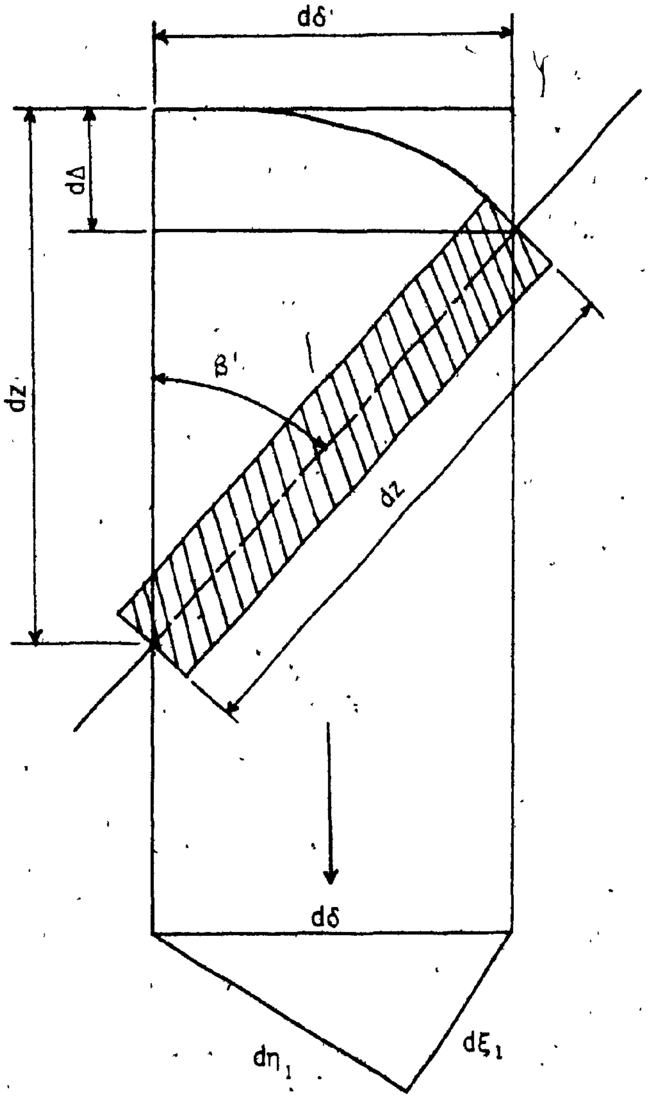

Fig. 2.4: Beam Element Before and After Deflection Showing the Relative Displacement dΔ of the Ends.

equation (2.23) can be written as

$$dT_z = -m\omega^2(R+z)dz \int_0^z \left\{\left(\frac{\partial\xi_1}{\partial z}\right)^2 + \left(\frac{\partial\eta_1}{\partial z}\right)^2\right\} dz \qquad (2.29)$$

Thus, for the entire blade the kinetic energy T_z, becomes

$$T_z = -\frac{\omega^2}{2}\int_0^L \left[m\ (R+z)\int_0^z \left\{\left(\frac{\partial\xi_1}{\partial z}\right)^2 + \left(\frac{\partial\eta_1}{\partial z}\right)^2\right\} dz\right] dz \qquad (2.30)$$

The total kinetic energy due to centrifugal effects,

$$T_R = T_\xi + T_\eta + T_z \qquad (2.31)$$

$$\text{i.e.}\quad T_R = -\frac{\omega^2}{2}\int_0^L \left[m(R+z)\int_0^z \left\{\left(\frac{\partial\xi_1}{\partial z}\right)^2 + \left(\frac{\partial\eta_1}{\partial z}\right)^2\right\} dz + m\eta_1^2\right] dz \qquad (2.32)$$

The above equation can be written as,

$$T_R = -\frac{\omega^2}{2}\int_0^L \left[\left\{\left(\frac{\partial\xi_1}{\partial z}\right)^2 + \left(\frac{\partial\eta_1}{\partial z}\right)^2\right\}\int_z^L \left[m(R+z)\right] dz + m\eta_1^2\right] dz \qquad (2.33)$$

Now, using the relationships,

$$\eta_1 = y\cos\theta - x\sin\theta \qquad (2.34)$$

$$\xi_1 = y\sin\theta + x\cos\theta \qquad (2.35)$$

equation (2.33), can be written as

$$T_R = \frac{\rho A\omega^2}{2}\int_0^L \Big\{(x^2\sin^2\theta - 2xy\sin\theta\cos\theta + y^2\cos^2\theta) -$$

$$\left[\left(\frac{\partial x}{\partial z}\right)^2 + \left(\frac{\partial y}{\partial z}\right)^2\right]\Big\} dz \int_z^L (R+z)\ dz\Big] \qquad (2.36)$$

Neglecting coupling of x and y deflections and ignoring higher order terms,

$$T_R = \frac{\rho A\omega^2}{2}\left[\int_0^L y^2\cos^2\theta\, dz - \int_0^L \left(\frac{\partial y}{\partial z}\right)^2 \left(RL + \frac{L^2}{2} - Rz - \frac{z^2}{2}\right) dz\right] \qquad (2.37)$$

The total kinetic energy of the system in terms of the non-dimensional parameter $\tilde{z}$ is,

$$T_{TOTAL} = T_f + T_r \qquad (2.38)$$

i.e. $$T_{TOTAL} = \frac{L}{2}\int_0^1 \rho A(\dot{y})^2 d\tilde{z} + \frac{1}{2L}\int_0^1 \rho I_x (\dot{y}')^2 d\tilde{z}$$

$$+ \frac{\rho A\omega^2}{2}\left[L\int_0^1 y^2\cos^2\theta d\tilde{z} - \frac{1}{L}\int (y')^2\left(RL + \frac{L^2}{2} - RL\tilde{z} - \frac{L^2\tilde{z}^2}{2}\right) d\tilde{z}\right] \qquad (2.39)$$

where a dot represents differentiation with respect to time and ( )' indicates differentiation with respect to $\tilde{z}$.

The equations of motion can be derived directly from the energy expressions by using the Lagrangian

$$L = T - U \qquad (2.40)$$

Assuming harmonic motion,

$$y = Y \exp(jpt) \qquad (2.41)$$

the time averaged value of the Lagrangian is obtained as

$$\bar{L} = \int_0^{2\Pi/p} L dt \qquad (2.42)$$

Incorporating the following dimensionless parameters

$$\left.\begin{aligned}
\tilde{R} &= R/L \\
\tilde{r}^2 &= I_x/AL^2 \\
\alpha^2 &= \lambda\omega^2 \\
\lambda &= \frac{\rho AL^4}{EI_x} \\
\eta^2 &= \lambda p^2
\end{aligned}\right\} \qquad (2.43)$$

the time averaged value of the Lagrangian can be written as

$$\bar{L} = \frac{\Pi EI_x}{2pL^3} \int_0^1 \Big[\eta^2 Y^2 + \eta^2 \tilde{r}^2 (Y')^2 + \alpha^2 Y^2 \cos^2\theta - \alpha^2 Y'^2 \Big\{ R(1-\tilde{z}) + \frac{1}{2}(1-\tilde{z}^2) - (Y'')^2 \Big\} \Big] d\tilde{z} \qquad (2.44)$$

To apply the Rayleigh-Ritz method, the shape function is assumed as a polynomial

$$Y = \sum_{n=2}^{N} C_n \tilde{z}^n \qquad (2.45)$$

where C_n are arbitrary coefficients which are to be determined. Substituting from equation (2.45), and applying the Ritz process, the following homogenous simultaneous equations are obtained,

$$\frac{\partial \bar{L}}{\partial C_n} = 0, \qquad i = 2,3,\ldots N \qquad (2.46)$$

$$\left[n^2 \sum_{K=2}^{N} \frac{C_K}{(n+K+1)} + \tilde{r}^2 \sum_{K=2}^{N} \frac{njC_K}{(n+K-1)} \right]$$

$$- \left[-\alpha^2 \cos^2\theta \sum_{K=2}^{N} \frac{C_K}{(n+K+1)} + \alpha^2 \int_0^1 \left\{ \tilde{R}\,(1-\tilde{z}) + \frac{1}{2}(1-\tilde{z}^2) \right\} \sum_{K=2}^{N} \frac{nKC_K}{(n+K-1)} \right.$$

$$\left. + \sum_{K=2}^{N} \frac{nK(n-1)(K-1)C_K}{(n+K-3)} \right] = 0 \qquad (2.47)$$

Equation (2.47) is in the form of a standard eigen-value problem.

$$\eta^2[A] - [B] = 0 \qquad (2.48)$$

and eigenvalues and eigenmodes are obtained by solving this equation. A computer algorithm developed to solve equation (2.48) is given in Appendix A.

2.3 Improved Strain Formulation in Rayleigh-Ritz Method

In the proposed method, a deflection shape of the form given in equation (2.45) is assumed

$$\text{i.e.} \quad Y = \sum_{n=2}^{N} C_n \tilde{z}^n \qquad (2.49)$$

This shape function as before satisfies the geometrical boundary conditions at the fixed end of the beam i.e. the deflection and slope at $\tilde{z} = 0$ are zero.

Instead of differentiating the deflection shape to be used in equations (2.8), (2.9), to obtain the strain energy, the deflection shape is used to obtain the distributed force over the beam, in the form,

$$q(\tilde{z}) = -mp^2 \sum_{n=2}^{N} C_n \tilde{z}^n \tag{2.50}$$

Integrating this distributed force to obtain the shear force at any sec-tion as [38].

$$Q(z) = \int_z^L q(z)\, dz \tag{2.51}$$

i.e. $$Q(\tilde{z}) = mp^2 L \sum_{n=2}^{N} \frac{C_n}{(n+1)} \left[\tilde{z}^{n+1} - 1\right] \tag{2.52}$$

Integrating the shear force once again gives the moment at any section as,

$$M(\tilde{z}) = L^2 mp^2 \sum_{n=2}^{N} \frac{C_n}{(n+1)} \left[\frac{1}{(n+2)} - \frac{\tilde{z}^{n+2}}{(n+2)} - 1 + \tilde{z}\right] \tag{2.53}$$

The strain energy of the beam is given by equations (2.8), (2.9) as,

$$U = \frac{1}{2EI_x} \int_0^1 M^2(\tilde{z})\, d\tilde{z} \tag{2.54}$$

To obtain the kinetic energy using equation (2.39) and assuming harmonic motion

$$y = Y \cos pt \tag{2.55}$$

$$T_{TOTAL} = \frac{L}{2} \int_0^1 \rho A Y^2 p^2\, d\tilde{z} + \frac{1}{2L} \int_0^1 \rho I_x p^2 (Y')^2\, d\tilde{z}$$

$$+ \frac{\rho A \omega^2}{2} \left[L \int_0^1 Y^2 \cos^2\theta\, d\tilde{z} - \frac{1}{L} \int_0^1 (Y')^2 \left(RL + \frac{L^2}{2} - RL\tilde{z} - \frac{L^2 \tilde{z}^2}{2}\right) d\tilde{z}\right] \tag{2.56}$$

where as before ( )', indicates differentiation with respect to $\tilde{z}$.

To obtain the slope $(y^*)'$ and deflection (y^*) to be used in the above equation, the moment distribution, (2.53), is integrated twice,

$$\text{i.e.}\quad (y^*)' = \frac{L}{EI_x}\int_0^{\tilde{z}} M(z)\,dz$$

$$= -\frac{L^3}{EI_x}mp^2\sum_{n=2}^{N}\frac{C_n}{(n+1)}\left[\frac{\tilde{z}}{(n+2)} - \frac{\tilde{z}^{n+3}}{(n+2)(n+3)} - \tilde{z} + \frac{\tilde{z}^2}{2}\right] + \text{Constant} \qquad (2.57)$$

at $\tilde{z} = 0$, $(y^*)' = 0$, therefore Constant = 0.

Integrating (2.57) again to obtain the deflection,

$$y^* = -\frac{L^4}{EI_x}mp^2\sum_{n=2}^{N}\frac{C_n}{(n+1)}\left[\frac{\tilde{z}^2}{2(n+2)} - \frac{\tilde{z}^{n+4}}{(n+2)(n+3)(n+4)} - \frac{\tilde{z}^2}{2} + \frac{\tilde{z}^3}{6}\right] + \text{Constant} \qquad (2.58)$$

at $\tilde{z} = 0$, $y^* = 0$, therefore Constant = 0.

Substituting equations (2.57), (2.58) in (2.56) gives,

$$T_{TOTAL} = \frac{L}{2}\int_0^1 \rho A Y^2 p^2 d\tilde{z} + \frac{1}{2L}\int_0^1 \rho I_x p^2 (Y')^2 d\tilde{z}$$

$$+ \frac{\rho A\omega^2 L}{2}\int_0^1\left[-\frac{L^2}{EI_x}\left\{L^2 mp^2\sum_{n=2}^{N}\frac{C_n}{(n+1)}\left(\frac{\tilde{z}^2}{2(n+2)} - \frac{\tilde{z}^{n+4}}{(n+2)(n+3)(n+4)}\right.\right.\right.$$

$$\left.\left.\left. - \frac{\tilde{z}^2}{2} + \frac{\tilde{z}^3}{6}\right)\right\}\right]^2 \cos^2\theta\, d\tilde{z} - \frac{\rho A\omega^2}{2L}\int_0^1\left[-L^4 mp^2\sum_{n=2}^{N}\frac{C_n}{(n+1)}\left(\frac{\tilde{z}}{(n+2)} - \right.\right.$$

$$\left.\left. \frac{\tilde{z}^{n+3}}{(n+2)(n+3)} - \tilde{z} + \frac{\tilde{z}^2}{z}\right)\right]^2\left(RL + \frac{L^2}{2} - RL\tilde{z} - L^2 + \frac{\tilde{z}^2}{z}\right) d\tilde{z} \qquad (2.59)$$

The Lagrangian is given by,

$$L = T - U \tag{2.60}$$

Applying the Ritz process, the following homogeneous equations are obtained,

$$\frac{\partial L}{\partial C_n} = 0 \qquad n = 2,3,\ldots N \tag{2.61}$$

Incorporating the dimensionless parameters given by equation (2.43), equation (2.61) can be written in the form of a standard eigenvalue problem as,

$$\eta^2 \, [A] - [B] = 0 \tag{2.62}$$

where the elements a_{nK} and b_{nK} of matrices [A] and [B] are given in Appendix B. The eigenvalues and eigenvectors are obtained by solving this equation.

A computer algorithm is developed to solve (2.62) for several parameter combinations of setting angle and hub radius and is given in Appendix C.

2.4 Discussion of the Results

Natural frequencies and mode shapes are obtained for a rotating cantilever beam at various rotational speeds for different values of setting angle and hub radius.

A convergence test was made by varying the number of terms considered in the polynomial shape functions. The results obtained using conventional Rayleigh-Ritz method with and without any improved strain energy formulation are shown in Tables 2.1-2.4. The variation of fundamental and second natural frequency for various values of Hub Radii and setting angle are presented in Tables 2.5-2.12.

Natural frequencies of the rotating beam for different rotational speeds and several parametical combinations are shown in Figs. 2.5 through 2.16.

Variation of natural frequency, η, with rotational speed, α, is shown in Figs. 2.5 and 2.6 for the first mode for various values of $\tilde{R}$ and setting angles. The increase in natural frequency is larger for higher setting angles and for any setting angle the increase is linear at higher rotational speeds.

The effect of hub radius $\tilde{R}$, on the natural frequencies of modes 1 to 5 are plotted against the rotational speed for setting angles of zero and 90° in Figs. 2.7 through 2.16. With higher value of, $\tilde{R}$, the natural frequencies are higher and increase faster with the rotational speed. The results are compared with those from Kumar [8], Wang et et [15] and Hoa [34] for the first mode and with conventional Rayleigh-Ritz method for higher modes.

The variation of the fundamental mode shape with the rotational speed is shown in Fig. 2.17. The mode shapes are normalized to a value of unity at the tip. It is observed that as the rotational speed α, increases, the beam tries to straighten itself more and more. The variation of the shape of second mode with rotational speed is shown in Fig. 2.18. The beam has a tendency to straighten itself as the rotational speed increases as in the case of fundamental mode.

In conclusion, natural frequencies and mode shapes of a rotating uniform cantilever beam are obtained using conventional Rayleigh-Ritz method with and without any improved strain energy formulation. A simple polynomial with arbitrary coefficients is used as shape function. When the arbitrary coefficients are determined, along with the natural frequencies, using Ritz method, the normal mode shapes are obtained as simple polynomials. Natural frequencies and mode shapes are obtained for different rotational speeds and for different parametric combinations such as setting angle, hub radius, etc.

In the following chapter, the dynamic analysis of the rotating beam is carried out using the finite element approach. SPAR, a finite element package, is used to model the beam taking into account the hub-radius and the setting angle.

TABLE 2.1: Convergence of Natural Frequency with Number of Terms Using Conventional Rayleigh-Ritz Method

Setting Angle	$\theta = 90°$
Angular Velocity	$\alpha = 0$
Hub Radius	$\tilde{R} = 0$
Non-Dimensional Parameter	$\tilde{r}^2 = 2.5 \times 10^{-5}$

Natural Frequency $\eta = p\sqrt{\lambda}$

No. of Terms	MODE 1	MODE 2	MODE 3	MODE 4	MODE 5
2	3.5325	34.7813			
3	3.5169	22.224	117.879		
4	3.5158	22.1437	63.2816	280.1555	
5	3.5158	22.0262	63.1768	128.2670	557.1312

TABLE 2.2: Convergence of Natural Frequency with Number of Terms Using Improved Strain Energy Formulation in Rayleigh-Ritz Method

Setting Angle	$\theta = 90°$				
Angular Velocity	$\alpha = 0$				
Hub Radius	$\tilde{R} = 0$				
Non-Dimensional Parameter	$\tilde{r}^2 = 2.5 \times 10^{-5}$				
Natural Frequency $\eta = p\sqrt{\lambda}$					
No. of Terms	MODE 1	MODE 2	MODE 3	MODE 4	MODE 5
2	3.5158	22.1004			
3	3.5158	22.0256	62.5269		
4	3.5158	22.0256	61.6434	124.228	
5	3.5158	22.0256	61.6389	120.4233	202.6457

TABLE 2.3: Convergence of Natural Frequency with Number of Terms Using Improved Strain Energy Formulation in Rayleigh-Ritz Method

Setting $\theta = 90°$					
Angular Velocity $\alpha = 5$					
Hub Radius $\tilde{R} = 0$					
Non-Dimensional Parameter $\tilde{r}^2 = 2.5 \times 10^{-5}$					
Natural Frequency $\eta = p\sqrt{\lambda}$					
No. of Terms	MODE 1	MODE 2	MODE 3	MODE 4	MODE 5
2	6.4607	25.5005			
3	6.4519	25.4433	65.8624		
4	6.4410	25.4387	65.1429	127.4728	
5	6.4494	25.4367	65.1423	124.0708	205.5518

TABLE 2.4: Convergence of Natural Frequency with Number of Terms Using Improved Strain Energy Formulation in Rayleigh-Ritz Method

Setting			θ = 90°		
Angular Velocity			α = 10		
Hub Radius			$\tilde{R}$ = 0		
Non-Dimensional Parameters			$\tilde{r}^2 = 2.5 \times 10^{-5}$		
Natural Frequency $\eta = p\sqrt{\lambda}$					
No. of Terms	MODE 1	MODE 2	MODE 3	MODE 4	MODE 5
2	11.2840	33.7397			
3	11.2284	33.7113	74.9903		
4	11.2111	33.6592	74.6069	136.7891	
5	11.2052	33.6382	74.6006	134.3606	213.9667

TABLE 2.5: Variation of Fundamental Natural Frequency for $\tilde{R} = 0$ and Various Values of Setting Angle using Improved Strain Energy Formulation in Rayleigh-Ritz Method

Angular Velocity	Natural Frequency ($\eta = p\sqrt{\lambda}$)			
α	$\tilde{R} = 0$			
	$\theta=0°$	$\theta=30°$	$\theta=60°$	$\theta=90°$
0	3.516	3.516	3.516	3.516
1	3.543	3.578	3.647	3.681
2	3.622	3.757	4.014	4.137
3	3.743	4.033	4.557	4.797
4	3.898	4.381	5.214	5.585
5	4.074	4.780	5.945	6.449
6	4.264	5.213	6.721	7.360
7	4.461	5.670	7.526	8.300
8	4.660	6.141	8.349	9.258
9	4.859	6.622	9.184	10.227
10	5.056	7.111	10.028	11.205

TABLE 2.6: Variation of Fundamental Natural Frequency for $\tilde{R}$ = 1 and Various Values of Setting Angle using Improved Strain Energy Formulation in Rayleigh-Ritz Method

Angular Velocity	Natural Frequency ($\eta = p\sqrt{\lambda}$)			
α	$\tilde{R}$ = 1			
	θ=0°	θ=30°	θ=60°	θ=90°
0	3.516	3.516	3.516	3.516
1	3.758	3.791	3.856	3.889
2	4.400	4.513	4.729	4.833
3	5.290	5.499	5.894	6.082
4	6.315	6.624	7.203	7.475
5	7.413	7.823	8.585	8.941
6	8.551	9.062	10.006	10.446
7	9.714	10.325	11.450	11.973
8	10.892	11.604	12.909	13.514
9	12.081	12.892	14.377	15.065
10	13.278	14.188	15.852	16.622

TABLE 2.7: Variation of Fundamental Natural Frequency for $\bar{R}$ = 5 and Various Values of Setting Angle using Improved Strain Energy Formulation in Rayleigh Ritz Method

Angular Velocity	Natural Frequency ($\eta = p\sqrt{\lambda}$)			
α	$\tilde{R}$ = 5			
	θ=0°	θ=30°	θ=60°	θ=90°
0	3.516	3.516	3.516	3.516
1	4.514	4.542	4.597	4.624
2	6.647	6.722	6.869	6.942
3	9.128	9.250	9.490	9.608
4	11.723	11.893	12.224	12.387
5	14.367	14.583	15.006	15.213
6	17.036	17.298	17.811	18.061
7	19.719	20.027	20.630	20.925
8	22.412	22.766	23.459	23.797
9	25.113	25.513	26.294	26.677
10	27.819	28.265	29.135	29.561

TABLE 2.8: Variation of Fundamental Natural Frequency for $\tilde{R}$ = 10 and Various Values of Setting Angle using Improved Strain Energy Formulation in Rayleigh Ritz Method

Angular Velocity	Natural Frequency ($\eta = p \cdot \bar{\lambda}$)			
α	$\tilde{R}$ = 10			
	θ=0°	θ=30°	θ=60°	θ=90°
0	3.516	3.516	3.516	3.516
1	5.308	5.318	5.378	5.402
2	8.657	8.715	8.829	8.885
3	12.318	12.409	12.589	12.678
4	16.066	16.189	16.435	16.556
5	19.849	20.006	20.0316	20.469
6	23.653	23.843	24.217	24.402
7	27.469	27.691	28.129	28.347
8	31.293	31.549	32.052	32.300
9	35.125	35,412	35.979	36.259
10	38.961	39.6280	39.912	40.223

TABLE 2.9: Variation of Second Natural Frequency for $\tilde{R}$ = 0 and Various Values of Setting Angle using Improved Strain Energy Formulation in Rayleigh Ritz Method

Angular Velocity	Natural Frequency ($\eta = p\sqrt{\lambda}$)			
α	$\tilde{R} = 0$			
	θ=0°	θ=30°	θ=60°	θ=90°
0	22.026	22.026	22.026	22.026
1	22.149	22.0155	22.166	22.170
2	22.517	22.539	22.583	22.605
3	23.117	23.165	23.262	23.311
4	23.932	24.015	24.181	24.264
5	24.941	25.066	25.313	25.436
6	26.120	26.292	26.632	26.800
7	27.448	27.670	28.108	28.326
8	28.902	29.178	29.720	29.988
9	30.465	30.795	31.446	31.766
10	32.118	32.505	33.264	33.630

TABLE 2.10: Variation of Second Natural Frequency for $\tilde{R}$ = 1 and Various Values of Setting Angle using Improved Strain Energy Formulation in Rayleigh-Ritz Method

Angular Velocity	Natural Frequency ($\eta = p\sqrt{\lambda}$)			
α	$\tilde{R}$ = 1			
	θ=0°	θ=30°	θ=60°	θ=90°
0	22.026	22.026	22.026	22.026
1	22.343	22.349	22.360	22.366
2	23.271	23.292	23.335	23.357
3	24.737	24.782	24.873	24.918
4	26.651	26.725	26.874	26.948
5	28.918	29.025	29.240	29.347
6	31.458	31.600	31.884	32.025
7	34.206	34.384	34.739	34.914
8	37.113	37.328	37.753	37.964
9	40.140	40.391	40.889	41.136
10	43.260	43.548	44.118	44.401

TABLE 2.11: Variation of Second Natural Frequency for $\tilde{R} = 5$ and Various Values of Setting Angle using Improved Strain Energy Formulation in Rayleigh-Ritz Method

Angular Velocity	Natural Frequency ($\eta = p\sqrt{\lambda}$)			
α	$\tilde{R} = 5$			
	θ=0°	θ=30°	θ=60°	θ=90°
0	22.026	22.026	22.026	22.026
1	23.103	23.108	23.119	23.124
2	26.058	26.077	26.116	26.134
3	30.320	30.357	30.432	30.468
4	35.396	35.446	35.559	35.615
5	40.945	41.021	41.173	41.249
6	46.797	46.893	47.084	47.180
7	52.839	52.955	53.186	53.301
8	59.010	59.146	59.415	59.549
9	65.272	65.427	65.735	65.888
10	71.600	71.774	72.121	72.293

TABLE 2.12: Variation of Second Natural Frequency for $\tilde{R} = 10$ and Various Values of Setting Angle using Improved Strain Energy Formulation in Rayleigh-Ritz Method

Angular Velocity	Natural Frequency ($\eta = p\sqrt{\lambda}$)			
α	$\tilde{R} = 10$			
	$\theta=0°$	$\theta=30°$	$\theta=60°$	$\theta=90°$
0	22.026	22.026	22.026	22.026
1	24.016	24.021	24.032	24.037
2	29.149	29.166	29.201	29.218
3	36.034	36.066	36.128	36.159
4	43.795	43.841	43.932	43.978
5	52.008	52.068	52.187	52.247
6	60.476	50.660	60.698	60.772
7	69.102	69.190	69.367	69.455
8	77.835	77.937	78.142	78.245
9	86.643	86.766	86.979	87.109
10	95.509	95.639	95.899	96.030

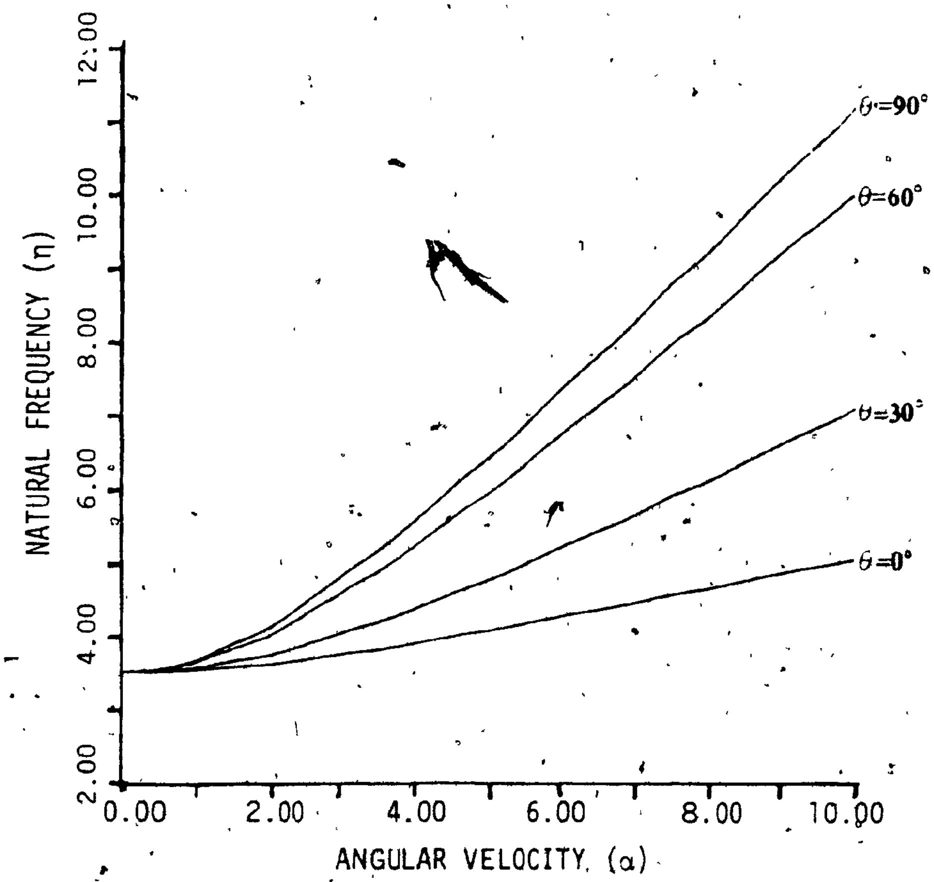

Fig. 2.5: Variation of First Natural Frequency with Speed for Different Setting Angles. ($\tilde{R} = 0$)

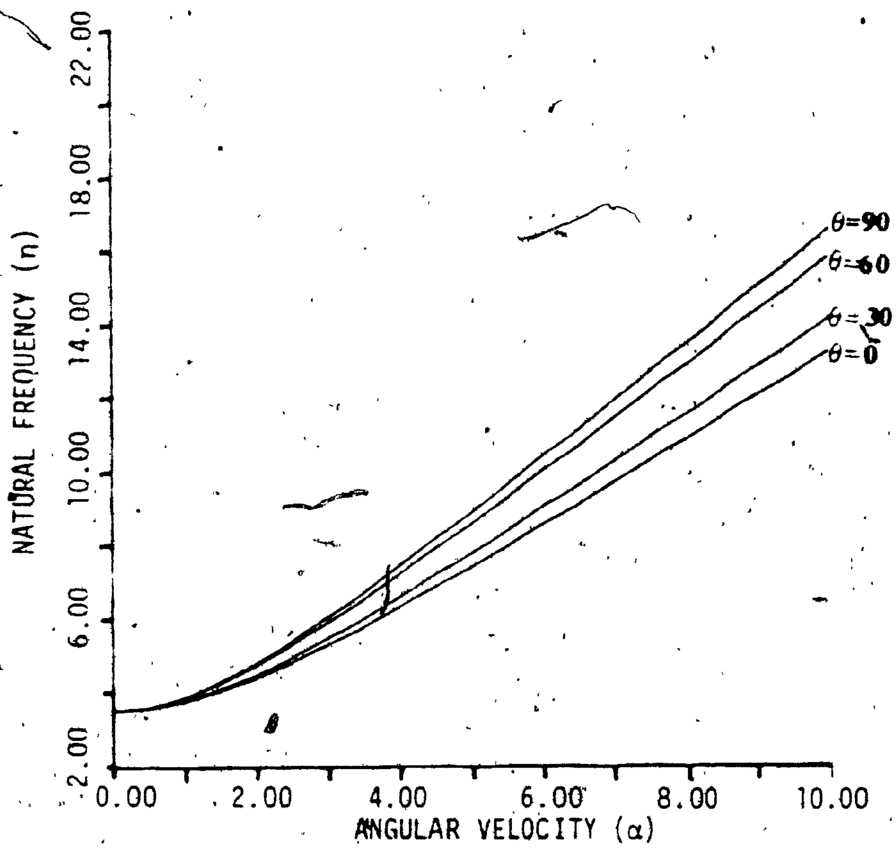

Fig. 2.6: Variation of First Natural Frequency with Speed for Different Setting Angles.

($\bar{R}$ = 1.0)

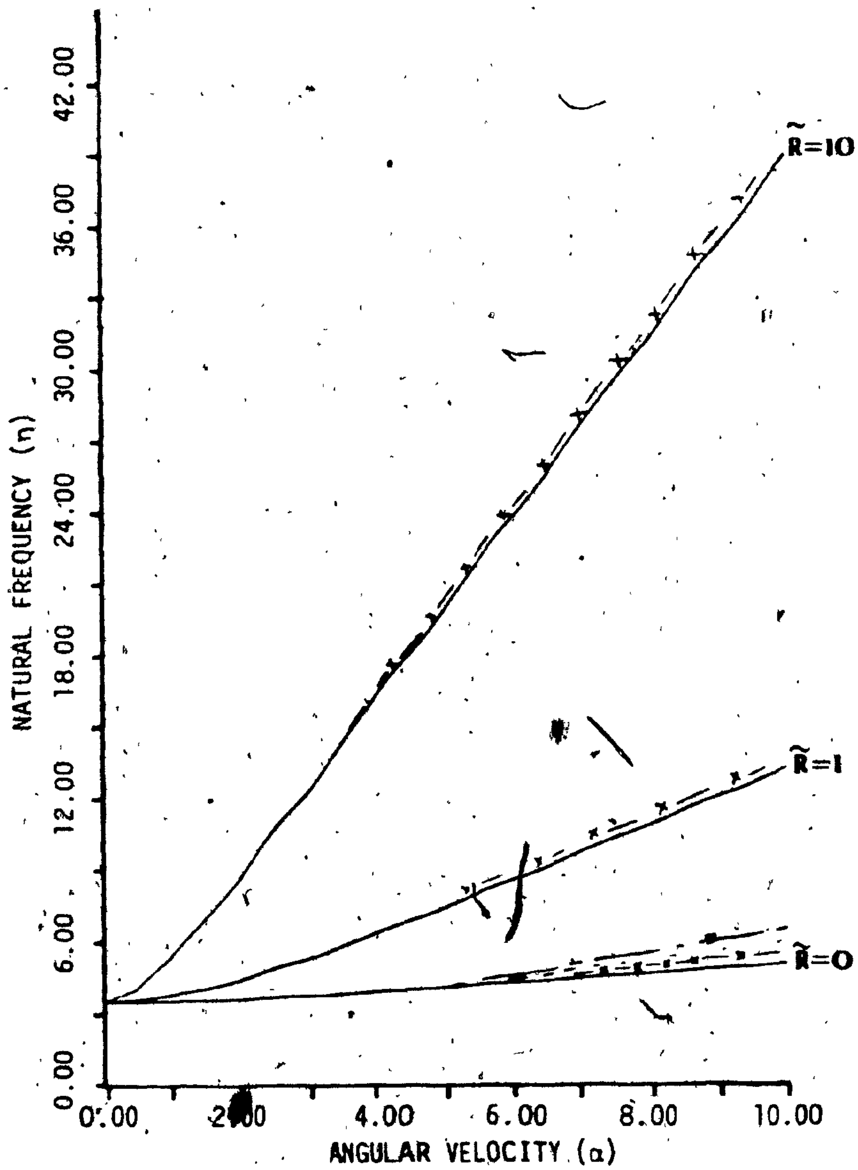

Fig. 2.7: Variation of First Natural Frequency with Speed for Different Hub-Radii

(-x-x-x- [8], ----[15], ----[34] θ = 0°)

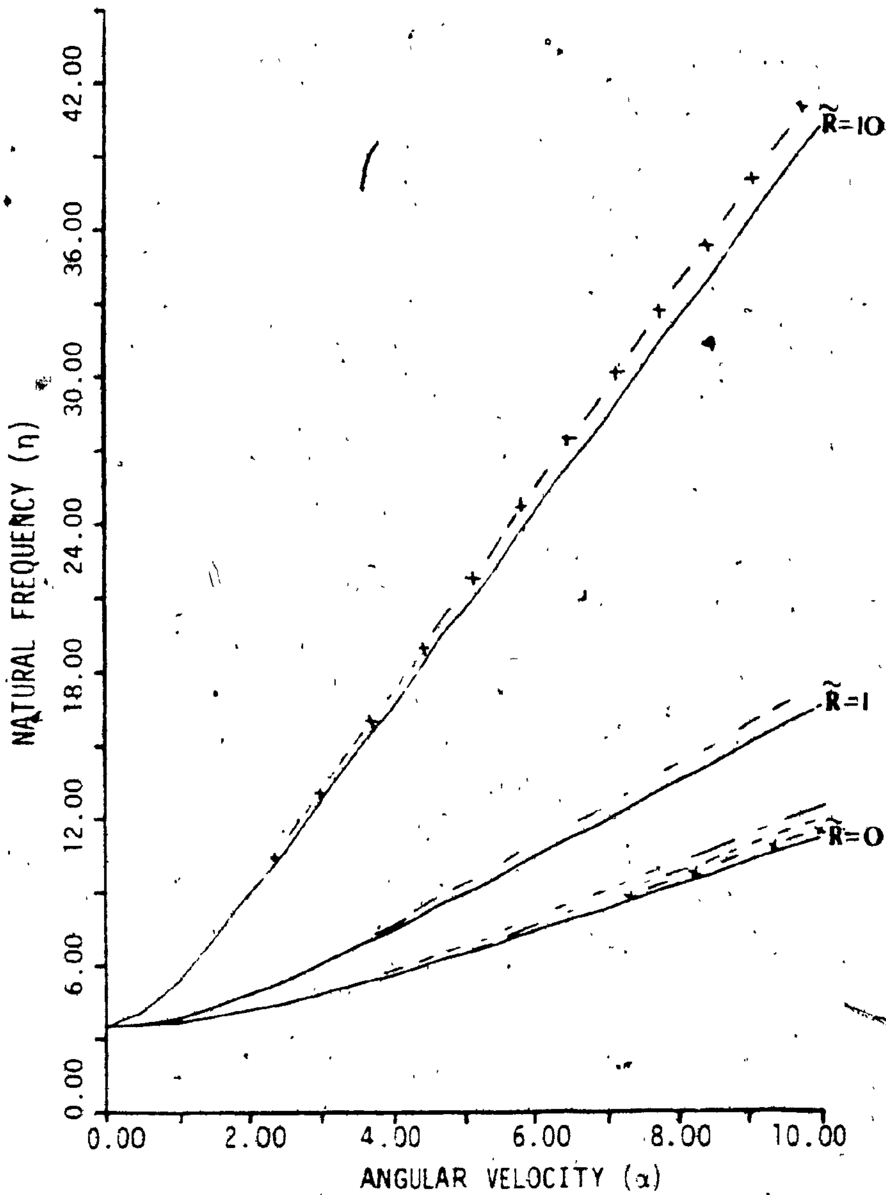

Fig. 2.8: Variation of First Natural Frequency with Speed for Different Hub-Radii

(-xx- [8], ----[15], ----[34], θ = 90°)

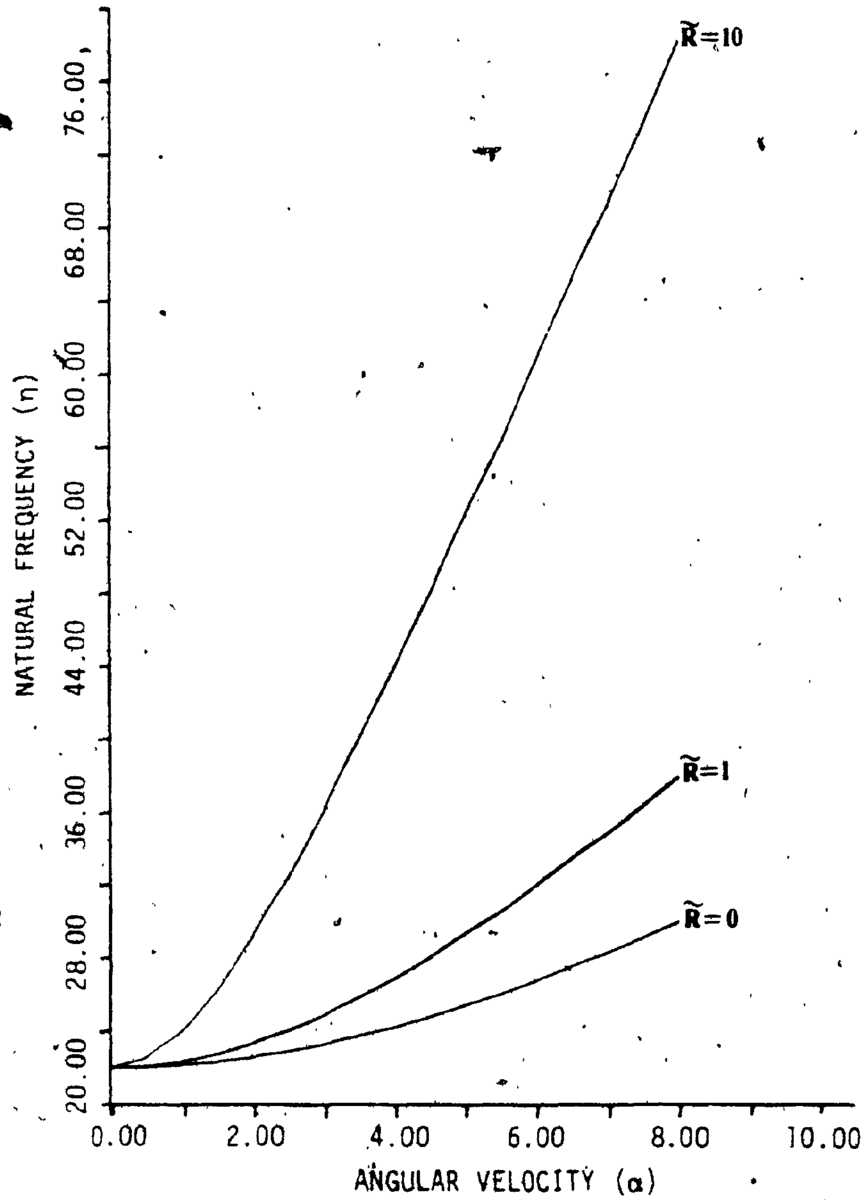

Fig. 2.9: Variation of Second Natural Frequency with Speed for Various Hub-Radii

($\theta = 0°$)

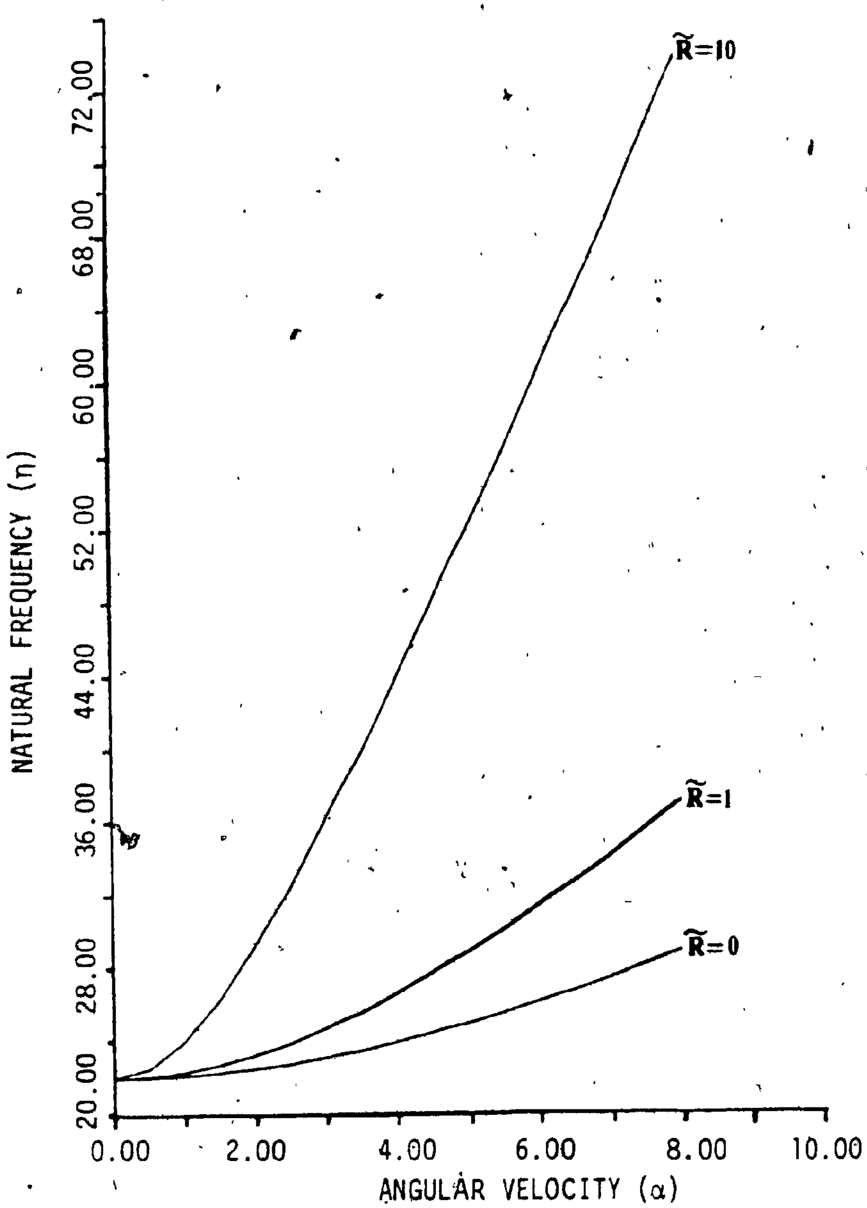

Fig. 2.10: Variation of Second Natural Frequency with Speed for Various Hub-Radii

(θ = 90°)

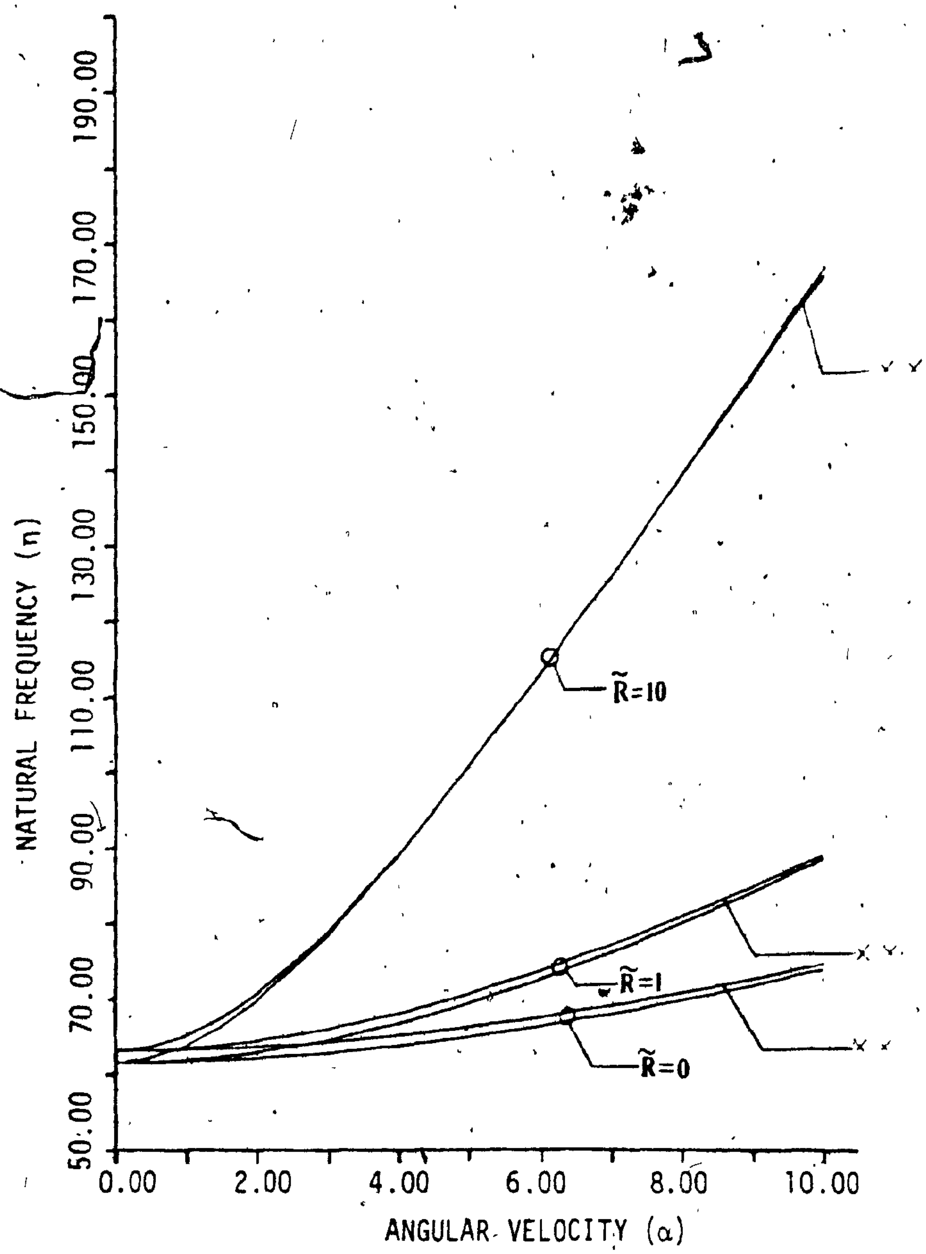

Fig. 2.11: Variation of Third Natural Frequency for Various Hub-Radii

(xx - Rayleigh Ritz Method, θ = 0°)

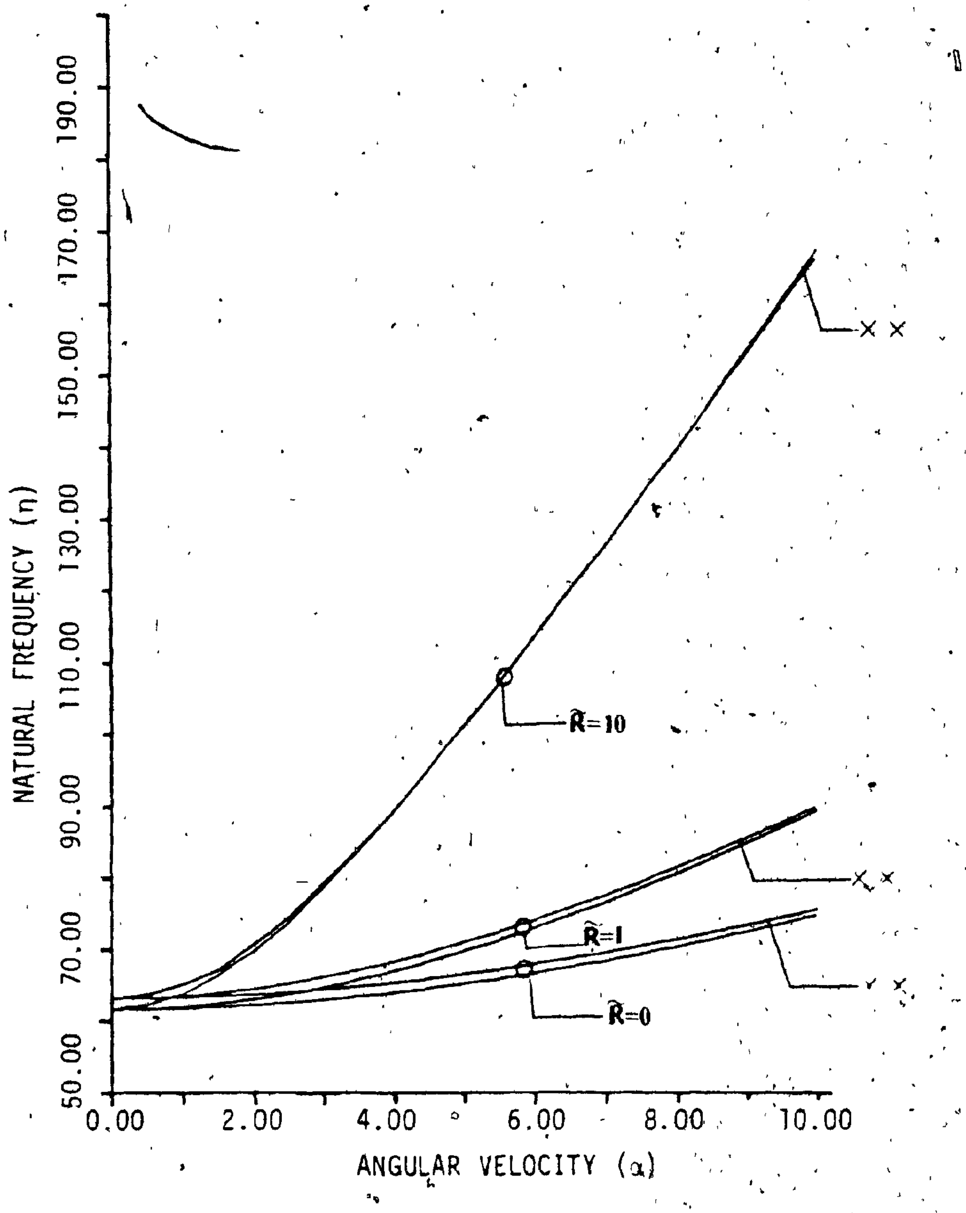

Fig. 2.12: Variation of Third Natural Frequency for Various Hub-Radii

(xx - Rayleigh Ritz Method, $\theta = 90°$)

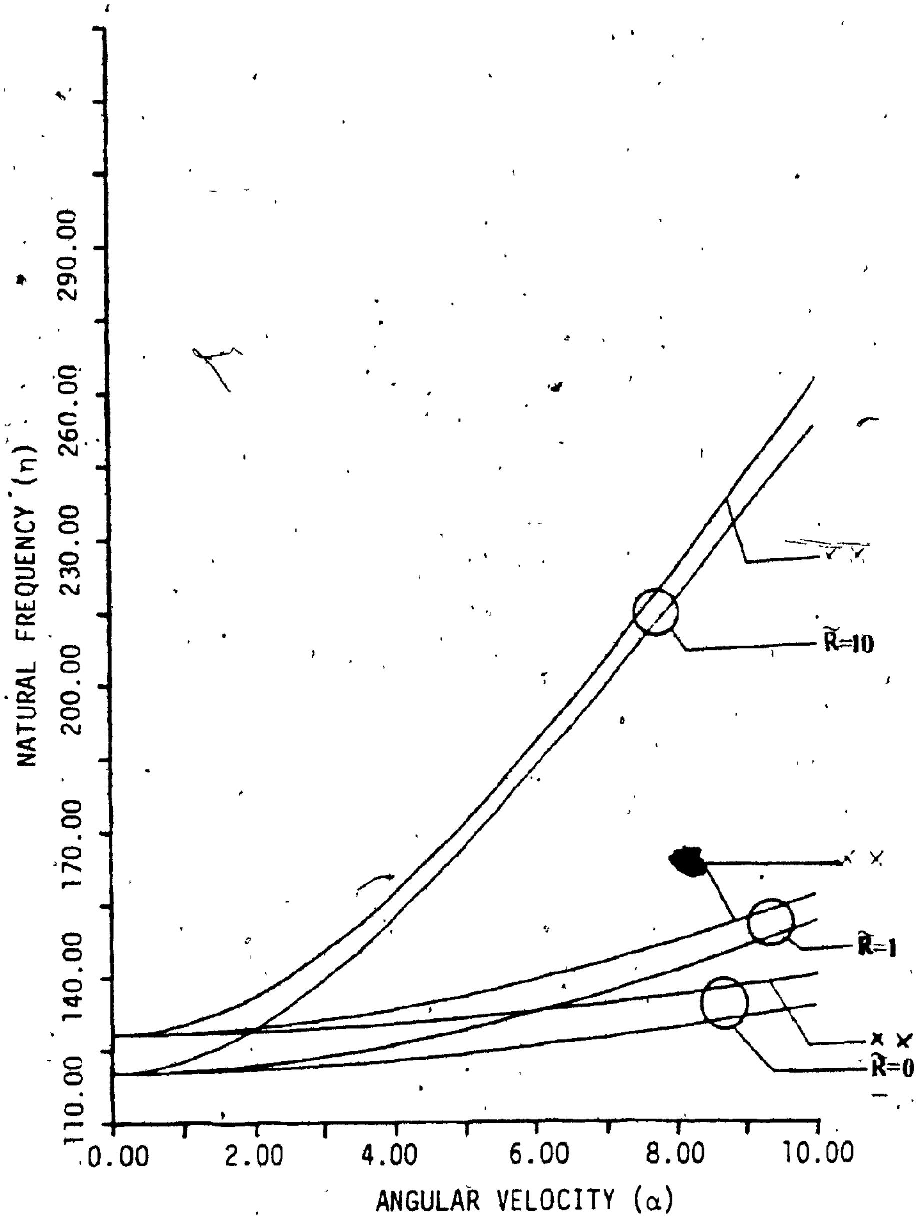

Fig. 2.13: Variation of Fourth Natural Frequency for Various Hub-Radii
(xx - Rayleigh-Ritz Method, θ = 0°)

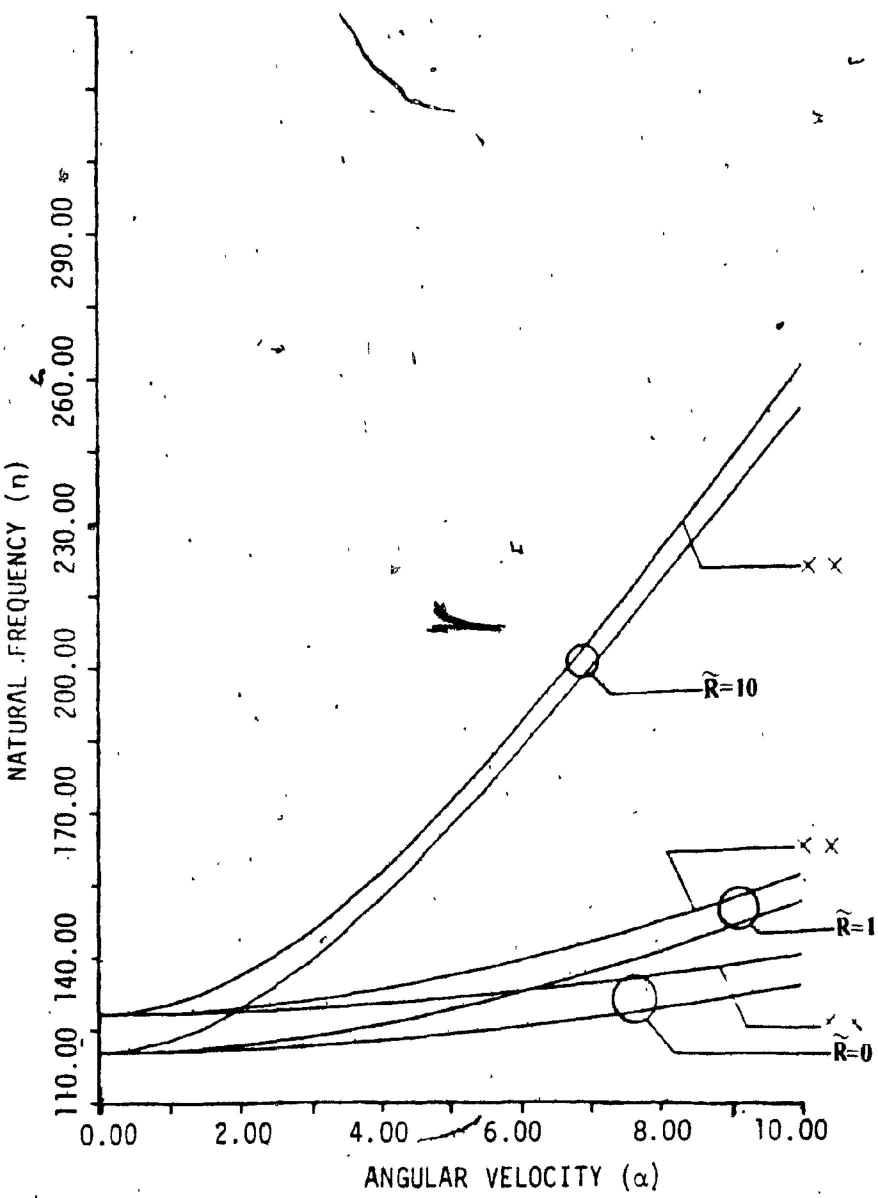

Fig. 2.14: Variation of Fourth Natural Frequency for Various Hub-Radii

(xx - Rayleigh Ritz Method, θ = 90°)

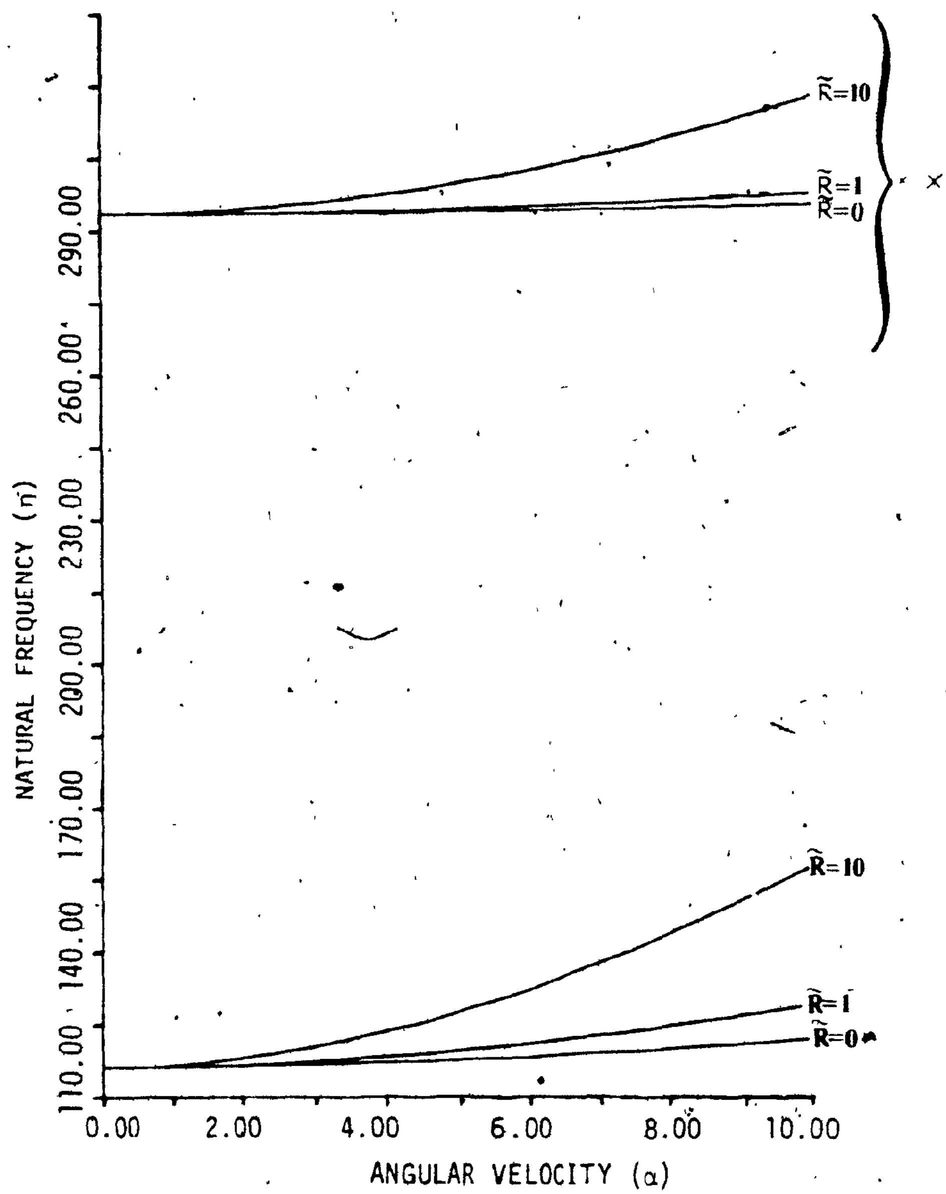

Fig. 2.15: Variation of Fifth Natural Frequency for Various Hub-Radii

(xx - Rayleigh Ritz-Method, $\theta = 0°$)

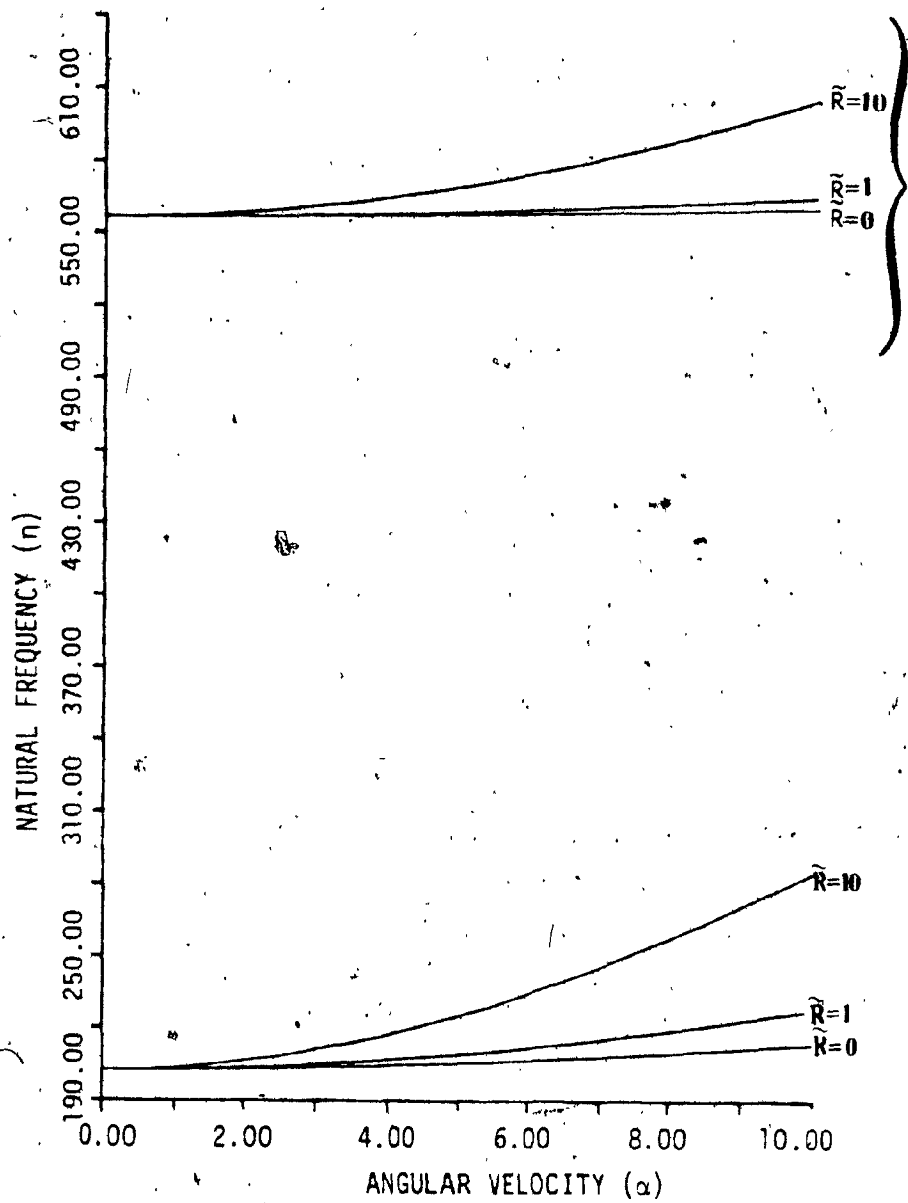

Fig. 2.16: Variation of Fifth Natural Frequency for Various Hub-Radii

(xx - Rayleigh-Ritz Method, θ = 90°)

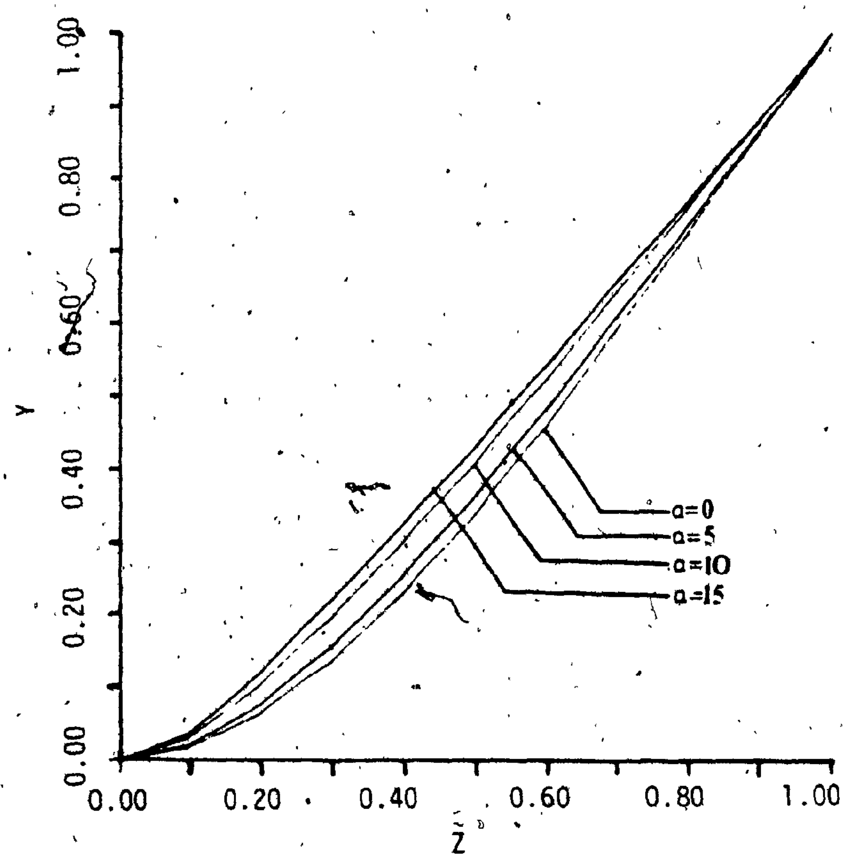

Fig. 2.17: Variation of First Mode Shape with Speed

($\tilde{R}$ = 0, θ = 90°)

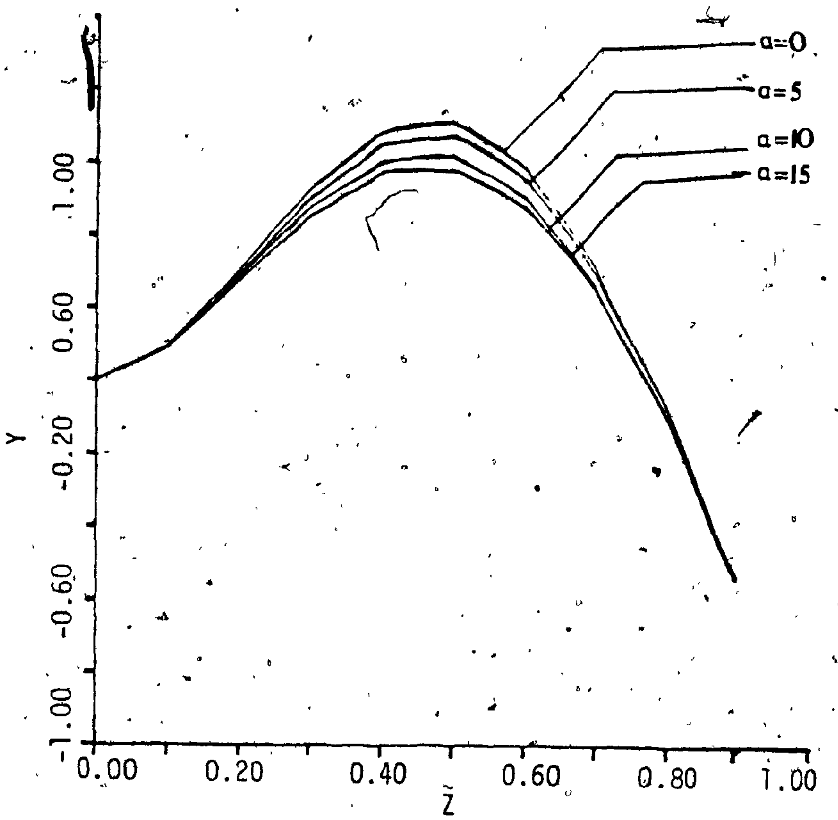

Fig. 2.18: Variation of Second Mode Shape with Speed

($\tilde{R}$ = 0, θ = 90°)

CHAPTER 3

DYNAMIC ANALYSIS USING FINITE ELEMENT APPROACH

CHAPTER 3

DYNAMIC ANALYSIS USING FINITE ELEMENT APPROACH

In this chapter, the dynamics of a rotating beam type structure is studied using an analyzer package based on a finite element program called SPAR, developed by NASA [39]. This program is written in modular form, that is, its various modules can be used in any desired combination to perform the required computations.

The natural frequencies for the rotating beam are obtained for different Hub-Radii, setting angle, rotational speed and are compared to the results obtained in chapter 2.

Pertinent descriptions of the finite element analysis program are discussed in the following sections.

3.1 General Description of the Software

The finite element package SPAR is a versatile general purpose finite element program for structural dynamic analysis. SPAR is an array of separate absolute programs called processors or modules. These processors obtain input from two sources, firstly, input records from terminals, and secondly, from a data base. The data base consists of one or more direct access libraries, which contain the data sets output from the different processors. These processors do not have to be executed in any particular order, provided all necessary source data sets reside in the data base. Each processor automatically extracts from the data base all of the data set it requires, and inserts into the data base the newly generated sets. Figure 3.1 shows the schematic of the general structure of the overall finite element program.

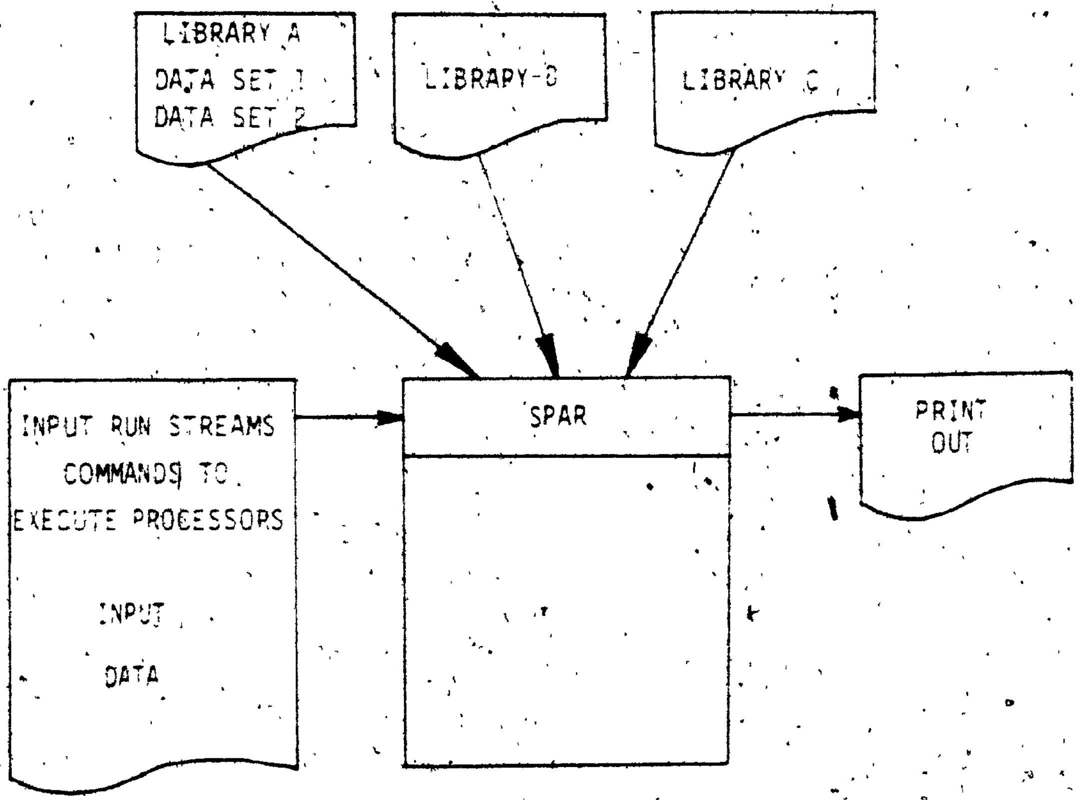

Fig. 3.1: SPAR Program Block Diagram

Each processor of SPAR performs a specific function e.g. processor TAB, contains an array of sub-processors which generate tables of material constants, section properties, constraint conditions and various other data sets comprising a substantial portion of the definition of the structure. Processor K assembles the unconstrained system stiffness matrices, processor M assembles the mass matrix of the structure etc. Further, the processor AUS performs matrix manipulations, such as multiplication, addition transpose etc. This processor provides a great deal of flexibility to the user in adopting SPAR program to suit any computational needs. Other program and analysis details about the SPAR processors are contained in reference [39].

In SPAR, the execution on a processor is carried out by processor basis. Each processor is commanded by a separate explicit command. A string of such commands interlaced with the input numerical data is written by the user for a problem at hand, and is called a run stream. Various run streams can be executed in any order.

SPAR program contains many different types of elements, way to connect these elements and other features which are described in detail in the SPAR reference manual [39].

SPAR is an extremely flexible and efficient computer program; it is modular in nature, has data base capability and can be easily modified for any particular application. SPAR data base contains all the information relevant to the type of structure being analyzed. Data base is located on the drum storage, the location of a particular data in the data base is given by the library number and the data set name. A table of contents (TOC) is used to store and relate the names and addresses of all data sets resident in the data base. A typical TOC listing is given in Appendix D.

3.2 Finite Element Model

The cantilever beam considered is mounted on the periphery of a rotating disc of radius R. The beam has an area of cross-section A, length L, modulus of elasticity of material E and material density ρ.

As shown in Fig. 3.2, xyz coordinate system is chosen such that the x and y axes are in the plane of the beam cross-section and are the principal centroidal axes of inertia in that plane. The z axis is along the beam. XYZ is another set of orthogonal axis system where Y is along the beam and the XY plane contains the plane of disc rotation. Origin of the XYZ coordinate axes is at the centre of the rotating disc while the xyz axes are located at the root of the beam where it is fixed to the disc. The angle θ, between the Z and x axes is the setting angle.

The rotating beam is modelled having 16 node points. Node 1 is fixed to the rotating disc and hence all the motion components (displacement and rotation) are identically zero at this node. The stiffness matrix for the formulation is assembled by considering the effects of elastic stiffness, centrifugal force and initial stress.

A listing of the sample program and the run stream used to compute the natural frequencies for different Hub-radii, setting angles etc. is given in Appendix D.

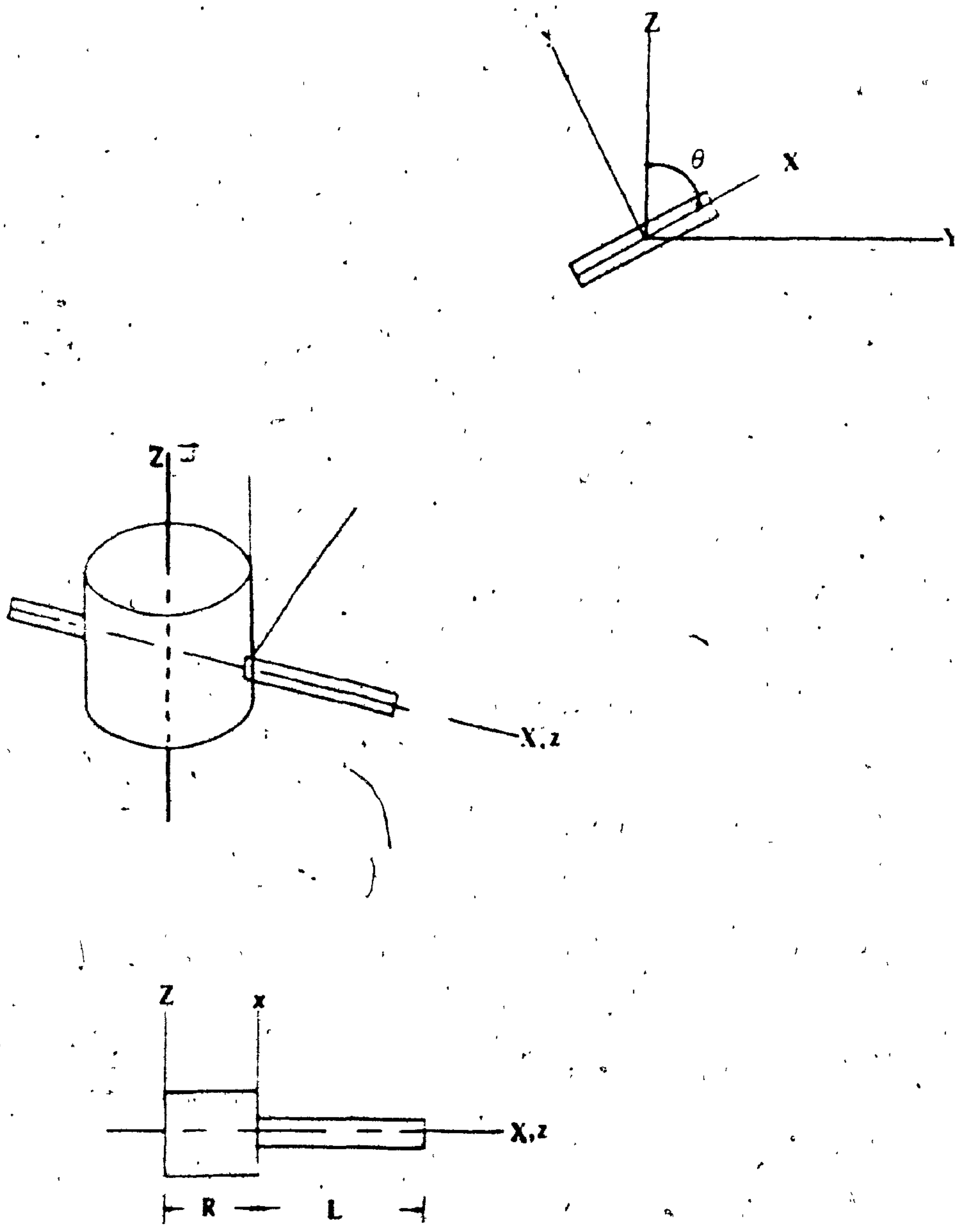

Fig. 3.2: Rotating Cantilever Beam Modelled Using SPAR

3.3 Discussion of the Results

Natural frequencies are obtained for a rotating cantilever beam at various rotational speeds for different values of setting angle and hub radii by using a finite element package 'SPAR'.

Table 3.1 shows the variation of fundamental natural frequency for different rotational speeds, and several parameter combinations. The results are compared to the ones obtained using improved strain energy formulation in Rayleigh Ritz in chapter 2.

The increase in natural frequency is larger for higher setting angles. With higher value of R, the natural frequency is higher and increase faster with the rotational speed. The results obtained using the finite element approach and the energy approach agree closely.

In this chapter, a finite element model of the rotating beam type structure is generated using SPAR. The natural frequencies are obtained for different rotational speed and several parameter combinations.

In the next chapter, the structure is modelled as a plate and the flexural vibrations of plates with different boundary conditions are studied using beam-characteristic orthogonal polynomials in Rayleigh-Ritz method.

TABLE 3.1: Variation of Fundamental Natural Frequency for Various Values of Setting Angle and Hub-Radii Using Finite Element Method

Angular Velocity (Hz)	Natural Frequency (Hz)							
	$\tilde{R} = 0$							
	$\theta = 0°$		$\theta = 30°$		$\theta = 60°$		$\theta = 90°$	
	SPAR	Ref. Ch. 2	SPAR	Ref. Ch. 2	SPAR	Ref. Ch. 2	SPAR	Ref. Ch. 2
0	13.71	13.6	13.71	13.6	13.71	13.6	13.6	13.71
5	13.88	13.71	14.07	13.72	14.19	14.07	14.76	14.76
10	14.37	13.88	14.82	14.65	15.97	15.34	17.35	17.24
	$\tilde{R} = 1$							
0	13.71	13.6	13.71	13.6	13.71	13.6	13.71	13.6
5	15.23	14.85	15.61	15.12	15.92	15.46	16.03	15.63
10	19.0	18.3	19.41	19.02	20.64	19.87	21.37	21.1
	$\tilde{R} = 5$							
0	13.71	13.6	13.71	13.6	13.71	13.6	13.71	13.6
5	19.69	19.2	19.81	19.4	19.98	19.6	20.03	19.8
10	31.26	30.9	31.71	31.42	32.54	31.87	32.78	32.3

CHAPTER 4

DYNAMIC ANALYSIS OF ROTATING PLATES

CHAPTER 4

DYNAMIC ANALYSIS OF ROTATING PLATES

Rotating structures in many applications cannot be strictly modelled as beams and must be modelled as flat or curved plates. In this chapter, the vibrational behavior of stationary and rotating plate type structures is studied using Rayleigh-Ritz method.

A class of beam characteristic orthogonal polynomials, constructed using Gram-Schmidt process, are employed as deflection functions for plates in Rayleigh-Ritz method to obtain their natural frequencies and mode shapes. A plate with all edges free is analyzed to obtain confidence in the proposed method. Natural frequencies and mode shapes of plates with (i) all edges free and (ii) three edges free and one fixed (cantilevered plate) are presented and compared with those obtained by other methods. Experimental results obtained by using modal testing techniques are also presented for a plate with all edges free.

4.1 Beam Characteristic Orthogonal Polynomials

The first member of the orthogonal polynomial set $\phi_i(x)$ is chosen as the simplest polynomial of the least order that satisfies both the geometrical and the natural boundary conditions of the beam. The other members of the orthogonal set in the interval $a < x < b$ are generated using Gram-Schmidt process as follows:

$$\phi_2(x) = (x - B_2)\ \phi_1(x) \tag{4.1}$$

$$\phi_K(x) = (x - B_K)\ \phi_{K-1}(x) - C_K\ \phi_{K-2}(x) \tag{4.2}$$

where

$$B_K = \left[\int_a^b xw(x)\ \phi_{K-1}^2(x)dx\right] \bigg/ \left[\int_a^b w(x)\ \phi_{K-1}^2(x)dx\right] \tag{4.3}$$

$$C_K = \left[\int_a^b xw(x)\ \phi_{K-1}(x)\ \phi_{K-2}(x)dx\right] \bigg/ \left[\int_a^b w(x)\ \phi_{K-2}^2(x)dx\right] \tag{4.4}$$

and $w(x)$ is the weighting function. For uniform beams the weighting function, $w(x)$, is unity. The polynomials $\phi_K(x)$ satisfy the orthogonality condition,

$$\begin{aligned}\int_a^b w(x)\ \phi_K(x)\ \phi_L(x)dx &= 0 \text{ if } K \neq L \\ &= a_{KL} \text{ if } K = L\end{aligned} \tag{4.5}$$

Even though $\phi_i(x)$ satisfies all the boundary conditions both geometric and natural, the other members of the orthogonal set satisfy only geometric boundary conditions and hence do not over-restrain the structure as in the case of classical beam functions.

4.2 Analysis

The deflection for a rectangular plate undergoing free flexural vibration can be expressed in terms of the beam characteristic orthogonal polynomials in x and y directions as

$$W(x,y) = \sum_m \sum_n A_{mn}\ \phi_m(\bar{x})\ \phi_n(\bar{y}) \tag{4.6}$$

where $\bar{x} = x/a$ and $\bar{y} = y/b$. x and y are the coordinates along the two sides of the plate and a and b are plate dimensions.

The strain energy of the plate can be obtained by assuming that the plate consists of a perfectly elastic, homogeneous, isotropic material. An element cut out of the plate by pairs of planes parallel to the xz and yz axes is shown in Fig. 4.1.

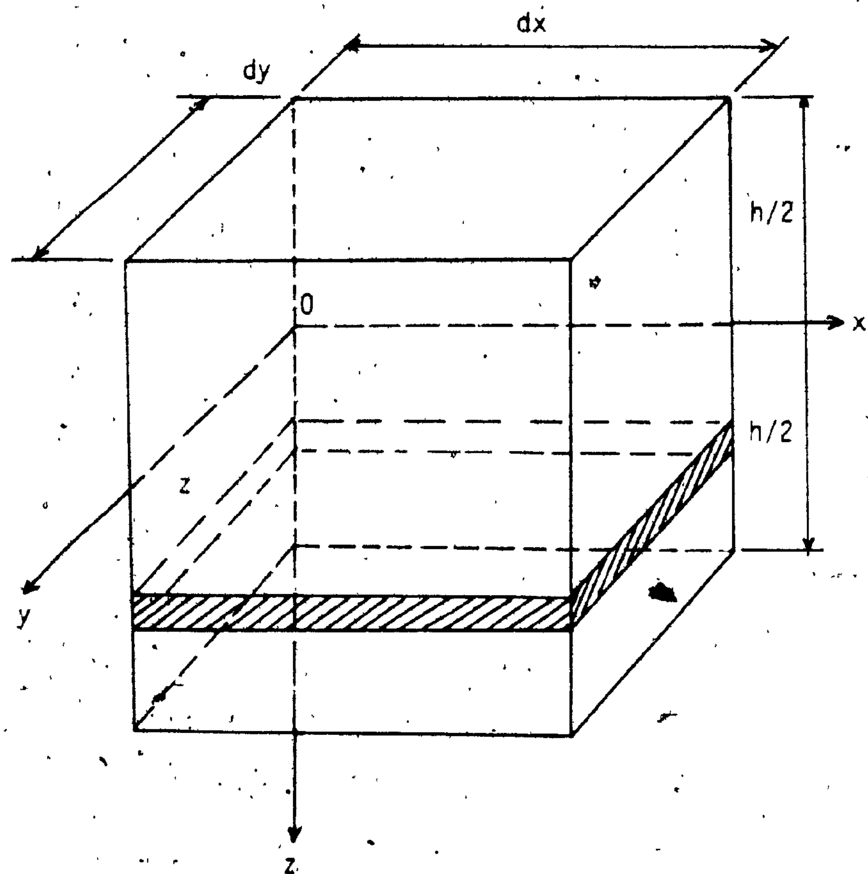

Fig. 4.1: Plate Element

W

The xy plane is taken as the middle plane of the plate and assuming that with small deflections, the lateral sides of an element cut out from the plate by planes parallel to zx and zy planes remain plane and rotate so as to be normal to the deflected middle surface of the plate. Then the strain in a thin layer of this element, indicated by the shaded area and distant z from the middle surface are equal to:

$$\varepsilon_{xx} = \frac{z}{R_2} = -z\,\frac{\partial^2 W}{\partial x^2} \tag{4.7}$$

$$\varepsilon_{yy} = \frac{z}{R_3} = -z\,\frac{\partial^2 W}{\partial y^2} \tag{4.8}$$

$$\varepsilon_{xy} = -2z\,\frac{\partial^2 W}{\partial x \partial y} \tag{4.9}$$

where ε_{xx}, ε_{yy} are unit elongations in the x and y directions, ε_{xy} is shear deformation in the xy plane, W is the deflection of the plate, and $\frac{1}{R_2}$ and $\frac{1}{R_3}$ are curvatures in the xz and yz planes respectively.

The corresponding stresses can be obtained by using Hooke's Law as:

$$\sigma_x = \frac{E}{1-\nu^2}\left(\varepsilon_{xx} + \nu\varepsilon_{yy}\right) = -\frac{E_z}{1-\nu^2}\left(\frac{\partial^2 W}{\partial x^2} + \frac{\partial^2 W}{\partial y^2}\right) \tag{4.10}$$

$$\sigma_y = \frac{E}{1-\nu^2}\left(\varepsilon_{yy} + \nu\varepsilon_{xx}\right) = -\frac{E_z}{1-\nu^2}\left(\frac{\partial^2 W}{\partial y^2} + \nu\,\frac{\partial^2 W}{\partial x^2}\right) \tag{4.11}$$

$$\tau = G\,\varepsilon_{xy} = -\frac{E_z}{(1+\nu)}\left(\frac{\partial^2 W}{\partial_x \partial_y}\right) \tag{4.12}$$

where ν is the Poissons ratio and E is the modulus of elasticity of the plate.

The potential energy accumulated in the shaded layer of the element during the deformation is,

$$dU = \left(\frac{\varepsilon_{xx}\sigma_x}{2} + \frac{\varepsilon_{yy}\sigma_y}{2} + \frac{\varepsilon_{xy}\tau}{2}\right) dx\ dy\ dz \qquad (4.13)$$

Using equations (4.7) through (4.12),

$$dU = \frac{Ez^2}{2(1-\nu^2)} \left\{\left(\frac{\partial^2 W}{\partial x^2}\right)^2 + \left(\frac{\partial^2 W}{\partial y^2}\right)^2 + 2\nu \frac{\partial^2 W}{\partial x^2}\frac{\partial^2 W}{\partial y^2} + 2(1-\nu)\left(\frac{\partial^2 W}{\partial x \partial y}\right)^2\right\} dx\ dy\ dz \qquad (4.14)$$

Integrating,

$$U = \iiint dV = \frac{D}{2}\iint\left\{\left(\frac{\partial^2 W}{\partial x^2}\right)^2 + \left(\frac{\partial^2 W}{\partial y^2}\right)^2 + 2\nu \frac{\partial^2 W}{\partial x^2}\frac{\partial^2 W}{\partial y^2} + 2(1-\nu)\left(\frac{\partial^2 W}{\partial x \partial y}\right)\right\} dx\ dy \qquad (4.15)$$

In term of dimensionless parameters $\hat{x}$ and $\hat{y}$,

$$U = \frac{1}{2}\ \frac{Dab}{a^4}\int_0^1\int_0^1 \left[W_{\hat{x}\hat{x}}^{\ 2} + \alpha_1^4 W_{\hat{y}\hat{y}}^{\ 2} + 2\nu\alpha_1^{\ 2}\, W_{\hat{x}\hat{x}}\, W_{\hat{y}\hat{y}} + 2(1-\nu)\,\alpha_1^{\ 2}\, W_{\hat{x}\hat{y}}^{\ 2}\right] d\hat{x}\ d\hat{y} \qquad (4.16)$$

The kinetic energy of the plate is

$$T = \frac{1}{2}\ \rho h a\ b\, p^2 \int_0^1\int_0^1 W^2(\hat{x},\hat{y})\ \ d\hat{x}\ d\hat{y} \qquad (4.17)$$

where ρ - density of plate material

h - thickness of the plate

D - flexural rigidity of the plate

α_1 - side ratio a/b

and the subscripts $\hat{x}$ and $\hat{y}$ refer to differentiation with respect to the subscript and the number of times the subscript appears denotes the order of differentiation.

The equations of motion are obtained by minimizing the Lagrangian with respect to the coefficient A_{ij} as,

$$\frac{\partial T}{\partial A_{ij}} - \frac{\partial U}{\partial A_{ij}} = 0 \tag{4.18}$$

i.e., $$\rho h a b p^2 \int_0^1\int_0^1 W \frac{\partial W}{\partial A_{ij}} d\hat{x}\, d\hat{y} - \frac{abD}{a^4} \int_0^1\int_0^1 \left[W_{\hat{x}\hat{x}} \frac{\partial W_{\hat{x}\hat{x}}}{\partial A_{ij}} + \alpha_1^4\, W_{\hat{y}\hat{y}} \frac{\partial W_{\hat{y}\hat{y}}}{\partial A_{ij}} \right.$$

$$\left. + \nu \alpha_1^2 \left(W_{\hat{x}\hat{x}} \frac{\partial W_{\hat{y}\hat{y}}}{\partial A_{ij}} + W_{\hat{y}\hat{y}} \frac{\partial W_{\hat{x}\hat{x}}}{\partial A_{ij}} \right) + 2\,(1-\nu^2)\alpha_1^2\, W_{\hat{x}\hat{y}} \frac{\partial W_{\hat{x}\hat{y}}}{\partial A_{ij}} \right] d\hat{x}\, d\hat{y} = 0 \tag{4.19}$$

4.3 Plates with Three Edges Free and One Fixed (Cantilevered Plates)

Rotating structures with low aspect ratio can be idealized as a cantilevered plate. Figure 4.2 shows such a plate which consists of beam problems with clamped-free and free-free conditions. The first member of polynomials which satisfy the free-free conditions is taken to be unity. To determine the first member of polynomials satisfying the clamped-free condition consider the deflection function,

$$\phi_1(\hat{x}) = a_0 + a_1\hat{x} + a_2\hat{x}^2 + a_3\hat{x}^3 + a_4\hat{x}^4 \tag{4.19}$$

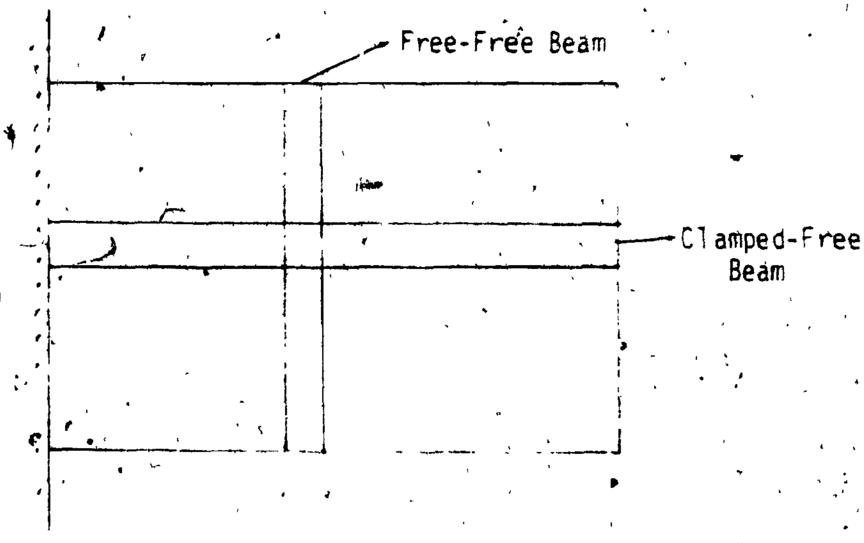

Fig. 4.2: Free-Free and Clamped-Free Beams used to Model the Cantilevered Plate

where x is the non-dimensional coordinate along the beam with the origin at one end of the beam. The boundary conditions for such a beam is that at $x = 0$, the deflection and slope are equal to zero and for $x = 1$, the moment and shear force are equal to zero,

$$\text{i.e.} \quad \phi_1(0) = \phi_1'(0) = \phi_1''(1) = \phi_1'''(1) = 0 \qquad (4.20)$$

Substituting these boundary conditions in equation (4.19), the coefficients a_i are determined to yield,

$$\phi_1(x) = a_1(6x^2 - 4x^3 + x^4) \qquad (4.21)$$

The coefficient a_1 is appropriately chosen so as to normalize $\phi_1(x)$ such that

$$\int_0^1 \phi_1^2(x)\, dx = 1 \qquad (4.22)$$

The other polynomials are generated using Gram-Schmidt process as outlined in Section 4.2.

Substituting these deflection functions into the equation of motion outlined in Section 4.3, leads to the eigen-value problem.

$$\left. \int_0^1\int_0^1 \left(\sum_{mn} A_{mn}\phi_m\psi_n \right) \phi_i\psi_j \; dx\, dy \right]$$

$$-\left[\int_0^1\int_0^1 \sum_{mn} A_{mn}\phi_m''''\psi_n\phi_i\psi_j \, dx\, dy + \alpha_1^4 \int_0^1\int_0^1 \sum_{mn} \psi_n''''\phi_m\psi_j\phi_i \; dx\, dy \right.$$

$$+ \ldots \left\{ \int_0^1\int_0^1 \sum_{mn} A_{mn} \phi_m''\psi_n\ldots\psi_j\phi_i \; dx\, dy \right.$$

$$\left. + \int_0^1\int_0^1 \sum_{mn} A_{mn} \psi_n\phi_m\phi_i''\psi_j \; dx\, dy \right\}$$

$$\left. + \, 2(1-\nu)\,\alpha_1^2 \int_0^1\int_0^1 \sum_{mn} A_{mn}\phi_m'\psi_n'\phi_i'\psi_j' \; dx\, dy \right] = 0 \qquad (4.23)$$

where $\lambda^2 = \frac{\rho h p^2 a^4}{D}$ and ' and ˙ represent differentiation with x and y respectively.

This resulting eigen-value problem was solved by using the computer algorithm outlined in Appendix E.

4.4 Plates with all Edges Free

The plates with all edges free consist of beam problems with both ends free. The first member of the polynomials which satisfy all the boundary conditions, $\phi_1(x)$, is chosen to be unity. This first member of the orthogonal polynomial set satisfies all the boundary conditions both geometric and natural. Using this first member, the other members of the orthogonal set are generated using the Gram-Schmidt process outlined in Section 4.2.

The resulting eigenvalue given by equation 4.23 is solved by using the computer algorithm given in Appendix F.

4.5 Experimental Verification Using Modal Testing Technique

Modal testing is the process of testing components to obtain their modal parameters. Essentially, modal testing involves identifying the natural frequencies of a structure and the associated deflected shapes when the structure is excited at one of the natural frequencies.

In this section, the natural frequencies and mode shapes for a square plate with free-free boundary conditions are obtained using an experimental modal analysis system. The experimental results obtained are compared with the computed analytical results.

4.6 General Description of the Software

The Modal Analysis program used consists of 13 transactions of which the 7 core one's are:

1) Geometry Entry.
2) Format data for display.
3) Identify Modal frequencies and damping.
4) Measure and extract Modal amplitudes.
5) Synthesize and plot transfer function.
6) Tabulate modal vectors or geometry.
7) Display mode shapes.

The core transactions shown above perform various portions of the experimental Modal Analysis procedure. The Geometry Transaction is used to store coordinates of the test points on the test structure. These test points form a "computer-sketch" of the test structure. The test points are connected by straight-line fashion in the Format Transaction.

The Identify Transaction is used to determine the natural frequency and damping ratio for each mode to be analyzed. Measurements from anywhere on the structure can be used by the Identify Transaction.

When Geometry, Format, and Identify Transactions have been completed, the Measure Transaction is used to collect and store transfer function data for each test point. This transaction is also used to curve-fit this stored data to extract modal parameters.

After transfer function data at each test point has been curve-fit, the Format transaction is used to create the display files necessary to animate the calculated mode shapes. The Display Transaction can then access these files to generate animated mode shape displays on the system terminal.

The Synthesis Transaction can be used to generate and compare transfer functions. A synthesized transfer function, generated from extracted modal parameters, may be compared with a live measurement.

The Tabulate Transaction can be used to generate "report-ready" listings of test point coordinates and extracted modal parameters. Other program and analysis details about the structural analysis system are contained in reference [40].

4.7 Experimental Model

The flat-plate tested was suspended by two flexible threads at two corners such that the plate surface was in the vertical plane. The plate was divided into twenty five test points and each of these test points were excited by impulse excitation with response measurement being taken from an accelerometer attached at the centre. The configuration is shown in Fig. 4.3.

Both the excitation signal and the input forcing signal were fed simultaneously into the FFT analyzer where the response time histories were transformed into frequency spectra. The ratio of these two functions which is the frequency response function of the structure was calculated and obtained as the output.

A complete experimental set up is given in Fig. 4.4. The frequency response function was further processed to obtain the modal parameters [39].

4.8 Natural Frequencies of a Rotating Plate

A simple configuration of a rotating plate is considered to use the orthogonal polynomial function approach. The setting angle is ninety degrees as shown in Fig. 4.5.

Consider an element of dimensions dx and dy. The radial displacement of this element towards the center due to deflection is

$$\Delta r = \frac{1}{2} \int_0^y \left(\frac{dW}{dy}\right)^2 dy \tag{4.24}$$

The work done on the element by the centrifugal forces acting on it during deflection is

$$\Delta W = -m\omega^2 \, (R + y) \, dx \, dy \quad \frac{1}{2} \int_0^y \left(\frac{dW}{dy}\right)^2 dy \tag{4.25}$$

The energy corresponding to the work of the centrifugal forces will be obtained by summing that due to all such elements and is obtained as

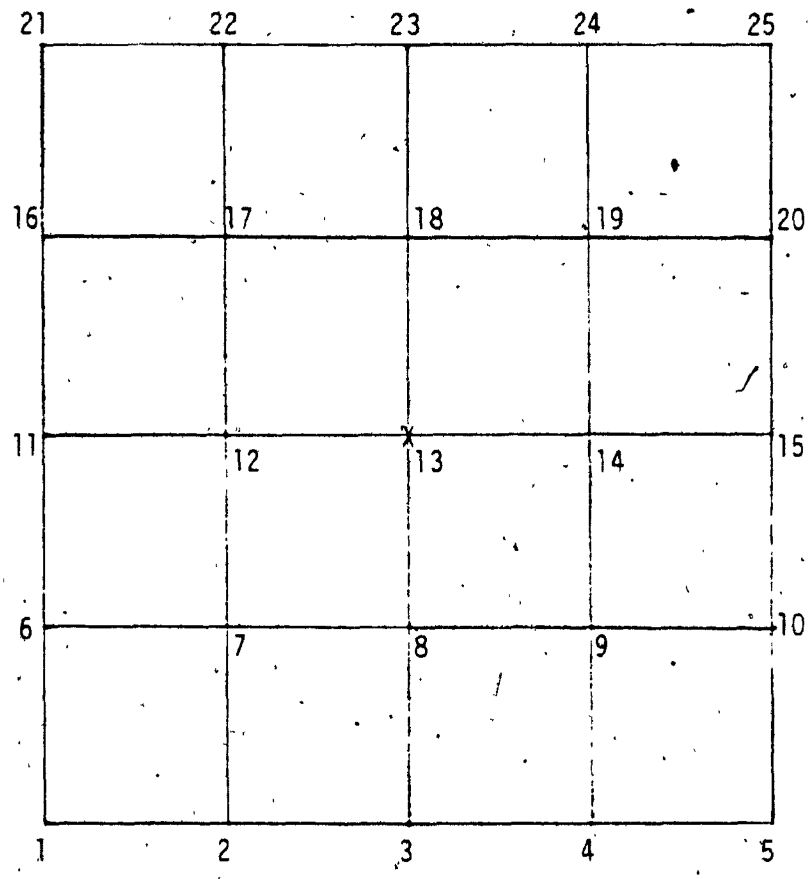

X - accelerometer attachment point

Fig. 4.3 : Measurement Points on Test Plate

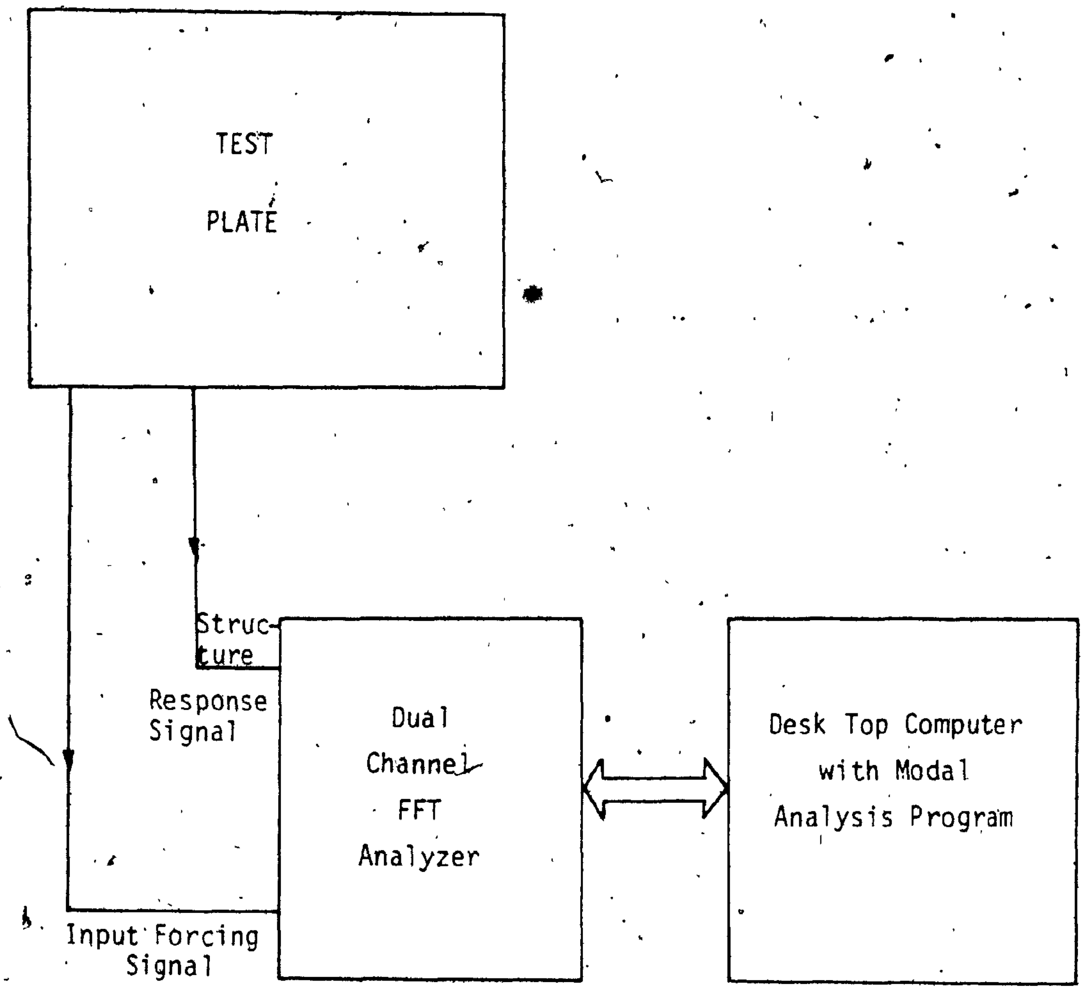

Fig. 4.4: Schematic of the Experimental Procedure

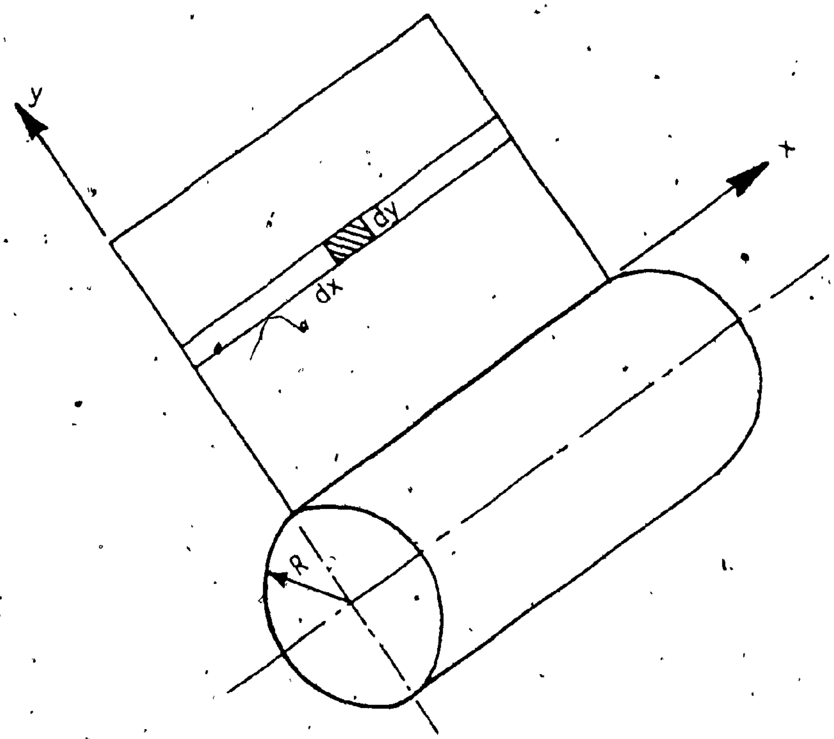

Fig. 4.5 : Rotating Cantilever Plate

$$U_r = -\int_0^a\int_0^b \Delta W$$

$$= \frac{1}{2} m\Omega^2 \int_0^a\int_0^b (R+y)\, dx\, dy \cdot \int \left(\frac{dW}{dy}\right) dy \qquad (4.26)$$

The additional strain energy U_r, due to centrifugal forces is added along with the bending strain energy U, given in eq. (4.15) to solve for the natural frequencies of the rotating plate.

Substituting eq. (4.6) for W(x,y) in eq. (4.26), the strain energy due to rotation can be written as

$$U_r = \alpha^2 \int_0^1 \phi_m \phi_i \, dx \left[\int_0^1 \frac{R}{b} dy \int_0^Y \dot{\psi}_n \dot{\psi}_j \, d\dot{y} \right.$$

$$\left. + \int_0^1 \dot{y}\, dy \int_0^{y} \dot{\psi}_n \dot{\psi}_j \, d\dot{y} \right] \qquad (4.27)$$

The natural frequencies of the rotating plate incorporating the strain energy due to rotation are numerically computed using Rayleigh's method. Results are tabulated in Table 4.3. Since only one term is used in the solution, flexure is considered only in the y direction and hence, the results are comparable to those for a rotating beam as can be verified by an inspection of Table 2.5. As to be expected, the natural frequency increases with speed of rotation showing the stiffening of the plate due to centrifugal forces.

4.9 Discussion of the Results

Natural frequencies, mode shapes and beam characteristic orthogonal polynomials are obtained for free-free and cantilevered plates.

A convergence test was carried out by taking equal number of terms for the series in both x and y directions. The results of this test are presented in Tables 4.1 and 4.2. The convergence is very rapid and the converged results are superior or equal to the comparison results. Experimental results obtained using modal analysis technique are also presented in Table 4.2.

The set of beam characteristic polynomials constructed using Gram-Schmidt process are presented and plotted in Tables 4.3-4.4 and Figs. 4.6-4.7 respectively.

The mode shape of the cantilevered plate is presented in Fig. 4.3. The animated mode shapes obtained using the experimental modal system are presented in Figs. 4.9 through 4.11.

The analytically computed first natural frequency could not be recorded experimentally due to the fact that the plate surface had a slight curvature when suspended by the flexible threads. Also, the first animated mode shape (Fig. 4.9) has a node point on one of its edges, probably due to an error in recording the transfer function. The other natural frequencies obtained experimentally agree closely with the analytical results and the results obtained by Leissa [21] and Dickinson [27] as shown in Table 4.2.

Natural frequencies of the rotating plate using Rayleigh's method are shown in Table 4.5. The natural frequencies increase with an increase in rotational speed α, and since flexure is considered only in the y direction, the results are comparable to the one's obtained for a rotating beam as shown in Table 2.5.

In this chapter, a set of beam characteristic orthogonal polynomials are used to obtain the natural frequencies and mode shapes of rotating and non-rotating plates. Experimental modal analysis is also carried out on a plate with free-free edges and the results are compared to the analytical results.

In the final chapter, conclusions, recommendations and scope for future work are presented.

TABLE 4.1: Frequency Parameters $(\rho h p^2 a^4/D)^{\frac{1}{2}}$ for Isotropic Cantilevered Plate ($\nu = 0.3$)

Side Ratio α_1	Mode No.	Values of m and n Taken in Deflection Function				Comparison Results	
		4	6	8	10	Ref [27]	Ref [21]
1.0	1	3.4881	3.4737	3.4717	3.4712	3.473	3.4917
	2	8.5472	8.5125	8.5089	8.5080		8.5246
	3	21.4727	21.3120	21.2913	21.2878	21.294	21.429

TABLE 4.2: Frequency Parameters $(\rho h p^2 a^4/D)^{\frac{1}{2}}$ for Isotropic Free-Free Plate ($\nu = 0.3$)

Side Ratio α_1	Mode No.	Values of m and n Taken in Deflection Function				Comparison Results		Experimental
		4	6	8	10	Ref [27]	Ref [21]	
1.0	1	13.6602	13.4687	13.4682	13.4682	13.468	13.489	
	2	22.4499	19.7257	19.5963	19.5961		19.789	21.461
	3	30.5941	24.5412	24.2707	24.2702		24.432	26.484

TABLE 4.3: Orthogonal Polynomials for Clamped-Free Beam

$$\phi_i(x) = \sum_{j=0} a_{ij}\, x^{j+2}$$

Coefficient \ i	1	2	3	4	5	6
a_{i0}	3.94676	20.0501	62.4439	152.106	317.665	596.162
a_{i1}	-2.63117	-38.3606	-225.033	-868.760	-2613.85	-6647.44
a_{i2}	6.57793	20.0043	259.361	1733.29	7900.08	28089.1
a_{i3}	0.	-4.16565	-115.023	-1512.98	-11321.0	-59107.0
a_{i4}	0.	0.	21.1140	591.069	8147.96	67318.5
a_{i5}	0.	0.	0.	-97.9188	-2861.11	-41733.8
a_{i6}	0.	0.	0.	0.	433.743	13350.5
a_{i7}	0.	0.	0.	0.	0.	-1869.89

TABLE 4.4: Orthogonal Polynomials for Free-Free Beam

$$\phi_i(x) = \sum_{j=0} a_{ij}\, x^j$$

coefficient i	1	2	3	4	5	6
a_{i0}	.999999	1.73205	2.23607	2.64575	2.99999	3.31662
a_{i1}	0.	-3.46410	-13.4164	-31.7490	-59.9999	-99.4987
a_{i2}	0.	0.	13.4164	79.3725	269.999	696.491
a_{i3}	0.	0.	0.	-52.9150	-419.999	-1857.31
a_{i4}	0.	0.	0.	0.	209.999	2089.47
a_{i5}	0.	0.	0.	0.	0.	-835.789
a_{i6}	0.	0.	0.	0.	0.	0.
a_{i7}	0.	0.	0.	0.	0.	0.

TABLE 4.5: Variation of Frequency Parameters $(\rho h p^2 a^4/D)^{\frac{1}{2}}$ for Isotropic Cantilevered Plate ($\nu = 0.3$; $\theta = 90°$)

Angular Velocity (α)	Frequency Parameters
0	3.531
1	3.692
2	4.142
3	4.797
4	5.588
5	6.464
6	7.395
7	8.149
8	9.356
9	10.367
10	11.3913

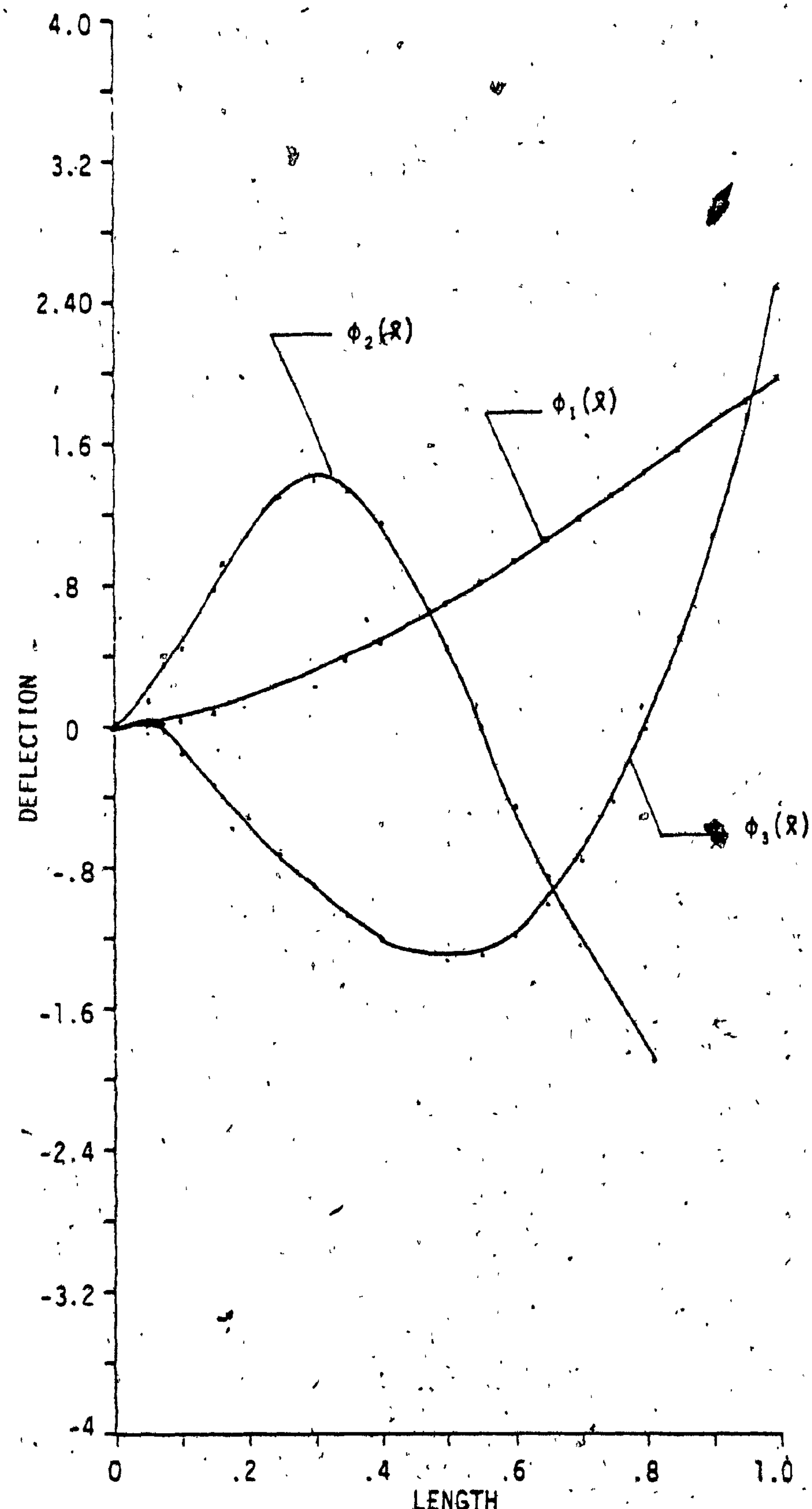

Fig. 4.6: Orthogonal Polynomial Deflection Functions for Clamped-Free Beam

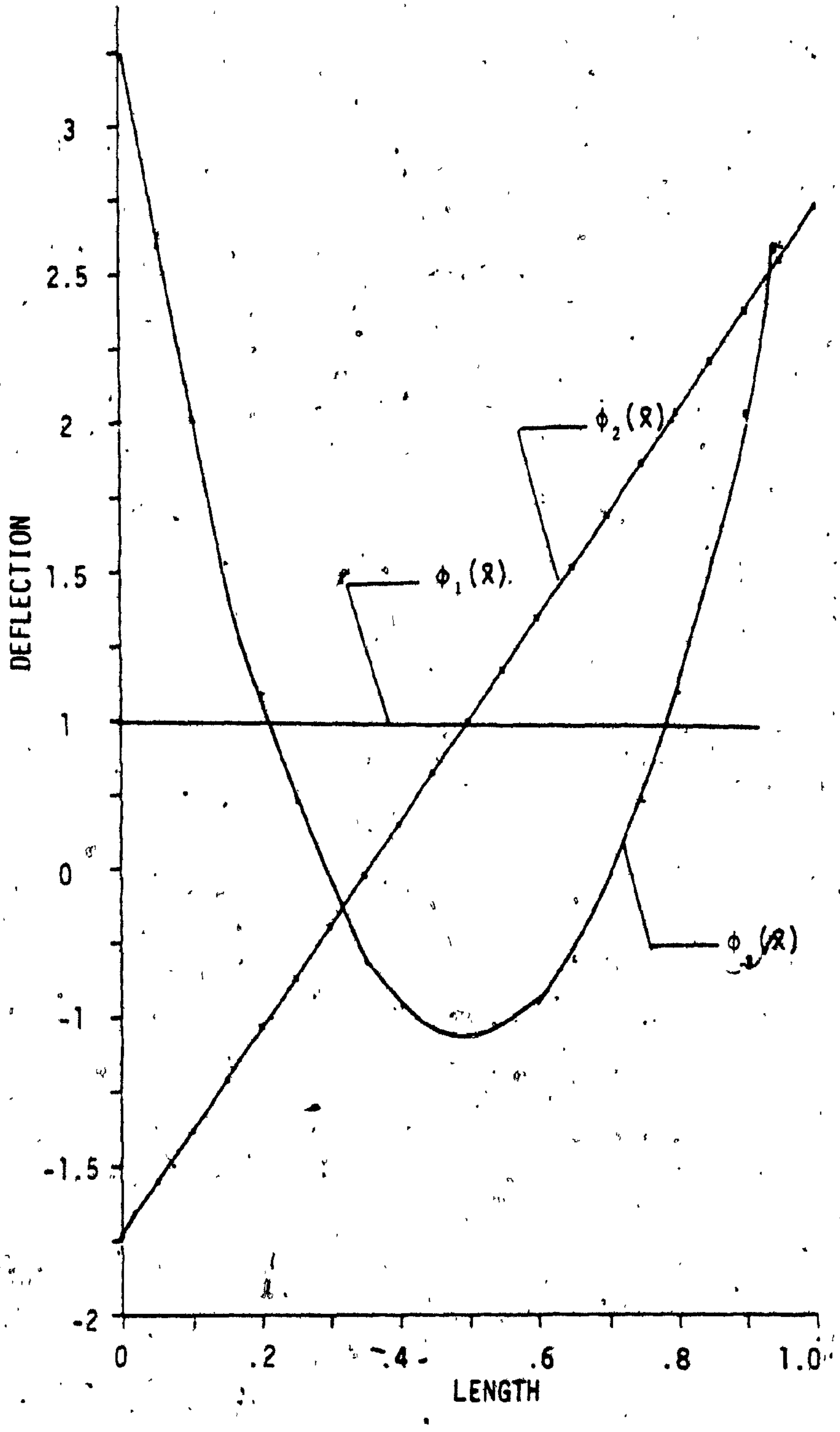

Fig. 4.7: Orthogonal Polynomial Deflection Functions for Free-Free Beam

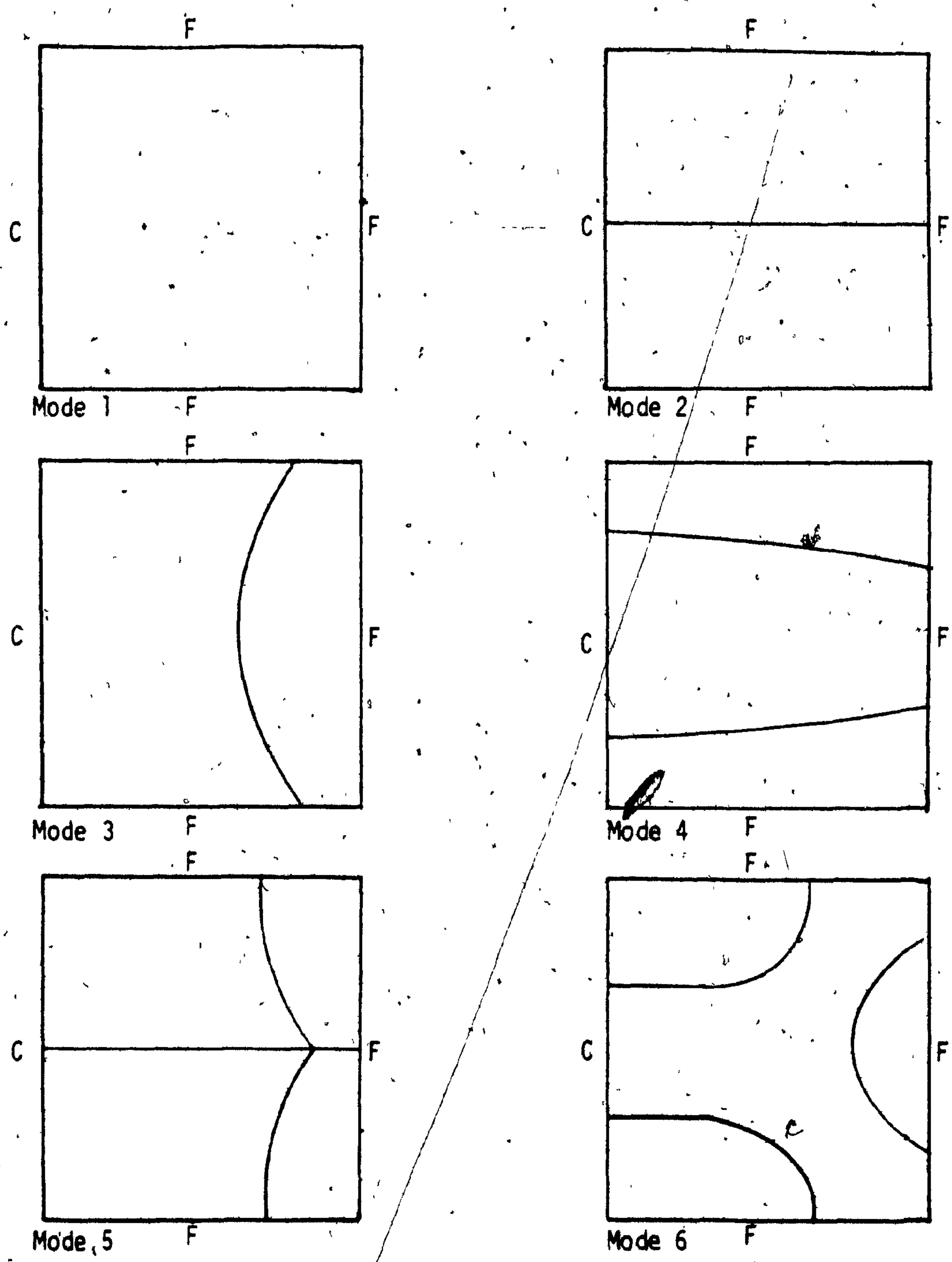

Fig. 4.8 : Nodal Lines for Cantilevered Plates

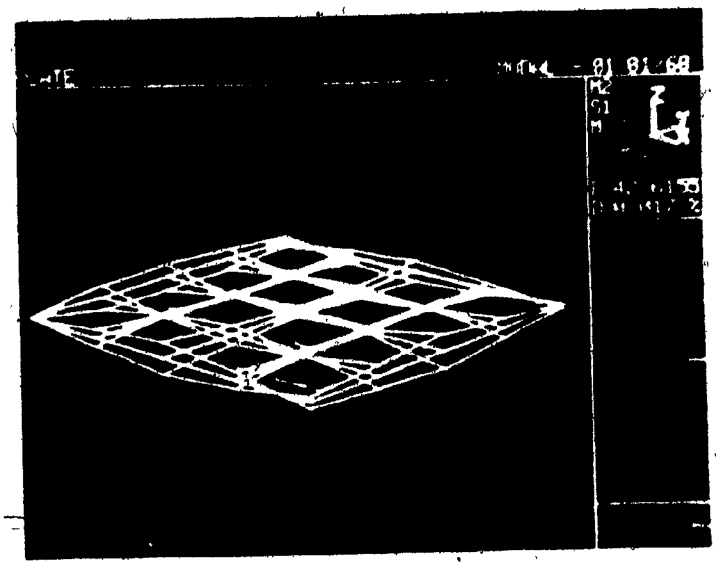

Fig. 4.9: First Animated Mode Shape Using Experimental Modal System

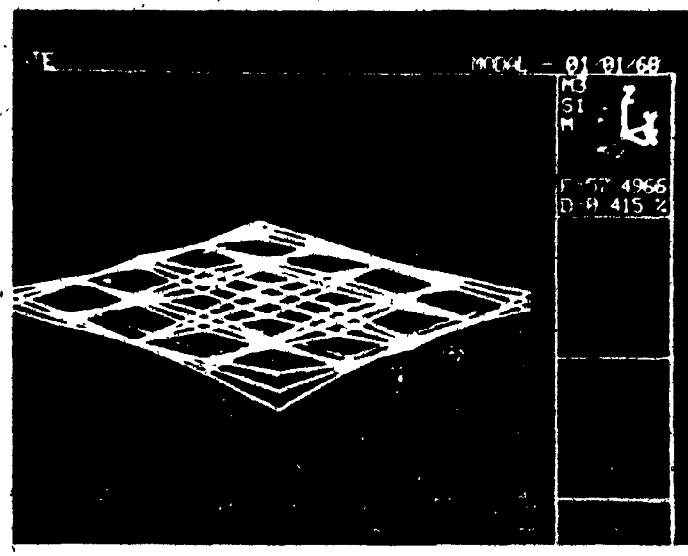

Fig. 4.10: Second Animated Mode Shape Using Experimental Modal System

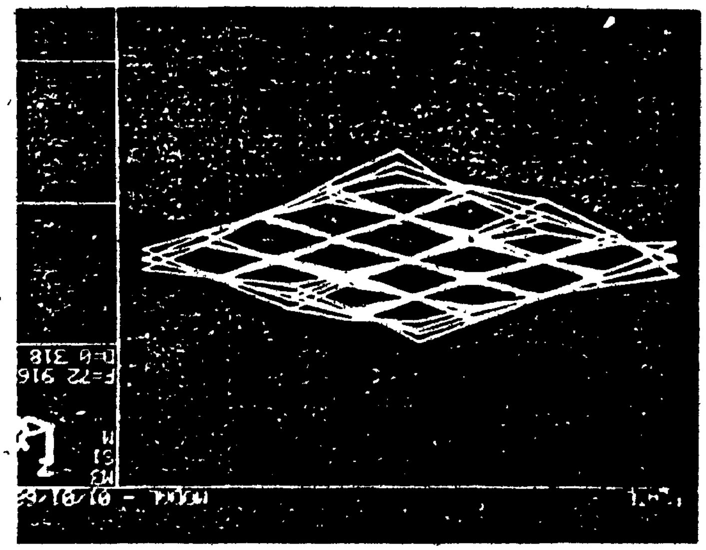

Fig. 4.11: Third Animated Mode Shape Using Experimental Modal System

CHAPTER 5

CONCLUSIONS AND RECOMMENDATIONS

CHAPTER 5

CONCLUSIONS AND RECOMMENDATIONS

Dynamics of a class of rotating structures by using improved methods in calculating their natural frequencies and mode shapes has been proposed where the rotating structure depending on the aspect ratio is modelled either as a beam or a plate.

Rayleigh-Ritz method with improved strain energy formulation is used to obtain the natural frequencies and mode shapes of a rotating beam type structure. The setting angle of the beam with respect to the plane of rotation and radius of hub on which the structure is mounted are also taken into account in the formulation. The variation of natural frequencies and mode shapes presented in a non-dimensional form against the rotational speed.

The finite element program SPAR has also been used to model this rotating beam type structure. The natural frequencies for the structure are obtained for different Hub-Radii, setting angle and rotational speed.

At low-aspect ratios, the structure is modelled as a plate. A class of beam characteristic orthogonal polynomials, constructed using Gram-Schmidt process, are employed as deflection functions to obtain the natural frequencies and mode shapes for a stationary and rotating plate type structure. Natural frequencies and mode shapes of plates with all edges free and three edges free and one fixed are presented.

Modal analysis technique to obtain the modal parameters for a free-free plate is also presented.

5.1 Conclusions

The conclusions arrived on the basis of the results presented in the different chapters of the thesis are summarized and given below:

1) The natural frequencies of the rotating beam type structure increase for higher setting angles and for any setting angle the increase is linear at higher rotational speeds.

2) With higher values of hub radius $\tilde{R}$, the natural frequencies are higher and increase faster with the rotational speed.

3) The beam tries to straighten itself more and more as the rotational speed α, is increased.

4) A convergency test was made by varying the number of terms considered in the polynomial shape and the convergence was good.

5) The natural frequencies for the non-rotating plate type structure using the beam characteristic orthogonal polynomials are superior than using other beam functions.

6) Gram-Schmidt process is used to generate sets of orthogonal polynomial functions, the first member of each set satisfying the geometric and natural boundary conditions of an appropriate equivalent beam, and the remainder of the set satisfying only the geometric boundary conditions of the beam. The lack of satisfaction of the natural boundary conditions of the equivalent beam by the higher members of the set relaxes the over-restraint encountered in the use of true beam functions and permits the treatement of a plate with all edges free with a degree of accuracy.

7) The results obtained by modal analysis techniques agree closely to the analytical computed ones, hence, validating the analytical analysis.

5.2 Recommendations for Future Work

Some suggestions for possible future work are given below:

1) Pretwist, shear deformation, taper, etc., can be incorporated in the formulation for the rotating beam type structure.

2) The influence of a tip mass on the natural frequencies and mode shapes of a rotating beam type structure using improved strain energy formulation outlined can be investigated.

3) Experimental Modal analysis techniques can be utilized to determine the natural frequencies and mode shapes of a rotating beam to verify the analtyical results.

4) Optimization of the beam can be carried out subject to the constraints of increase in natural frequency due to rotation, setting angle, hub radii, etc.

5) Rayleigh's method can be extended over to Rayleigh-Ritz method for rotating plates by incorporating the additional energy due to rotation.

6) Improved energy formulation can be carried out in Rayleigh-Ritz method for analyzing the plates.

7) Effect of setting angle, Hub-Radii on the natural frequencies of rotating plates can be studied.

8) Modal analysis techniques can be utilized to study rotating plates.

REFERENCES

REFERENCES

1. Rao, J.S., "Natural Frequencies of Turbine Blading - a Survey", Shock and Vibration Digest, 5, 1, 1973.

2. Carnegie, W., "Vibrations of Rotating Cantilever Blading: Theoretical Approaches to the Frequency Problem Based on Energy Methods", Journal of Mechanical Engineering Science, Vol. 1, No. 3, 1959, pp. 235-240.

3. Schilhansl, M.J., "Bending Frequency of a Rotating Cantilever Beam", Journal of Applied Mechanics, Vol. 25, 1958, pp. 28-30.

4. Rubinstein, N. and Stadter, J.T., "Bounds to Bending Frequencies of a Rotating Beam", Journal of Franklin Institute, Vol. 294, 1972, pp. 217-229.

5. Pnuelli, D., "Natural Bending Frequency Comparable to Rotational Frequency in Rotating Cantilever Beam", Journal of Applied Mechanics, Vol. 39, 1972, pp. 602-604.

6. Subrahmanyam, K.B., Kulkarni, S.V. and Rao, J.S., "Coupled Bending-Torsion Vibrations of Rotating Blades of Asymmetric Aerofoil Cross Section with Allowance for Shear Deflection and Rotary Inertia by use of the Reissner Method", Journal of Sound and Vibration, Vol. 75, No. 1, 1981, pp. 17-36.

7. Sutherland, R.L., "Bending Vibration of a Rotating Blade Vibrating in the Plane of Rotation", Journal of Applied Mechanics, Transactions ASME, 16, 1949, pp. 389-394.

8. Kumar, K., "Vibrations of Space Boom under Centrifugal Force Field", Transactions of C.A.S.I., Vol. 7, 1974, pp. 1-5.

9. Isakson, G. and Eisley, J.G., "Natural Frequencies in Bending of Twisted Rotating and Non-Rotating Blades", 1960, NASA TND-371.

10. Slypez, H.A., "Coupled Bending Vibrations of Pretwisted Cantilever Beams", Journal of Mechanical Engineering Science 10, 1968, pp. 365-379.

11. Wright, A.D., Smith, C.E., Thrishen, R.W. and Wang, J.L.C., "Vibration Modes of Centrifugally Stiffened Beams", Journal of Applied Mechanics, Vol. 49, 1982, pp. 197-201.

12. Handleman, G., Boyce, W. and Cohen, H., "Vibration of a Uniform Rotating Beam with Tip Mass", Third U.S. National Congress of Applied Mechanics, Vol. 27, 1960, pp. 548-550.

13. Lo, H., Goldberg, J.E. and Bogdanoff, J.H., "Effect of Small Hub Radius Change on Bending Frequencies of a Rotating Beam", Journal of Applied Mechanics, Vol. 27, 1960, pp. 548-550.

14. Boyce, W.E. and Handleman, G., "Vibrations of Rotating Beams with Tip Mass", Zeitschaift fur Angewandte Mathematik und Physik, Vol. 12, 1961, pp. 369-392.

15. Wang, J.T.H., Mahrenholtz, O. and Bohm, J., "Extended Galerkin's Method for Rotating Beam Vibrations Using Legendre Polynomials", Solid Mechanics Archives, Vol. 1, 1976, pp. 341-365.

16. Kaushal, A. and Bhat, R.B., "Natural Frequencies and Mode Shapes of Rotating Structures Using Improved Strain Energy Formulation in Rayleigh-Ritz Method", Proceedings of the 3rd International Modal Aanalysis Conference, 1985.

17. Bhat, R.B., "Transverse Vibrations of a Rotating Uniform Cantilever Beam with Tip Mass Using Beam Characteristic Orthogonal Polynomials in Rayleigh-Ritz Method", Journal of Sound and Vibration, Vol. 104, No. 3, 1985.

18. Ritz, W., "Uber Eine Neue Method Zur Losung Gewisser Variation Sprobleme Der Mathematische Physik", Journal Fur Reine Und Angewandte Mathematik, Vol. 135, 1909, pp. 1-61.

19. Ritz, W., "Theorie Der Transverscilschwingungen Einer Quadratischen Platten Mit Freien Randem", Annalen Der Physik, Viente Folge, Vol. 28, 1909, pp. 737-786.

20. Young, D., "Vibration of Rectangular Plates by the Ritz Method", Journal of Applied Mechanics 17, 1950, pp. 448-453.

21. Leissa, A.W., "The Free Vibration of Rectangular Plates", Journal of Sound and Vibration 31, 1973, pp. 257-293.

22. Dickinson, S.M., "The Buckling and Frequency of Flexural Vibration of Rectangular Orthotropic Plates using Rayleigh's Method", Journal of Sound and Vibration 61, 1978, pp. 1-8.

23. Trefftz, E., "Konvergenz und Fehterschatzung Beim Ritzchen Verfahren", Mathematische Annalen, Vol. 100, 1928, p. 503.

24. Courant, R., "Variational Methods for the Solution of Problems of Equilibrium and Vibration", Bulletin of the American Mathematical Society, New York, N.Y., Vol. 49, 1939, pp. 1-23.

25. Colatz, L., "Eigenwertprobleme", Chelsa Publishing Company, New York, N.Y., 1948.

26. Pickett, G., "Solution of Rectangular Clamped Plate with Lateral Lead by Generalized Energy Method", Journal of Applied Mechanics, Transaction ASME, Vol. 61, 1931, p. A-178.

27. Bassily, S.F., Dickinson, S.M., "On the Use of Beam Functions for Problems of Plates Involving Free Edges", Transactions of the ASME, 1975, pp. 858-864.

28. Dickinson, S.M. and Li, E.K.H., "On the Use of Simply Supported Plate Functions in Rayleigh's Method Applied to the Flexural Vibration of Rectangular Plates", Journal of Sound and Vibration 80, 1982, pp. 292-297.

29. Laura, P.A.A., "Comments on the Use of Simply-Supported Plate Functions in the Rayleigh-Ritz Method Applied to the Flexural Vibration of Rectangular Plates", Journal of Sound and Vibration, 84, 1982, pp. 595-597.

30. Goldfracht, E. and Rosenhouse, G., "Use of Lagrange Multipliers with Polynomial Series for Dynamic Analysis of Constrained Plates, Part 1: Polynomial Series", Journal of Sound and Vibration, 92, 1984, pp. 83-93.

31. Bhat, R.B., "Natural Frequencies of Rectangular Plates using Characteristic Orthogonal Polynomials in Rayleigh-Ritz Method", Journal of Sound and Vibration, Vol. 102, No. 3, 1985.

32. Chihara, T.S., "Introduction to Orthogonal Polynomials", Gordon and Breach Science Publishers, London, 1978.

33. Putter, S. and Manor, H., "Natural Frequencies of Radial Rotating Beams", Journal of Sound and Vibration, Vol. 56, 1978, pp. 175-185.

34. Hoa, S.V., "Vibration of a Rotating Beam with Tip Mass", Journal of Sound and Vibration, Vol. 67, 1979, pp. 369-381.

35. Dokainish, M.A. and Rawtani, S., "Vibration Analysis of Rotating Cantilever Plates", International Journal of Numerical Methods in Engineering, Vol. 3, 1971, pp. 233-248.

36. Henry, R. and Lalanne, M., "Vibration Analysis of Rotating Compressor Blades", Transactions of the ASME, 1974, pp. 1028-1035.

37. Shigley, J.E., "Mechanical Engineering Design", McGraw Hill Series in Mechanical Engineering, 1977.

38. Thompson, W.T., "Theory of Vibrators with Application", Englewood Cliffs, New Jersey, Prentice Hall, 1981, pp. 270-271.

39. Whetstone, W.D., "SPAR Structural Analysis Reference Manual", NASA CR-158970-1, 1978.

40. "Structural Analysis System Model 6602", Nicolet Scientific Corporation, 1982.

41. Wang, J.T.H., Mahrenholtz, O. and Bohm, J., "Extended Galerkin's Method for Rotating Beam Vibrations Using Legendre Polynomials", Solid Mechanics Archives, Vol. 1, 1976, pp. 341-365.

APPENDIX A

CONVENTIONAL RALYEIGH-RITZ PROGRAM

This Fortran program computes the natural frequencies and mode shapes for a rotating cantilever beam using conventional Rayleigh-Ritz method.

This program has been referenced in Section 2.2 of Chapter 2.

```
C     ***********************************************************
C     THIS PROGRAM IS USED TO COMPUTE EIGEN-VALUES AND EIGEN-
C     VECTORS FOR A ROTATING STRUCTURE(CANTILEVER BEAM).
C     THE SETTING ANGLE OF THE BLADE WITH RESPECT TO THE
C     PLANE OF ROTATION AND THE HUB RADIUS(RBAR) ON WHICH THE BLADE
C     IS MOUNTED ARE TAKEN INTO ACCOUNT IN THE FORMULATION.
C           THE VARIATION OF NATURAL FREQUENCES AND MODE SHAPES
C     WITH THE SPEED OF ROTATION(ALPHA),SETTING ANGLE(THETA) AND
C     HUB RADIUS ARE STUDIED.
C***********************************************************
       PROGRAM REF(INPUT,OUTPUT)
       DIMENSION A(5,5),B(5,5),AREAL(5),
      1WK(800),BETA(5),BREAL(5),ZREAL(5,5),ZPLEX(5,5),
      1THETA(4),SUMY(10),EIGEN(10)
       COMPLEX ALFA(5),Z(5,5)
C   2   READ*,LIM
        LIM=5
        LIMM=LIM-1
        LIMN=LIM+1
C       IF (LIM.EQ.0) STOP
       PI=ATAN(1.0)*4.
       THETA(1)=0.0
       THETA(2)=PI/6.0
       THETA(3)=PI/3.0
       THETA(4)=PI/2.0
 3     DO 5 MM=1,4
       ANGLE=THETA(MM)*180.0/PI
       PRINT 1000,ANGLE
 1000  FORMAT(20X,*SETTING ANGLE=*,F5.2,1X,*DEGREES*)
       EMU=0.0
       SIGMA=0.0
       AREA=3.14E-4
       SLENGTH=0.1
       EIXX=7.85E-9
       SRBAR=SQRT(EIXX/AREA*SLENGTH**2)
       RBAR=10.0
       ALPHA=0.0
 4     DO 10 I=2,LIMN
       DO 15 J=2,LIMN
       AT1=(COS(THETA(MM)))**2/(I+J+1.)
       AT2=I*J*((RBAR+.5)/(I+J-1.)-RBAR/(I+J)-.5/(I+J+1.))
       AT3=((I*J)/(I+J-1.))*(RBAR+1.)*EMU
       AT4=EMU*(COS(THETA(MM)))**2
       AT5=(I-1.)*(J-1.)*((I*J)/(I+J-3.))
       BT1=(1.)/(I+J+1.)+EMU
       BT2=(SRBAR**2*I*J)/(I+J-1.)
       BT3=SIGMA*I*J
       AJ1=ALPHA**2*(-AT1+AT2+AT3-AT4)+AT5
       BJ1=BT1+BT2+BT3
       A((I-1),(J-1))=AJ1
       B((I-1),(J-1))=BJ1
 15     CONTINUE
 10     CONTINUE
       CALL EIGZF(A,5,B,5,5,2,ALFA,BETA,Z,5,WK,IER)
```

```
      DO 50 I=1,LIM
      DO 55 J=1,LIM
      ZREAL(I,J)=REAL(Z(I,J))
      ZPLEX(I,J)=AIMAG(Z(I,J))
55    CONTINUE
50    CONTINUE
      PRINT 100
100    FORMAT(2X,*NATURAL FREQUENCY WHEN*)
      PRINT 150, ALPHA
150    FORMAT(2X,*ANGULAR VELOCITY=*,F5.2)
      DO 30 I=1,LIM
      AREAL(I)=REAL(ALFA(I))
      BREAL(I)=BETA(I)
30    CONTINUE
      DO 35 I=1,LIM
      EIGEN(I)=SQRT(AREAL(I)/BREAL(I))
 35      CONTINUE
        IF(LIM.EQ.1) GO TO 211
        DO 9 I=1,LIMM
        M=I+1
        DO 11 J=M,LIM
        XXX=(EIGEN(I)-EIGEN(J))
        IF(XXX)12,12,13
 13     TEMP=EIGEN(I)
         EIGEN(I)=EIGEN(J)
         EIGEN(J)=TEMP
 12      CONTINUE
       DO 14 N1=1,LIM
       TEMP1=Z(N1,I)
       Z(N1,I)=Z(N1,J)
       Z(N1,J)=TEMP1
 14    CONTINUE
  11     CONTINUE
   9     CONTINUE
  211 PRINT 400,(EIGEN(I),I=1,LIM)
 400  FORMAT(2X,E16.8)
C5      CONTINUE
        ALPHA=ALPHA+0.5
        IF(ALPHA.GT.10.)GO TO 6
        GO TO 4
 6      CONTINUE
 5      CONTINUE
C       GO TO 2
        END
```

APPENDIX B

ELEMENTS OF THE MATRICES

This appendix gives the elements a_{nk} and b_{nk} of matrices [A] and [B] as mentioned in Section 2.3 of Chapter 2.

The elements a_{nk} and b_{nk} of matrices $[A]$ and $[B]$ are given by:

$$a_{nk} = \frac{1}{(n+1)(k+1)} (A_1 + A_2 + \ldots + A_{16})$$

$$+ \frac{\tilde{r}^2}{(n+1)(k+1)} (A_{17} + A_{18} + \ldots + A_{32})$$

$$b_{nk} = \frac{\alpha^2}{(n+1)(k+1)} (B_1 + B_2 + \ldots + B_{64})$$

$$- \frac{\alpha^2 \cos^2\theta}{(n+1)(k+1)} (A_1 + A_2 + \ldots + A_{16}) +$$

$$+ \frac{1}{(n+1)(k+1)} (B_{65} + B_{66} + \ldots + B_{72})$$

where

$$A_1 = \frac{1}{20(n+2)(k+2)}$$

$$A_2 = -\frac{1}{2(n+7)(n+4)(n+3)(n+2)(k+2)}$$

$$A_3 = -\frac{1}{20(k+2)}; \quad A_4 = \frac{1}{72(k+2)}$$

$$A_5 = \frac{-1}{2(n+2)(k+2)(k+3)(k+4)(k+7)}$$

$$A_6 = \frac{1}{(n+k+9)(k+2)(k+3)(k+4)(n+2)(n+3)(n+4)}$$

$$A_7 = \frac{1}{2(k+2)(k+3)(k+4)(k+7)}$$

$$A_8 = -\frac{1}{6(k+2)(k+3)(k+4)(k+8)}$$

$$A_9 = -\frac{1}{20(n+2)}$$

$$A_{10} = \frac{1}{2(n+2)(n+3)(n+4)(n+7)}$$

$$A_{11} = \frac{1}{20}; \quad A_{12} = -\frac{1}{72}$$

$$A_{13} = \frac{1}{72(n+2)}$$

$$A_{14} = -\frac{1}{6(n+2)(n+3)(n+4)(n+8)}$$

$$A_{15} = -\frac{1}{72}; \quad A_{16} = \frac{1}{252}; \quad A_{17} = \frac{1}{3(n+2)(k+2)}$$

$$A_{18} = -\frac{1}{(n+5)(n+3)(n+2)(k+2)}$$

$$A_{19} = -\frac{1}{3(k+2)} \; ; \; A_{20} = \frac{1}{8(k+2)}$$

$$A_{21} = -\frac{1}{(k+5)(n+2)(k+3)(k+2)}$$

$$A_{22} = \frac{1}{(n+k+7)(n+3)(n+2)(k+3)(k+2)}$$

$$A_{23} = \frac{1}{(k+5)(k+3)(k+2)}$$

$$A_{24} = -\frac{1}{2(k+6)(k+3)(k+2)}$$

$$A_{25} = -\frac{1}{3(n+2)}$$

$$A_{26} = \frac{1}{(n+5)(n+3)(n+2)} \; ; \; A_{27} = \frac{1}{3}$$

$$A_{28} = -\frac{1}{8} \; ; \; A_{29} = \frac{1}{8(n+2)}$$

$$A_{30} = -\frac{1}{2(n+6)(n+3)(n+2)}$$

$$A_{31} = -\frac{1}{8} \; ; \; A_{32} = \frac{1}{20}$$

$$B_1 = \frac{\tilde{R}}{3(n+2)(k+2)}$$

$$B_2 = -\frac{\tilde{R}}{(n+5)(n+3)(n+2)(k+2)}$$

$$B_3 = -\frac{\tilde{R}}{3(k+2)} \; ; \; B_4 = \frac{\tilde{R}}{8(k+2)}$$

$$B_5 = -\frac{\tilde{R}}{(k+5)(n+2)(k+3)(k+2)}$$

$$B_6 = \frac{\tilde{R}}{(n+k+7)(n+3)(n+2)(k+3)(k+2)}$$

$$B_7 = \frac{\tilde{R}}{(k+5)(k+3)(k+2)}$$

$$B_8 = -\frac{\tilde{R}}{2(k+6)(k+3)(k+2)}$$

$$B_9 = -\frac{\tilde{R}}{3(n+2)}$$

$$B_{10} = \frac{\tilde{R}}{(n+5)(n+3)(n+2)} \; ; \quad B_{11} = \frac{\tilde{R}}{3}$$

$$B_{12} = -\frac{\tilde{R}}{8} \; ; \quad B_{13} = \frac{\tilde{R}}{8(n+2)}$$

$$B_{14} = -\frac{\tilde{R}}{2(n+6)(n+3)(n+2)}$$

$$B_{15} = -\frac{\tilde{R}}{8} \; ; \quad B_{16} = \frac{\tilde{R}}{20}$$

$$B_{17} = \frac{1}{6(n+2)(k+2)}$$

$$B_{18} = -\frac{1}{2(n+5)(n+3)(n+2)(k+2)}$$

$$B_{19} = -\frac{1}{6(k+2)} \; ; \quad B_{20} = \frac{1}{16(k+2)}$$

$$B_{21} = -\frac{1}{2(k+5)(n+2)(k+3)(k+2)}$$

$$B_{22} = \frac{1}{2(n+k+7)(n+3)(n+2)(k+3)(k+2)}$$

$$B_{23} = \frac{1}{2(k+5)(k+3)(k+2)}$$

$$B_{24} = -\frac{1}{4(k+6)(k+3)(k+2)}$$

$$B_{25} = -\frac{1}{6(n+2)} \; ; \quad B_{26} = \frac{1}{2(n+5)(n+3)(n+2)}$$

$$B_{27} = \frac{1}{6} \; ; \quad B_{28} = -\frac{1}{16} \; ; \quad B_{29} = \frac{1}{16(n+2)}$$

$$B_{30} = -\frac{1}{4(n+6)(n+3)(n+2)}$$

$$B_{31} = -\frac{1}{16} \; ; \quad B_{32} = \frac{1}{40}$$

$$B_{33} = -\frac{\tilde{R}}{4(n+2)(k+2)}$$

$$B_{34} = \frac{\tilde{R}}{(n+6)(n+3)(n+2)(k+2)}$$

$$B_{35} = \frac{\tilde{R}}{4(k + 2)}; \quad B_{36} = -\frac{\tilde{R}}{10(k + 2)}$$

$$B_{37} = \frac{\tilde{R}}{(k + 6)(n + 2)(k + 3)(k + 2)}$$

$$B_{38} = -\frac{\tilde{R}}{(n + k + 8)(n + 3)(n + 2)(k + 3)(k + 2)}$$

$$B_{39} = -\frac{\tilde{R}}{(k + 6)(k + 3)(k + 2)}$$

$$B_{40} = \frac{\tilde{R}}{2(k + 7)(k + 3)(k + 2)}$$

$$B_{41} = \frac{\tilde{R}}{4(n + 2)}; \quad B_{42} = -\frac{\tilde{R}}{(n + 6)(n + 3)(n + 2)}$$

$$B_{43} = -\frac{\tilde{R}}{4}; \quad B_{44} = \frac{\tilde{R}}{10}; \quad B_{45} = -\frac{\tilde{R}}{10(n + 2)}$$

$$B_{46} = \frac{\tilde{R}}{2(n + 7)(n + 3)(n + 2)}$$

$$B_{47} = \frac{\tilde{R}}{10}; \quad B_{48} = -\frac{\tilde{R}}{24}$$

$$B_{49} = -\frac{1}{10(n + 2)(k + 2)}$$

$$B_{50} = \frac{1}{2(n + 7)(n + 3)(n + 2)(k + 2)}; \quad B_{51} = \frac{1}{10(k + 2)}$$

$$B_{52} = -\frac{1}{24(k + 2)}; \quad B_{53} = -\frac{1}{2(k + 7)(n + 2)(k + 3)(k + 2)}$$

$$B_{54} = -\frac{1}{2(n + k + 9)(n + 3)(n + 2)(k + \ )(k + 2)}$$

$$B_{55} = -\frac{1}{2(k + 7)(k + 3)(k + 2)}; \quad B_{56} = \frac{1}{4(k + 8)(k + 3)(k + 2)}$$

$$B_{57} = \frac{1}{10(n + 2)}; \quad B_{58} = -\frac{1}{2(n + 7)(n + 3)(n + 2)}$$

$$B_{59} = -\frac{1}{10}; \quad B_{60} = \frac{1}{24}; \quad B_{61} = -\frac{1}{24(n + 2)}$$

$$B_{62} = \frac{1}{4(n + 8)(n + 3)(n + 2)}; \quad B_{63} = \frac{1}{24}$$

$$B_{64} = -\frac{1}{56}; \quad B_{65} = \frac{1}{3}; \quad B_{66} = -\frac{1}{(k + 2)(n + 2)}$$

$$B_{67} = -\frac{(n+k)}{2(k+2)(n+2)}; \quad B_{68} = \frac{(n+1)}{(k+2)(n+2)(k+3)}.$$

$$B_{69} = \frac{(k+1)}{(k+2)(n+2)(n+3)}$$

$$B_{70} = -\frac{(n+2)}{(n+2)(k+2)(k+4)}$$

$$B_{71} = -\frac{(k+2)}{(k+2)(n+2)(n+4)}$$

$$B_{72} = \frac{1}{(n+2)(k+2)(n+k+5)}$$

APPENDIX C

PROGRAM FOR IMPROVED STRAIN ENERGY FORMULATION IN RAYLEIGH-RITZ METHOD

This Fortran program is used to obtain the natural frequencies and mode shapes for a rotating cantilever beam using improved strain energy formulation in Rayleigh-Ritz method. This program was referenced in Section 2.3 of Chapter 2.

```
C     ************************************************************
C     THIS PROGRAM IS USED TO COMPUTE EIGEN-VALUES AND EIGEN-
C     VECTORS FOR A ROTATING STRUCTURE(CANTILEVER BEAM).AN
C     IMPROVED STRAIN-ENERGY FORMULATION IN RAYLEIGH-RITZ
C     METHOD IS CARRIED OUT BY SUCCESIVE INTEGRATION OF THE
C     ASSUMED DEFLECTION FUNCTION TO OBTAIN THE MOMENT
C     DISTRIBUTION WHICH IS USED TO OBTAIN THE STRAIN ENERGY OF
C     THE BLADE.THE SETTING ANGLE OF THE BLADE WITH RESPECT TO THE
C     PLANE OF ROTATION AND THE HUB RADIUS(RBAR) ON WHICH THE BLADE
C     IS MOUNTED ARE TAKEN INTO ACCOUNT IN THE FORMULATION.
C           THE VARIATION OF NATURAL FREQUENCES AND MODE SHAPES
C     WITH THE SPEED OF ROTATION(ALPHA),SETTING ANGLE(THETA) AND
C     HUB RADIUS ARE STUDIED.
C*****************************************************************
      PROGRAM CANTI(INPUT,OUTPUT)
      COMPLEX ALFA(10),Z(10,10)
       REAL LAB
       DIMENSION A(10,10),B(10,10),BETA(10),WK(300),EIG(10)
     1 ,THETA(4),LAB(10),ZZ(5,5),YY(10)
C2      READ*,LIM
      LIM=5
      LIMM=LIM-1
       LIMN=LIM+1
C     IF (LIM.EQ.0) STOP
      PI=ATAN(1.0)*4
      THETA(1)=0.0
      THETA(2)=PI/6.0
      THETA(3)=PI/3.0
      THETA(4)=PI/2.0
   3  DO 5 MM=1,4
      ANGLE=THETA(MM)*180.0/PI
      PRINT 1000,ANGLE
 1000 FORMAT(20X,*SETTING ANGLE=*,F5.2,1X,*DEGREES*)
      AREA=3.14E-4
      SLENGTH=1.0
      EIXX=7.85E-9
      SRBAR=(EIXX/(AREA*SLENGTH**2))
      RBAR=0.0
      DO 6 II=5,20,5
      ALPHA=II-5
   4  DO 7 K=2,LIMN
      DO 7 N=2,LIMN
      KK=K-1
      NN=N-1
      P=K
      Q=N
      AT1=(COS(THETA(MM)))**2
      AT2=(1.)/((Q+1.)*(P+1.))
      AT3=(1.)/(20.*(Q+2.)*(P+2.))
      AT4=(1.)/(2.*(Q+7.)*(Q+4.)*(Q+3.)*(Q+2.)*(P+2.))
      AT5=(1.)/(20.*(P+2.))
      AT6=(1.)/(72.*(P+2.))
      AT7=(1.)/(2.*(Q+2.)*(P+2.)*(P+3.)*(P+4.)*(P+7.))
      AT8=(1.)/((Q+P+9.)*(P+2.)*(P+3.)*(P+4.)*(Q+2.)*(Q+3.)
     1*(Q+4.))
      AT9=(1.)/(2.*(P+2.)*(P+3.)*(P+4.)*(P+7.))
```

```
      BT48=(RBAR)/10.
      BT49=(RBAR)/24.
      BT50=(1.)/(10.*(Q+2.)*(P+2.))
      BT51=(1.)/(2.*(Q+7.)*(Q+3.)*(Q+2.)*(P+2.))
      BT52=(1.)/(10.*(P+2.))
      BT53=(1.)/(24.*(P+2.))
      BT54=(1.)/(2.*(P+7.)*(Q+2.)*(P+3.)*(P+2.))
      BT55=(1.)/(2.*(Q+P+9.)*(Q+3.)*(Q+2.)*(P+3.)*(P+2.))
      BT56=(1.)/(2.*(P+7.)*(P+3.)*(P+2.))
      BT57=(1.)/(4.*(P+8.)*(P+3.)*(P+2.))
      BT58=(1.)/(10.*(Q+2.))
      BT59=(1.)/(2.*(Q+7.)*(Q+3.)*(Q+2.))
      BT60=(1.)/10.
      BT61=(1.)/24.
      BT62=(1.)/(24.*(Q+2.))
      BT63=(1.)/(4.*(Q+8.)*(Q+3.)*(Q+2.))
      BT64=(1.)/24.
       BT65=(1.)/56.
C      ***********************************************************
      CT1=(1.)/((Q+1.)*(P+1.))
      CT2=(1.)/3.
      CT3=(1.)/((P+2.)*(Q+2.))
      CT4=1.
      CT5=0.5*(Q+P)
      CT6=((Q+1.)/(P+3.))
      CT7=((P+1.)/(Q+3.))
      CT8=((Q+2.)/(P+4.))
      CT9=((P+2.)/(Q+4.))
      CT10=(1.)/(Q+P+5.)
C         ***********************************************************
      DT1=(1.)/((Q+1.)*(P+1.))
      DT2=(1.)/(3.*(Q+2.)*(P+2.))
      DT3=(1.)/((Q+5.)*(Q+3.)*(Q+2.)*(P+2.))
      DT4=(1.)/(3.*(P+2.))
      DT5=(1.)/(8.*(P+2.))
      DT6=(1.)/((P+5.)*(Q+2.)*(P+3.)*(P+2.))
      DT7=(1.)/((Q+P+7.)*(Q+3.)*(Q+2.)*(P+3.)*(P+2.))
      DT8=(1.)/((P+5.)*(P+3.)*(P+2.))
      DT9=(1.)/(2.*(P+6.)*(P+3.)*(P+2.))
      DT10=(1.)/(3.*(Q+2.))
      DT11=(1.)/((Q+5.)*(Q+3.)*(Q+2.))
      DT12=(1.)/3.
      DT13=(1.)/8.
      DT14=(1.)/(8*(Q+2.))
      DT15=(1.)/(2.*(Q+6.)*(Q+3.)*(Q+2.))
      DT16=(1.)/8.
      DT17=(1.)/20.
      DTT1=AT2*(AT3-AT4-AT5+AT6-AT7+AT8+AT9-AT10-AT11
     1+AT12+AT13-AT14+AT15-AT16-AT17+AT18)
      DTT2=SRBAR*DT1*(DT2-DT3-DT4+DT5-DT6+DT7+DT8-DT9-DT10
     1+DT11+DT12-DT13+DT14-DT15-DT16+DT17)
      DTT=DTT1+DTT2
C          ***********************************************************
       ATT=(ALPHA**2*(AT1*AT2)*(AT3-AT4-AT5+AT6-AT7+AT8+AT9-AT10-AT11
     1+AT12+AT13-AT14+AT15-AT16-AT17+AT18))
```

```
      AT10=(1.)/(6.*(P+2.)*(P+3.)*(P+4.)*(P+8.))
      AT11=(1.)/(20.*(Q+2.))
      AT12=(1.)/(2.*(Q+2.)*(Q+3.)*(Q+4.)*(Q+7.))
      AT13=(1.)/20.
      AT14=(1.)/72.
      AT15=(1.)/(72.*(Q+2.))
      AT16=(1.)/(6.*(Q+2.)*(Q+3.)*(Q+4.)*(Q+8.))
      AT17=(1.)/72.
      AT18=(1.)/(252.)
C      ****************************************************
       BT1=(1.)/((Q+1)*(P+1))
      BT2=RBAR/(3.*(Q+2.)*(P+2.))
      BT3=(RBAR)/((Q+5.)*(Q+3.)*(Q+2.)*(P+2.))
      BT4=(RBAR)/(3.*(P+2.))
      BT5=(RBAR)/(8.*(P+2.))
      BT6=(RBAR)/((P+5.)*(Q+2.)*(P+3.)*(P+2.))
      BT7=(RBAR)/((Q+P+7.)*(Q+3.)*(Q+2.)*(P+3.)*(P+2.))
      BT8=(RBAR)/((P+5.)*(P+3.)*(P+2.))
      BT9=(RBAR)/(2.*(P+6.)*(P+3.)*(P+2.))
      BT10=(RBAR)/(3.*(Q+2.))
      BT11=(RBAR)/((Q+5.)*(Q+3.)*(Q+2.))
      BT12=(RBAR)/3.
      BT13=(RBAR)/8.
      BT14=(RBAR)/(8.*(Q+2.))
      BT15=(RBAR)/(2.*(Q+6.)*(Q+3.)*(Q+2.))
      BT16=(RBAR)/8.
      BT17=(RBAR)/20.
      BT18=(1.)/(6.*(Q+2.)*(P+2.))
      BT19=(1.)/(2.*(Q+5.)*(Q+3.)*(Q+2.)*(P+2.))
      BT20=(1.)/(6.*(P+2.))
      BT21=(1.)/(16.*(P+2.))
      BT22=(1.)/(2.*(P+5.)*(Q+2.)*(P+3.)*(P+2.))
      BT23=(1.)/(2.*(Q+P+7.)*(Q+3.)*(Q+2.)*(P+3.)*(P+2.))
      BT24=(1.)/(2.*(P+5.)*(P+3.)*(P+2.))
      BT25=(1.)/(4.*(P+6.)*(P+3.)*(P+2.))
      BT26=(1.)/(6.*(Q+2.))
      BT27=(1.)/(2.*(Q+5.)*(Q+3.)*(Q+2.))
      BT28=(1.)/6.
      BT29=(1.)/16.
      BT30=(1.)/(16.*(Q+2.))
      BT31=(1.)/(4.*(Q+6.)*(Q+3.)*(Q+2.))
      BT32=(1.)/16.
      BT33=1./(40.)
      BT34=(RBAR)/(4.*(Q+2.)*(P+2.))
      BT35=(RBAR)/((Q+6.)*(Q+3.)*(Q+2.)*(P+2.))
      BT36=(RBAR)/(4.*(P+2.))
      BT37=(RBAR)/(10.*(P+2.))
      BT38=(RBAR)/((P+6.)*(Q+2.)*(P+3.)*(P+2.))
      BT39=(RBAR)/((Q+P+8.)*(Q+3.)*(Q+2.)*(P+3.)*(P+2.))
      BT40=(RBAR)/((P+6.)*(P+3.)*(P+2.))
      BT41=(RBAR)/(2.*(P+7.)*(P+3.)*(P+2.))
      BT42=(RBAR)/(4.*(Q+2.))
      BT43=(RBAR)/((Q+6.)*(Q+3.)*(Q+2.))
      BT44=(RBAR)/4.
      BT45=(RBAR)/10.
      BT46=(RBAR)/(10.*(Q+2.))
      BT47=(RBAR)/(2.*(Q+7.)*(Q+3.)*(Q+2.))
```

```
      BTT=(ALPHA**2*((BT1)*(BT2-BT3-BT4+BT5-BT6+BT7+BT8-BT9-BT10
     1+BT11+BT12-BT13+BT14-BT15-BT16+BT17+BT18-BT19-BT20
     1+BT21-BT22+BT23+BT24-BT25-BT26+BT27+BT28-BT29+BT30
     1-BT31-BT32+BT33-BT34+BT35+BT36-BT37+BT38-BT39-BT40
     1+BT41+BT42-BT43-BT44+BT45-BT46+BT47+BT48-BT49-BT50
     1+BT51+BT52-BT53+BT54-BT55-BT56+BT57+BT58-BT59-BT60+BT61
     1-BT62+BT63+BT64-BT65)))
      CTT=((CT1)*(CT2+(CT3*(-1.*CT4-CT5+CT6+CT7-CT8-CT9+CT10))))
      A(KK,NN)=CTT+BTT-ATT
      B(KK,NN)=BTT
7     CONTINUE
      CALL EIGZF(A,10,B,10,LIM,2,ALFA,BETA,Z,10,WK,IER)
      PRINT 500
500   FORMAT(2X,*NATURAL FREQUENCY WHEN*)
      PRINT 550,ALPHA
550   FORMAT(2X,*ANGULAR VELOCITY=*,F5.2)
      DO 8 I=1,LIM
      EIG(I)=(ALFA(I))/BETA(I)
      LAB(I)=SQRT(EIG(I))
8      CONTINUE
      IF(LIM.EQ.1)GO TO 211
      DO 9 I=1,LIMM
      M=I+1
      DO 10 J=M,LIM
      XXX=(LAB(I)-LAB(J))
      IF(XXX)11,11,12
12    TEMP=LAB(I)
      LAB(I)=LAB(J)
      LAB(J)=TEMP
11       CONTINUE
      DO 13 N1=1,LIM
      TEMP1=Z(N1,I)
      Z(N1,I)=Z(N1,J)
      Z(N1,J)=TEMP1
13      CONTINUE
10    CONTINUE
9     CONTINUE
211   PRINT 600,(LAB(I),I=1,LIM)
600   FORMAT(E16.8)
      PRINT 700
700   FORMAT(/2X,*CORRESPONDING EIGEN VECTORS*/)
      DO 14 I=1,LIM
      DO 14 J=1,LIM
      ZZ(I,J)=REAL(Z(I,J))
14    CONTINUE
      DO 15 I=1,LIM
      PRINT 800,(ZZ(I,J),J=1,LIM)
800   FORMAT(2X,5F12.4)
15    CONTINUE
```

```
C       ALPHA=ALPHA+0.5
C       IF(ALPHA.GT.10.) GO TO 20
        DO 16 J=1,LIM
        DO 17 LL=1,10
        ZBAR=LL/10.0
        SUM=0.0
        DO 18 I=1,5
        SUM=ZZ(I,J)*ZBAR**(1.+I)+SUM
 18     CONTINUE
        YY(LL)=SUM
 17     CONTINUE
        DO 19 LL=1,10
        YY(LL)=YY(LL)/ABS(YY(10))
 19     CONTINUE
        PRINT 900,(YY(LL),LL=1,10)
 900    FORMAT(2X,*Y=*,1X,10E12.4,/)
 16     CONTINUE
 20     CONTINUE
  6     CONTINUE
  5     CONTINUE
C       GO TO 2
        END
```

APPENDIX D

SAMPLE LISTING OF TABLE OF CONTENTS AND A RUN STREAM USED IN SPAR

This appendix gives a listing of table of contents stored in SPAR data base and a typical run stream used to calculate the natural frequencies for a rotating cantilever beam.

Each line of the table contains information denoting when the data was created, the name of the data set and the number of words in the data sets.

References were made to this appendix in Section 3.1 and Section 3.2 of Chapter 3 respectively.

Example of TOC

TABLE OF CONTENTS, LIBRARY 2

SEQ	PR	DATE	TIME	ER	WORDS	NJ	NI*NJ	TY	DATA SET NAME N1	N2	N3	N4
1	-17	080775	172617	0	18	1	18	0	JDF1	BTAB	1	9
2	-18	080775	172617	0	5	5	5	0	JREF	BTAB	2	6
3	-19	080775	172617	0	12	1	12	1	ALTR	BTAB	2	4
4	20	080775	172617	0	18	1	18	0	JDF1	BTAB	1	8
5	21	080775	172617	0	5	5	5	0	JREF	BTAB	2	6
6	22	080775	172617	0	12	1	12	1	ALTR	BTAB	2	4
7	23	080775	172617	0	15	5	15	1	JLOC	BTAB	2	5
8	24	080775	172617	0	10	1	10	1	MATC	BTAB	2	2
9	25	080775	172617	0	5	1	5	1	MREF	BTAB	2	7
10	26	080775	172617	0	31	1	31	1	BA	BTAB	2	9
11	28	080775	172617	0	5	5	5	0	CON		1	0
12	29	080775	172617	0	45	5	45	1	OUJT	BTAB	2	19
13	31	080775	172617	0	64	4	896	0	DEF	E21	1	2
14	34	080775	172617	0	2	1	2	0	GD	E21	1	2
15	35	080775	172617	0	15	1	15	0	GTIT	E21	1	2
16	36	080775	172617	0	12	12	12	0	NELS	BTAB	1	11
17	37	080775	172617	0	5	1	5	0	*E		0	0
18	38	080775	172617	0	7	1	7	0	NS		0	0
19	39	080775	172617	0	1	1	1	3	ELTS	NAME	0	0
20	40	080775	172617	0	1	1	1	0	ELTS	LTYP	0	0
21	41	080775	172617	0	1	1	1	0	ELTS	NNOD	0	0
22	42	080775	172617	0	1	1	1	0	ELTS	ISCT	0	0
23	43	080775	172617	0	1	1	1	0	ELTS	NELS	0	0
24	44	080775	172617	0	1	1	1	0	ELTS	LE3	0	0
25	45	080775	172617	0	560	4	140	4	E21	EFIL	1	2
26	65	080775	172617	0	20	20	20	0	DIR	E21	1	2
27	66	080775	172617	0	30	5	30	-1	DEM	DIAG	0	0
28	68	080775	172617	0	996	5	996	0	*MAP		9	3
29	100	080775	172617	0	1792	5	1792	0	AMAP	aaaa	9	3
30	164	080775	172617	0	2240	5	2240	1	*	SPAR	36	0
31	244	080775	172617	0	3584	5	3584	1	INV	*	1	0
32	272	080775	172617	0	30	5	30	-1	APPL	FORC	1	1
33	288	080775	172617	0	15	1	15	4	CASE	TITL	1	1
34	389	080775	172617	0	30	5	30	-1	STAT	DISP	1	1
35	391	080775	172617	0	30	5	30	-1	STAT	REAC	1	1
36	393	080775	172617	0	204	4	5600	-1	STRS	E21	1	1
37	401	080775	172617	0	2240	5	2240	1	*G	SPAR	36	0
38	-431	080775	172617	0	18	1	18	4	NDAL		0	0
39	432	080775	173455	0	18	1	18	4	NDAL		0	0

```
[XQT TAB
START 16
MATC;1
JLOC;1
BB
1; 8.6815-5;;;;$
2; 4.3047-5;;;;$
[XQT ELD
E25; NSECT=1;2 2;3 3;4 4;5 5;6 6;7 7;8 8
              9 9;10 10;11 11;12 12;13 13;14 14;15 15
     NSECT=2;1 1;16 16
[XQT TOPO
[XQT E
[XQT EKS
[XQT K
[XQT EXIT
[XQT DCU
COPY 1,2 K SPAR 36 0
CHANGE 2 K SPAR 36 0,G SPAR 36 0
CHANGE 1 K SPAR 36 0, NO NEED 36 0
[XQT TAB
       START 16
       MATC$
       1,10.0+6,0.3,0.1
ALTREF$
2,1,0,2,0,3,0
       JLOC$
1,0,0,0,0,40,0,16,1
       E21 SECTION PROPERTIES$
       GIVN 1 4.-5 0. 6.-5 0. 1.-3 .7954-4
       MREF$
       1 1 3 1  0
       CONSTRAINT DEFINITION 1
       ZERO 1 2 3 4 5 6 ;1
       [XQT ELD
       E21
       1 2 1 15
       [XQT TOPO
       [XQT E
       RESET G=386.
       [XQT EKS
       [XQT K
       [XQT INV
       [XQT EIG
       RESET INIT=6
```

```
        [XQT AUS
        SYSVEC;WS
        I=1 2;J=1,16;3947.8418 3947.8418
        KC=PROD(WS,DEM)
        KEKC=SUM(K,-1.0 KC)
        TABLE(NI=6,NJ=16);P
        TRAN(SOURCE=JLOC,ILIM=3,JLIM=16,DSKIP=3)
        APPLIED FORCE 1 0=PRODUCT(KC,P)
        [XQT INV
        RESET K=KEKC
        [XQT SSOL
        RESET K=KEKC
        [XQT GSF
        RESET EMBED=1
        [XQT KG
        [XQT AUS
        KECG=SUM(KEKC,KG)
        [XQT DCU
        COPY 2,1 G SPAR 36 0
[XQT INV
        RESET K=KECG
        [XQT AUS
        DEFINE V=VIBR MODE 1 1
        DEFINE E=VIBR RVAL 1 1
        RVEC CEIG 1 1=UNION(V)
        IVEC CEIG 1 1=UNION(0. V)
        RVAL CEIG 1 1=UNION(0. E)
        IVAL CEIG 1 1=SQRT(E)
        [XQT CEIG
        RESET HIST=1
        RESET NREQ=4
        RESET CBAL=1
        M=1 DEM
        K=1 KECG
        G= 1 G
        KINV= 1 INV KECG
        [XQT EXIT
```

APPENDIX E

PROGRAM FOR COMPUTING NATURAL FREQUENCIES AND MODE SHAPES FOR CANTILEVER PLATE USING ORTHOGONAL POLYNOMIALS

This Fortran program is used to calculate the natural frequencies and mode shapes for a cantilever plate using beam characteristic orthogonal polynomials as deflection functions in Rayleigh-Ritz method.

Reference was made to this program in Section 4.3 of Chapter 4.

```
      PROGRAM PLTFF3(INPUT,OUTPUT)
C*****************************************************************
C       THIS PGM IS USED TO CALCULATE EIGEN VALUES AND   *
C       EIGEN VECTORS FOR A CANTILEVER PLATE.            *
C*****************************************************************
      EXTERNAL PHI,PHI11,PHI20,PHI22,PHIQX,PHIQY
      COMPLEX ALFA(36),Z(36,36),TEMPC
      DIMENSION ENT(12,12),AKS(36,36),AMS(36,36),
     1WK(6000),BETA(36),DEFL(11),F(36)
      COMMON/PARA/A(12,12),C(12,12),L,M,N,LIM
      READ*,ALPHA,ENU,MMMM,NNNN
      PRINT 4,ALPHA,ENU,MMMM,NNNN
 4    FORMAT(2X,'ALPHA=',F3.1/,2X,'ENU=',F3.2/,2X,'MMMM=',I3/,
     12X,'NNNN=',I3)
      LIM=1
      LOOP=1
 5    CONTINUE
      DO 10 I=1,12
      DO 10 J=1,12
      A(I,J)=0.
   10 CONTINUE
      IF(LOOP.EQ.2) GO TO 7
      A(1,3)=6.0
      A(1,4)=-4.0
      A(1,5)=1.0
      IF(LOOP.EQ.1) GO TO 6
 7    A(1,1)=1.0
 6    CONTINUE
      L=0
      M=1
      N=1
      CALL QG10(0.,1.,PHI,EI2)
      DO 12 J=1,12
      A(1,J)=A(1,J)/(SQRT(EI2))
   12 CONTINUE
      PRINT 100,1
      PRINT 110,(A(1,J),J=1,12)
      CK=0.
      K2=1
      DO 20 K=2,12
      M=K-1
      N=K-1
      L=1
      CALL QG10(0.,1.,PHI,EI1)
      L=0
      CALL QG10(0.,1.,PHI,EI2)
      BK=EI1/EI2
      IF(K.EQ.2)GO TO 16
      M=K-1
      N-K-2
      L=1
      CALL QG10(0.,1.,PHI,EI3)
      M=K-2
      N=K-2
      L=0
```

```
      CALL QG10(0.,1.,PHI,EI4)
      CK=EI3/EI4
      K2=K-2
   16 K1=K-1
      A(K,1)=-BK*A(K1,1)-CK*A(K2,1)
      DO 25 J=2,12
      J1=J-1
      A(K,J)=A(K1,J1)-BK*A(K1,J)-CK*A(K2,J)
   25 CONTINUE
      M=K
      N=K
      L=0
      CALL QG10(0.,1.,PHI,EN)
      ENSQ=SQRT(EN)
C     FACTOR=A(K,1)/(ABS(A(K,1)))
      DO 30 J=1,12
      A(K,J)=A(K,J)/ENSQ
   30 CONTINUE
      PRINT 100,K
  100 FORMAT(2X,'A(K,J),K=',I3)
      PRINT 110,(A(K,J),J=1,12)
  110 FORMAT(2X,5E20.8)
   20 CONTINUE
      DO 50 I=1,12
      DO 50 J=1,12
      M=I
      N=J
      CALL QG10(0.,1.,PHI,ENTEG)
      ENT(I,J)=ENTEG
   50 CONTINUE
      PRINT 120
  120 FORMAT(2X,'ORTHOGONALITY PRINCIPLE')
      PRINT 130,((ENT(I,J),I=1,12),J=1,12)
  130 FORMAT(2X,5E20.8)
      IF(LOOP.EQ.2) GO TO 132
      DO 131 I=1,12
      DO 131 J=1,12
      C(I,J)=A(I,J)
131   CONTINUE
      LOOP=LOOP+1
      IF(LOOP.EQ.2) GO TO 5
132   CONTINUE
      L=0
      DO 70 II=1,MMMM
      DO 70 JJ=1,NNNN
      KK=JJ+NNNN*(II-1)
      DO 75 MM=1,MMMM
      DO 75 NN=1,NNNN
      LL=NN+NNNN*(MM-1)
      M=MM
      N=II
      LIM=1
      CALL QG10(0.,1.,PHI,TM1)
      CALL QG10(0.,1.,PHI22,TK1)
      CALL QG10(0.,1.,PHI20,TK2)
      CALL QG10(0.,1.,PHI11,TK3)
      M=II
```

```
      N=MM
      CALL QG10(0.,1.,PHI20,TK4)
      M=NN
      N=JJ
      LIM=2
      CALL QG10(0.,1.,PHI,TM2)
      CALL QG10(0.,1.,PHI22,TK5)
      CALL QG10(0.,1.,PHI20,TK6)
      CALL QG10(0.,1.,PHI11,TK7)
      M=JJ
      N=NN
      CALL QG10(0.,1.,PHI20,TK8)
C     PRINT 1001,TM1,TM2,TK1,TK2,TK3,TK4,TK5,TK6,TK7,TK8
C1001 FORMAT(2X,*TM, TK=*,5E15.8)
      AMS(KK,LL)=TM1*TM2
      TEMP1=TK1*TM2
      TEMP2=ALPHA**4*TK5*TM1
      TEMP3=ENU*ALPHA**2*(TK2*TK8+TK4*TK6)
      TEMP4=2.*(1.-ENU)*ALPHA**2*TK3*TK7
      AKS(KK,LL)=TEMP1+TEMP2+TEMP3+TEMP4
   75 CONTINUE
  70  CONTINUE
      MMNN=MMMM*NNNN
C     PRINT 150,((AMS(KK,LL),LL=1,MMNN),KK=1,MMNN)
      CALL EIGZF(AKS,36,AMS,36,MMNN,2,ALFA,BETA,Z,36,WK,IER)
      DO 90 I=1,MMNN
      F(I)=REAL(ALFA(I))/BETA(I)
      F(I)=SQRT(F(I))
  90    CONTINUE
        PRINT 150,(F(I),I=1,MMNN)
      MMNN1=MMNN-1
       DO 105 I=1,MMNN1
      L=I+1
       DO 105 J=L,MMNN
       IF(F(I)-F(J))105,105,115
  115   TEMP=F(I)
       F(I)=F(J)
       F(J)=TEMP
       DO 125 NI=1,MMNN
       TEMPC=Z(NI,I)
       Z(NI,I)=Z(NI,J)
       Z(NI,J)=TEMPC
 125    CONTINUE
 105    CONTINUE
      PRINT 140
  140 FORMAT(2X,'EIGENVALUES AND EIGENVECTORS',/)
       PRINT 150,(F(I),I=1,MMNN)
  150 FORMAT(2X,8E12.6)
      PRINT 2000
 2000  FORMAT(2X,'ORTHOGONAL POLYNOMIAL FUNCTION VALUES')
      DO 300 IM=1,MMMM
      M=IM
      DO 300 I=1,21
      X=(I-1)/20.
      FVAL=POLY(X)
```

```
      PRINT 2001,X,FVAL
300    CONTINUE
      DO 301 IN=1,NNNN
      N=IN
      DO 301 I=1,21
      Y=(I-1)/20.
      FVAL=POLLY(Y)
      PRINT 2001,Y,FVAL
301    CONTINUE
2001   FORMAT(2X,F8.3,E15.5)
      DO 400 K=1,6
      DO 401 KX=1,11
      X=(KX-1)/10.
      DO 405 KY=1,11
      Y=(KY-1)/10.
      DEFL(KY)=0.
      DO 402 I=1,MMMM
      M=I
      TEMPX=POLY(X)
      DO 403 J=1,NNNN
      IJ=J+NNNN*(I-1)
      N=J
      TEMPY=POLLY(Y)
      DEFL(KY)=DEFL(KY)+Z(IJ,K)*TEMPX*TEMPY
403    CONTINUE
402    CONTINUE
405    CONTINUE
      PRINT 3001,X,(DEFL(KY),KY=1,11)
401    CONTINUE
400    CONTINUE
3001   FORMAT(2X,F6.2,11F10.6,///////)
      STOP
      END
      FUNCTION PHI(X)
      COMMON/PARA/A(12,12),C(12,12),L,M,N,LIM
      PHIM=0.
      PHIN=0.
      DO 10 J=1,12
      K=J-1
      IF(LIM.EQ.2) GO TO 20
      PHIM=A(M,J)*X**K+PHIM
      PHIN=A(N,J)*X**K+PHIN
      GO TO 30
   20 PHIM=C(M,J)*X**K+PHIM
      PHIN=C(N,J)*X**K+PHIN
   30   CONTINUE
   10 CONTINUE
      IF(L.EQ.1)PHIM=PHIM*X
      PHI=PHIM*PHIN
      RETURN
      END
```

```
      FUNCTION POLY(X)
      COMMON/PARA/A(12,12),C(12,12),L,M,N,LIM
      PHIMT=A(M,1)
      DO 10 J=2,12
      K=J-1
      PHIMT=A(M,J)*X**K+PHIMT
 10    CONTINUE
      POLY=PHIMT
      RETURN
      END
      FUNCTION POLLY(Y)
      COMMON/PARA/A(12,12),C(12,12),L,M,N,LIM
      PHINT=C(N,1)
      DO 10 J=2,12
      K=J-1
      PHINT=C(N,J)*Y**K+PHINT
 10   CONTINUE
      POLLY=PHINT
      RETURN
      END
      FUNCTION PHI11(X)
      COMMON/PARA/A(12,12),C(12,12),L,M,N,LIM
      PHIM1=0.
      PHIN1=0.
      DO 10 J=2,12
      K=J-1
      KN=J-2
      IF(LIM.EQ.2) GO TO 20
      PHIM1=K*A(M,J)*X**KN+PHIM1
      PHIN1=K*A(N,J)*X**KN+PHIN1
      GO TO 30
   20 PHIM1=K*C(M,J)*X**KN+PHIM1
      PHIN1=K*C(N,J)*X**KN+PHIN1
   30 CONTINUE
   10 CONTINUE
      PHI11=PHIM1*PHIN1
      RETURN
      END
      FUNCTION PHI20(X)
      COMMON/PARA/A(12,12),C(12,12),L,M,N,LIM
      PHIM2=0.
      PHIN=0.
      DO 10 J=3,12
      IF(LIM.EQ.2) GO TO 30
      K=J-1
      KN=J-2
```

```
      KM=J-3
      PHIM2=K*KN*A(M,J)*X**KM+PHIM2
10    CONTINUE
      DO 20 J=1,12
      K=J-1
      PHIN=A(N,J)*X**K+PHIN
20     CONTINUE
      GO TO 50
   30 DO 60 J=3,12
      K=J-1
      KN=J-2
      KM=J-3
      PHIM2=K*KN*C(M,J)*X**KM+PHIM2
60    CONTINUE
      DO 70 J=1,12
      K=J-1
      PHIN=C(N,J)*X**K+PHIN
   70 CONTINUE
   50 CONTINUE
      PHI20=PHIM2*PHIN
      RETURN
      END
      FUNCTION PHI22(X)
      COMMON/PARA/A(12,12),C(12,12),L,M,N,LIM
      PHIM2=0.
      PHIN2=0.
      DO 10 J=3,12
      K=J-1
      KN=J-2
      KM=J-3
      IF(LIM.EQ.2) GO TO 20
      PHIM2=K*KN*A(M,J)*X**KM+PHIM2
      PHIN2=K*KN*A(N,J)*X**KM+PHIN2
      GO TO 30
   20 PHIM2=K*KN*C(M,J)*X**KM+PHIM2
      PHIN2=K*KN*C(N,J)*X**KM+PHIN2
   30 CONTINUE
   10 CONTINUE
      PHI22=PHIM2*PHIN2
      RETURN
      END
```

APPENDIX F

PROGRAM FOR COMPUTING NATURAL FREQUENCIES AND MODE SHAPES FOR FREE-FREE PLATE USING ORTHOGONAL POLYNOMIALS

This Fortran program is used to calculate the natural frequencies and mode shapes for a free-free plate using beam characteristic orthogonal polynomials as deflection functions in Rayleigh-Ritz method.

Reference was made to this program in Section 4.4 of Chapter 4.

```
      PROGRAM PLFRFR(INPUT,OUTPUT)
      EXTERNAL PHI,PHI11,PHI20,PHI22
      COMPLEX ALFA(36),Z(36,36),TEMPC
      DIMENSION ENT(12,12),AMS(36,36),AKS(36,36),
     1WK(6000),BETA(36),DEFL(11),F(36)
C**********************************************
C        THIS PROGRAM IS USED TO CALCULATE THE
C     NATURAL FREQUENCIES AND MODE SHAPESOF A
C     FREE-FREE PLATE.
C**********************************************
      COMMON/PARA/A(12,12),L,M,N
      READ *,ALPHA,ENU,MMMM,NNNN
       PRINT 5,ALPHA,ENU,MMMM,NNNN
  5   FORMAT(2X,'ALPHA=',F3.1/,2X,'ENU=',F3.2/,2X,'MMMM=',I
     12X,'NNNN=',I3)
      DO 10 I=1,12
      DO 10 J=1,12
      A(I,J)=0.
   10 CONTINUE
      A(1,1)=1.
      L=0
      M=1
      N=1
      CALL QG10(0.,1.0,PHI,EI2)
      DO 12 J=1,12
      A(1,J)=A(1,J)/(SQRT(EI2))
   12 CONTINUE
      PRINT 100,1
      PRINT 110,(A(1,J),J=1,12)
      CK=0.
      K2=1
      DO 20 K=2,12
      M=K-1
      N=K-1
      L=1
      CALL QG10(0.,1.0,PHI,EI1)
      L=0
      CALL QG10(0.,1.0,PHI,EI2)
      BK=EI1/EI2
      IF(K.EQ.2)GO TO 16
      M=K-1
      N=K-2
      L=1
      CALL QG10(0.,1.0,PHI,EI3)
      M=K-2
      N=K-2
      L=0
      CALL QG10(0.,1.0,PHI,EI4)
      CK=EI3/EI4
      K2=K-2
   16 K1=K-1
```

```
      A(K,1)=-BK*A(K1,1)-CK*A(K2,1)
      DO 25 J=2,12
      J1=J-1
      A(K,J)=A(K1,J1)-BK*A(K1,J)-CK*A(K2,J)
   25 CONTINUE
      M=K
      N=K
      L=0
      CALL QG10(0.,1.0,PHI,EN)
      ENSQ=SQRT(EN)
      DO 30 J=1,12
      A(K,J)=A(K,J)/ENSQ
   30 CONTINUE
      PRINT 100,K
  100 FORMAT(2X,'A(K,J),K=',I3)
      PRINT 110,(A(K,J),J=1,12)
  110 FORMAT(2X,6E20.8)
   20 CONTINUE
      DO 50 I=1,12
      DO 50 J=1,12
      M=I
      N=J
      CALL QG10(0.,1.0,PHI,ENTEG)
      ENT(I,J)=ENTEG
   50 CONTINUE
      PRINT 120
  120 FORMAT(2X,'ORTHOGONALITY PRINCIPLE')
      PRINT 130,((ENT(I,J),I=1,12),J=1,12)
  130 FORMAT(2X,6E20.8)
      L=0
      DO 70 II=1,MMMM
      DO 70 JJ=1,NNNN
      KK=JJ+NNNN*(II-1)
      DO 75 MM=1,MMMM
      DO 75 NN=1,NNNN
      LL=NN+NNNN*(MM-1)
      M=MM
      N=II
      CALL QG10(0.,1.0,PHI,TM1)
      CALL QG10(0.,1.0,PHI22,TK1)
      CALL QG10(0.,1.0,PHI20,TK2)
      CALL QG10(0.,1.0,PHI11,TK3)
      M=II
      N=MM
      CALL QG10(0.,1.0,PHI20,TK4)
      M=NN
      N=JJ
      CALL QG10(0.,1.0,PHI,TM2)
      CALL QG10(0.,1.0,PHI22,TK5)
      CALL QG10(0.,1.0,PHI20,TK6)
      CALL QG10(0.,1.0,PHI11,TK7)
```

```
      M=JJ
      N=NN
      CALL OG10(0.,1.0,PHI20,TK8)
      PRINT 1001,TM1,TM2,TK1,TK2,TK3,TK4,TK5,TN6,TK7,TK8
 1001 FORMAT(2X,'TM,TK=',5E15.8)
      AMS(KK,LL)=TM1*TM2
      TEMP1=TK1*TM2
      TEMP2=ALPHA**4*TK5*TM1
      TEMP3=ENU*ALPHA**2*(TK2*TK8+TK4*TK6)
      TEMP4=2.*(1.-ENU)*ALPHA**2*TK3*TK7
      AKS(KK,LL)=TEMP1+TEMP2+TEMP3+TEMP4
   75 CONTINUE
   70 CONTINUE
      MMNN=MMMM*NNNN
      PRINT 150,((AMS(KK,LL),LL=1,MMNN),KK=1,MMNN)
      PRINT 150,((AKS(KK,LL),LL=1,MMNN),KK=1,MMNN)
      CALL EIGZF(AKS,36,AMS,36,MMNN,2,ALFA,BETA,Z,36,WK,IER
      PRINT *, 'ALFA AND BETA'
      PRINT *, (ALFA(IXX), IXX=1,MMNN)
      PRINT *, (BETA(IXX), IXX=1,MMNN)
      DO 90 I=1,MMNN
      F(I)=REAL(ALFA(I))/BETA(I)
      F(I)=SQRT(F(I))
   90 CONTINUE
      MMNN1=MMNN-1
      DO 105 I=1,MMNN1
      L=I+1
      DO 105 J=L,MMNN
      XXX=(F(I)-F(J))
      IF(XXX) 106,106,115
  115 TEMP=F(I)
      F(I)=F(J)
      F(J)=TEMP
  106    CONTINUE
      DO 125 NI=1,MMNN
      TEMPC=Z(NI,I)
      Z(NI,I)=Z(NI,J)
      Z(NI,J)=TEMPC
  125 CONTINUE
  105 CONTINUE
      PRINT 140
  140 FORMAT(2X,'EIGENVALUES AND EIGENVECTORS',/)
      PRINT 150,(F(I),I=1,MMNN)
      PRINT 150,((Z(I,J),I=1,MMNN),J=1,MMNN)
  150 FORMAT(2X,8E12.6)
      PRINT 2000
 2000 FORMAT(2X,'ORTHOGONAL POLYNOMIAL FUNCTION VALUES')
      DO 300 IM=1,6
      M=IM
      DO 300 I=1,21
      X=(I-1)/20.
```

```
      FVAL=POLY(X)
      PRINT 2001,X,FVAL
300   CONTINUE
2001  FORMAT(2X,F8.3,E15.5)
      DO 400 K=1,6
      DO 401 KX=1,11
      X=(KX-1)/10.
      DO 405 KY=1,11
      Y=(KY-1)/10.
      DEFL(KY)=0.
      DO 402 I=1,MMMM
      M=I
      TEMPX=POLY(X)
      DO 403 J=1,NNNN
      IJ=J+NNNN*(I-1)
      M=J
      TEMPY=POLY(Y)
      DEFL(KY)=DEFL(KY)+Z(IJ,K)*TEMPX*TEMPY
403   CONTINUE
402   CONTINUE
405   CONTINUE
      PRINT 3001,K,X,(DEFL(KY),KY=1,11)
401   CONTINUE
400   CONTINUE
 3001 FORMAT(2X,I3,F6.2,11F10.3,///////)
      STOP
      END
      FUNCTION PHI(X)
      COMMON/PARA/A(12,12),L,M,N
      PHIM=0.
      PHIN=0.
      DO 10 J=1,12
      K=J-1
      PHIM=A(M,J)*X**K+PHIM
      PHIN=A(N,J)*X**K+PHIN
   10 CONTINUE
      IF(L.EQ.1)PHIM=PHIM*X
      PHI=PHIM*PHIN
      RETURN
      END
      FUNCTION POLY(X)
      COMMON/PARA/A(12,12),L,M,N
      PHIMT=A(M,1)
      DO 10 J=2,12
      K=J-1
      PHIMT=A(M,J)*X**K+PHIMT
10    CONTINUE
      POLY=PHIMT
      RETURN
      END
      FUNCTION PHI11(X)
```

```
      COMMON/PARA/A(12,12),L,M,N
      PHIM1=0.
      PHIN1=0.
      DO 10 J=2,12
      K=J-1
      KN=J-2
      PHIM1=K*A(M,J)*X**KN+PHIM1
      PHIN1=K*A(N,J)*X**KN+PHIN1
   10 CONTINUE
      PHI11=PHIM1*PHIN1
      RETURN
      END
      FUNCTION PHI20(X)
      COMMON/PARA/A(12,12),L,M,N
      PHIM2=0.
      PHIN=0.
      DO 10 J=3,12
      K=J-1
      KN=J-2
      KM=J-3
      PHIM2=K*KN*A(M,J)*X**KM+PHIM2
10    CONTINUE
      DO 20 J=1,12
      K=J-1
      PHIN=A(N,J)*X**K+PHIN
   20 CONTINUE
      PHI20=PHIM2*PHIN
      RETURN
      END
      FUNCTION PHI22(X)
      COMMON/PARA/A(12,12),L,M,N
      PHIM2=0.
      PHIN2=0.
      DO 10 J=3,12
      K=J-1
      KN=J-2
      KM=J-3
      PHIM2=K*KN*A(M,J)*X**KM+PHIM2
      PHIN2=K*KN*A(N,J)*X**KM+PHIN2
   10 CONTINUE
      PHI22=PHIM2*PHIN2
      RETURN
      END
```